Monitoring Complex Reactions using Tandem Mass Spectrometric Methods

by

Michelle Yan Chi Ting
Bachelor of Science, York University, 2016

A Thesis Submitted in Partial Fulfillment
of the Requirements for the Degree of

Master of Science

in the Department of Chemistry

Supervisory Committee

Monitoring Complex Reactions Using Tandem Mass spectrometry Methods

by

Michelle Yan Chi Ting
B.Sc. (Hons), York University, 2016

Supervisory Committee

Dr. J. Scott McIndoe, Department of Chemistry
Supervisor

Dr. Fraser Hof, Department of Chemistry
Departmental Member

Abstract

Supervisory Committee
Dr. J. Scott McIndoe, Department of Chemistry
Supervisor
Dr. Fraser Hof, Department of Chemistry
Departmental Member

Suzuki-Miyaura cross-coupling is a well-known method for making biaryls. With bifunctional monomers, Suzuki polycondensation (SPC) can be used to make polyaryls. Given the complexity of the reacting solution, studying the mechanism of SPC is extremely tough. To solve this problem, we used tandem mass spectrometric (MS/MS) methods to observe the dynamic behaviour of catalytically relevant species in real time.

Catalysis involves a complex soup of reactants, intermediates and products. We used an ESI-MS with a triple quadrupole mass analyzer to monitor the SPC in positive ion mode using pressurized sample infusion (PSI) in real time. Full scan, selected ion recording (SIR), product ion scan, neutral loss scan (NLS) and multiple reaction monitoring (MRM) MS/MS methods were applied. Tetrakistriphenylphosphine palladium(0) was the catalyst of this reaction and a positively charged phosphonium aryl iodide tag (*m/z* 478) was implemented into the first catalytic cycle, enabling us to track all the intermediate oligomers up to the 4^{th} addition. Product ion scan revealed all the intermediate oligomers lose a triphenylphosphine fragment (*m/z* 262) which would either come from the complex or the charged tag. Three significant intermediate types were observed in each stage of the catalysis, oxidative addition, transmetallation and reductive elimination and their behavior was studied in a chronogram, normalized to the total ion current. As expected, the use of selected ion recording, and neutral loss scan dramatically improved the signal-to-noise ratio. Ultimately, multiple reaction monitoring showed the best chronogram data due to the fact that this scan acts as a "double filter" in a soup of reactive species and contaminants.

Real time reaction monitoring has proven to provide detailed insights regarding a reaction. MS/MS methods are promising for improving data quality, selectivity and sensitivity in reaction monitoring. The principle is broadly applicable to other systems, from an intricate catalytic reaction with short-lived ionic intermediates to a reaction with only a single product generated. Reaction dynamics for an exceptionally complex reaction can be made simple and easy by utilizing tandem mass spectrometry methods in time resolved reaction monitoring.

Table of Contents

List of Tables

List of Scheme

List of Figures

List of Abbreviation

CID	collision-induced dissociation
CRM	charge residue model
Da	Dalton
EI	electron ionization
ESI	electrospray ionization
IEM	ion evaporation model
IMS	ion mobility mass spectrometry
IR	infra-red spectroscopy
m/z	mass-to-charge ratio
MALDI	matrix-assisted laser desorption ionization
MRM	multiple reaction monitoring
MS	mass spectrometry
MS/MS	tandem mass spectrometry
MS1/2	first and the second mass analyzer in a triple quadrupole
NLS	neutral loss scan
NMR	nuclear magnetic resonance
OLED	organic light emitting diode
PEEK	polyether ether ketone
PPh_3	triphenylphosphine
PSI	pressurized-sample infusion
q	collision cell
S:N	Signal-to-noise ratio
SIR	selected ion recording
SMC	Suzuki-Miyaura cross-coupling reaction
SPC	Suzuki polycondensation
TIC	total ion current
UV-VIS	ultraviolet–visible spectroscopy

Acknowledgments

I would like to express my gratitude to Dr. Scott McIndoe for giving me the opportunity to work in his research lab and never closing his office door on me. His generosity, patience, and encouragements are out of my understanding at times and without his guidance, this work would be impossible. I also would like to express my gratitude to Dr. Fraser Hof and Dr. Matthew Bush for being my committee members and taking the time to read this work. Everyone questions I got from each of you filled every loophole and doubts I had about my thesis and I am extremely grateful to that.

I would also like to further express my gratitude to Elena Liles for her genuine friendship and advices; her kindness was like a warm summer breeze during a cold and rainy BC winter. As for my office neighbours Cameron and Andy from the Leitch group; Tong and Jon from the Wulff group; and Jin from the Rosenberg group, I am extremely grateful to all your friendships, suggestions and never-ending patience to explain synthetic concepts to an analytical chemist without losing your temper and always ready to offer your helping hand and brain on my silly questions and rants.

I would also like to express my admiration to the newest addition of the McIndoe group, Gilian and Sofia. I am truly humbled by Gilian's dedication towards research and her passion on mass spectrometry and am very inspired to meet her level of perseverance. I really hope we will meet again in the future. Also, I am thankful to the Friday crew for always including me and I apologize for MIA during my thesis crunching time.

I am extremely thankful to the staff in the Department of Chemistry especially to Lori because she has always hyped along with my ideas in decorating the chemistry office but she usually does all the work. I am also thankful for Dr. Jane Browning's teaching and always lending me her ear. I am blown away by her level of kindness, empathy and knowledge on teaching and in analytical chemistry. I would also like to thank all the undergraduates I have taught at UVic for letting me grow as a teacher and I have learned just as much as they have learn from me.

I am also thankful to Peter Sidhu for being the first person to push me to start graduate school and the original chemfam in Toronto for always rooting and cheering for me. I

would also like to thank my undergraduate thesis supervisor, Dr. Damien Ifa for igniting my passion in mass spectrometry by showing me the power of DESI-MS imaging.

Last but not least, I am thankful to the Tingster family and friends for their love and support. I am happy to know that the title page of my thesis and the paper I published during my graduate studies will have a place on the refrigerator. As for everyone I have met along the way in this journey, I thank you because it would not have been the same without you.

Dedication

To Momma and Papa Ting

And

Future McIndoe Graduate Students

Chapter 1 Reaction Monitoring by Mass spectrometry

Brief history and fundamentals of Mass spectrometry

Mass spectrometry is a powerful analytical technique since its discovery in the early 1900s and has been countlessly explored and improved over the years.[1–6] The making of this well-established technique was a collaborative effort between numerous physicists and chemists. Following the studies of "cathode rays" by Eugene Goldstein[7,8], scientists are able to generate charged particles in which Joseph John (J.J) Thomson introduced the first mass spectrometer with the idea of measuring the mass-to-charge (*m/z*) ratio of Neon-20 and Neon-22.[9] Thomson's student, Francis Aston later revamped Thomas's original instrument with a higher signal intensity and resolution and discovered the existence of isotopes of stable elements.[9,10] Since then, mass spectrometry has been made available to scientists of various fields, and it is the versatility of mass spectrometry that makes it such an applicable tool, and applications are continuously expanding.

There are three major components in a given mass spectrometer: an ionization source, a mass analyzer(s) and a detector. An analyte first enters the ionization source through an inlet to generate gas-phase ions, which are then accelerated to the mass analyzer for separation under vacuum, and finally reach the detector that converts the ion count into readable signals. The relative abundance of ions is expressed in mass-to-charge (*m/z*) ratio, where the mass (m) is the atomic mass unit (u) or Dalton (Da), and the charge (z), is an integer number elementary charges (e). A mass spectrum is a plot of ion intensity versus *m/z* ratio, and each peak indicates the presence of an ion at that particular *m/z*.[9]

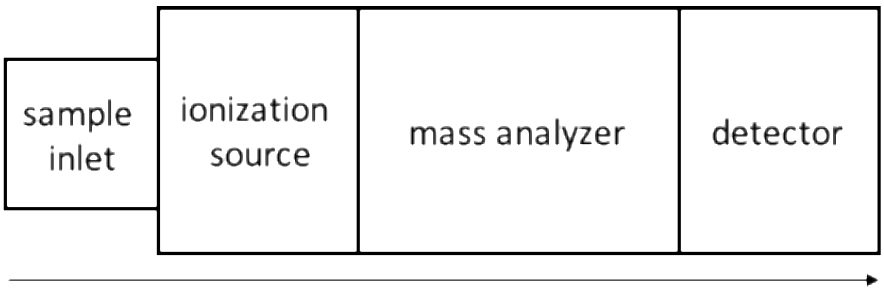

Figure 1-1. Illustration of the components in a mass spectrometer.

A sample must be charged in the gas phase to be analyzed in a mass spectrometer. Each ionization method is unique and is suitable for a specific class of analyte. Ionization methods can be classified as "hard" ionization and "soft" ionization. Hard ionization, such as electron ionization (EI) employs energetic electron to ionize small volatile organic molecules to produce extensive fragmentation of the analyte before it is introduced to the mass analyzer.[11,12] Whereas soft ionization, induces minimal fragmentation and allows sample ions to be intact in the gas phase.[6,13] Electrospray ionization (ESI) is a prime example of soft ionization because the process is done under atmospheric condition, making it a popular way to introduce several samples, including inorganic and organometallic compounds for analysis.[14–17] Recent groundbreaking development in ambient ionization methods receives much attention due to the simplicity of the setup and how they address the limitations that traditional mass spectrometry experiments bring.[18–22]

Electrospray Ionization

Electrospray ionization (ESI) was first developed by Malcolm Dole in 1968 and later improved by John Fenn and Yamashita in the late 1980s.[14,23–25] Fenn was awarded the Nobel prize in chemistry in 2002 for his contribution in electrospray mass spectrometry. The ESI-MS process starts with a continuous flow of the analyte solution that passes

through a stainless-steel capillary connected to a high voltage (2-5 kV). This creates a stream of charged droplets to form a Taylor cone at the end of the capillary tip due to the presence of the high electric field.[26] These charged droplets are then desolvated by a nebulizing gas (usually argon or nitrogen gas) and shrink in size, causing the charge density of each droplet to overcome the surface tension and draw to the mass analyzer.

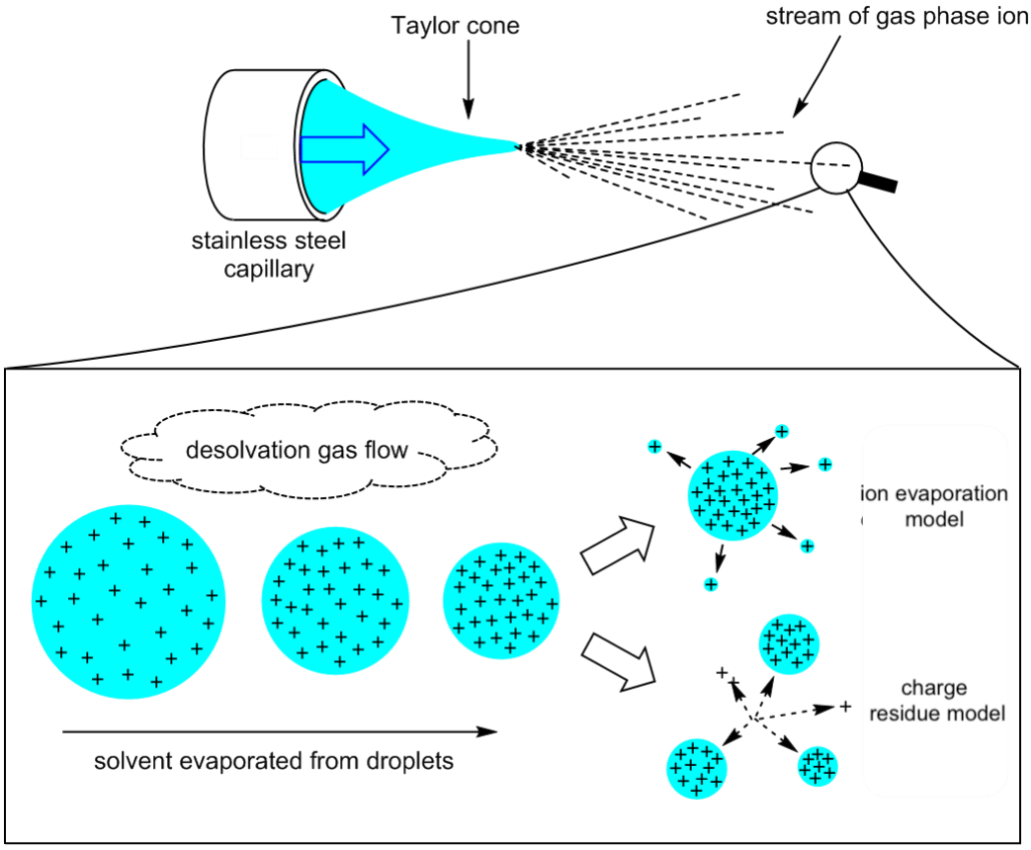

Figure 1-2. Illustration of the electrospray process.

There are two generally accepted ionization mechanism, the ion evaporation model (IEM) and the charged residue model (CRM).[27] The IEM suggests that the high electric field cause charged ions to expel from the droplet surface and is used to explain the

ionization process for low molecular weight organic compounds. The CRM model explains a simpler ionization process on protein samples. It describes solvated charged droplet as a shell, and as the solvent shell evaporates, the charges are transferred onto the analyte residue.

ESI-MS is suitable for small, large, and polar compounds. It is a fast technique, with one spectrum taking one second or less to process, and can be applied to reactions that are a minute to hours long. Whatever the time period, it gives the opportunity for studying not only products and reactants, but also intermediates, resting states, and decomposition material.[18,28] It is also far more sensitive than other techniques such as nuclear magnetic resonance spectroscopy (NMR) with observations of species in the parts per million range. Even more importantly, it has a high dynamic range that spans several orders of magnitude and it can analyze complex mixtures with great resolution of different species (providing they have different mass to charge ratios – ESI-MS does not discriminate between isomers). The "softness" of ESI-MS makes it ideal for the analysis of catalytic reactions when applied to olefin polymerization and metathesis,[29,30] hydroformylation,[31] decarboxylation,[32] esterification,[33] and of course, palladium-catalyzed cross-coupling.[34–40] In fact, palladium-catalyzed cross-coupling reactions have been analyzed by mass spectrometry since 1994.[35] Because it is a soft ionization technique, there is a complete desolvation of large, charged species with minimal fragmentation. These species are separated based on their *m/z* which makes it possible to analyze the contents of a reaction through mass and isotope patterns.

Sample Introduction: Pressurized-sample Infusion (PSI-ESI-MS)

Mass spectrometry is an extremely powerful tool with diverse methods that deliver samples from solution to the gas phase and ionize them for mass separation. Pressurize sample infusion (PSI) is a sample introduction technique that allows a reaction mixture to be directly injected into the mass spectrometer to collect real time data of an experiment.[41,42] The setup of a PSI is simple and easy to implement to ESI-MS: a Schenk flask containing the reaction mixture is sealed with a rubber septum and is connected to an inert gas supply. A piece of chromatography capillary like a fused silica or apolyetheretherketone (PEEK) capillary tubing can be used to punctured through the septum and submerged into the reaction solution. The overpressure inside the flask is enough to push the reaction solution through the capillary tubing to enter the ESI inlet. This is called cannula transfer and the flow rate can be determined by the Hagen-Poiseuille equation,[42,43] where the change in pressure is measured, the length and the inner diameter of the capillary tubing, and the viscosity of the reaction mixture (solvent) is known. The inert gas provides the system with 1-5 psi is usually nitrogen or argon and the flow rate of the solution is usually between 5-10 μL/min.

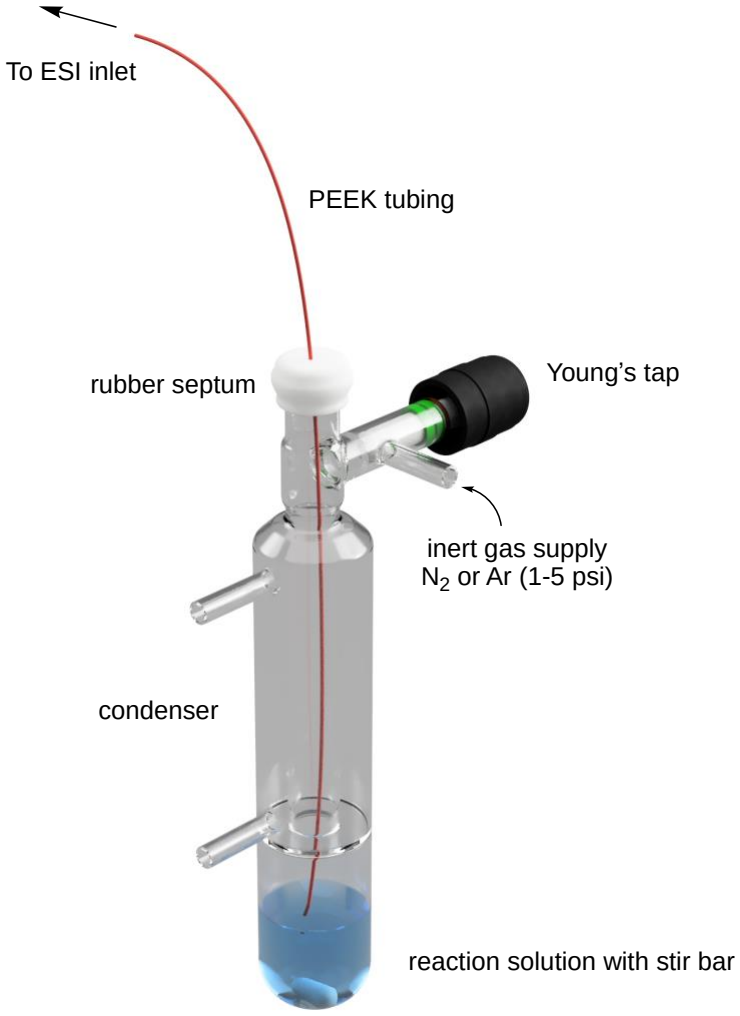

Figure 1-3. Pressurized-sample infusion with a customized Schlenk flask set.

PSI setup also allows air or water sensitive reaction to be analyzed as the Schlenk flask is sealed and degassed with an inert gas. It can be conveniently brought into a glovebox to prepare reaction starting material before an ESI-MS experiment. Alternatively, solvent and reagents can be added into the flask using a syringe through the rubber septum. Alterations can be incorporated to the Schlenk flask, such as an integrated condenser so that reflux condition can be achieved or additional outlet can be designed onto the Schlenk flask to couple with another analytical probe, e.g., UV-VIS spectrometer.

Mass Analyzer, Tandem Mass Spectrometry and Collision-Induced Dissociation

The mass analyzer is the heart of a mass spectrometer and it carries out the most crucial task of separating ions coming from the ion source then passing them to the detector. Mass analyzer uses either a magnetic or an electric field (sometimes both) to separate ions base on their *m/z* ratio.[9] Modern mass analyzers include quadrupole, ion-trap (IT), time-of-flight (TOF) and orbitrap in which the resolution, mass range, and cost vary from each mass analyzer.[7,44–46] A high vacuum is also required in the mass analyzer to prevent excessive collision between ions, which results in fragmentation and lower the resolution between mass peaks.

Tandem mass spectrometry also known as mass spectrometry/mass spectrometry (MS/MS),[7,46,47] is a two-stage process where precursor ions are analyzed and undergo a fragmentation process to produce a product ion and a neutral fragment of different masses that is displayed on the mass spectrum. There are various ways to perform MS/MS analysis and collision-induced dissociation (CID) is one of the most commonly employed method.[7,45,48,49] In CID, fast travelling intact molecular ions are introduced with a collision gas (usually an inert gas, e.g. argon or nitrogen) at high pressure in the first mass spectrometer and applied with a collision voltage. Eventually, the high internal energy in these ions induces ion dissociation into fragmented ions, which is then detected by the secondary mass spectrometer. The fragmentation pattern of the product ion is acquired in the mass spectrum. MS^n is used to describe the number of times of ions that have been through the collision process.[48] Ion trap mass analyzer is one example that can carry out MS^n experiments, where $n > 2$. Mass analyzers can be coupled together to carry out tandem

mass spectrometry, most famously the triple quadrupole mass spectrometer. Other hybrid instruments such as quadrupole time-of-flight (qTOF), tandem time-of-flight (TOF/TOF), and quadruople ion trap (QIT) combine two mass analyzers in the same instrument to take advantage of the best of both worlds.[47]

Quadrupole Mass Analyzer

Quadrupole is made up of four symmetrical cylindrical hyperbolic rod-like electrodes (Figure 1-4) that are connected to both radio frequency (RF) alternating current (AC) and direct current (DC).[46,50,51] Each pair of parallel electrodes are applied with the same voltage but different signs $(+/-)$. As ions are accelerated into the quadrupole field from the ion source, they travel through the center of the electrodes along the z-axis. The signs of the voltage on the electrode pairs alternate periodically, positive ion is attracted to the negative electrodes and as the sign of the voltage switches, these ions then repel from the original electrodes to move to the opposite electrodes and vice versa for negative ions.

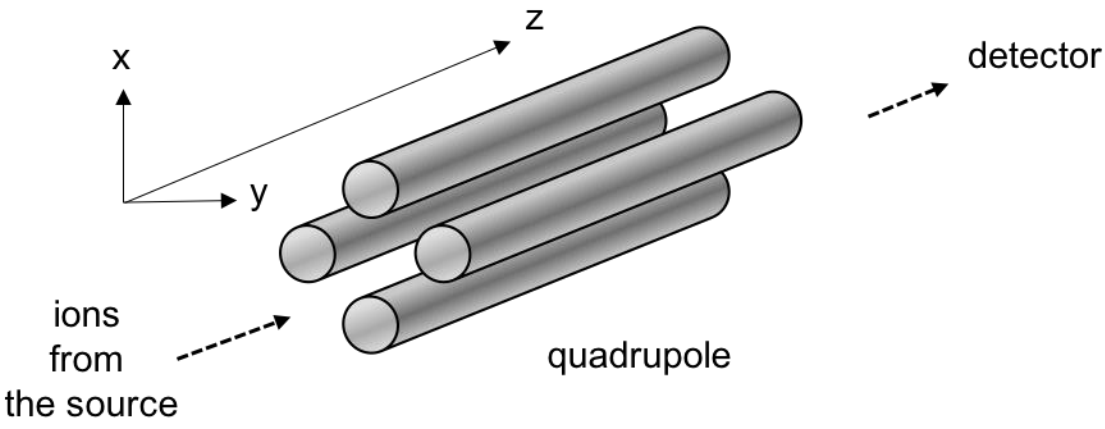

Figure 1-4. Diagram of a single quadruople mass analyzer.

Quadrupole is known as a mass filter because ions with a particular *m/z* ratio or within a selected range can successfully pass through the quadrupole and reach the detector to give out signals; all other ions will collide with the electrodes, discharge and never reach the detector. The Mathieu equation is used to explain the principle of ion motion the along the ion path under the influence of the RF and DC ratio: [50–52]

$$\Phi_0 = +(U - V\cos\omega t)$$

$$-\Phi_0 = -(U - V\cos\omega t)$$

Φ_0 represents the total potential applied to the electrodes, U is the DC voltage, V is the RF voltage, ω is the angular frequency, and t is the time. The integration of the Mathieu equation explains the motion of ions in the quadrupole but is complicated and is beyond the scope of the study. It is important to recognize that at each *m/z* there is a range of DC and RF voltage values that are set to safely transverse ions across the z-axis without hitting the electrodes on the x-y plane (See Figure 1-4).

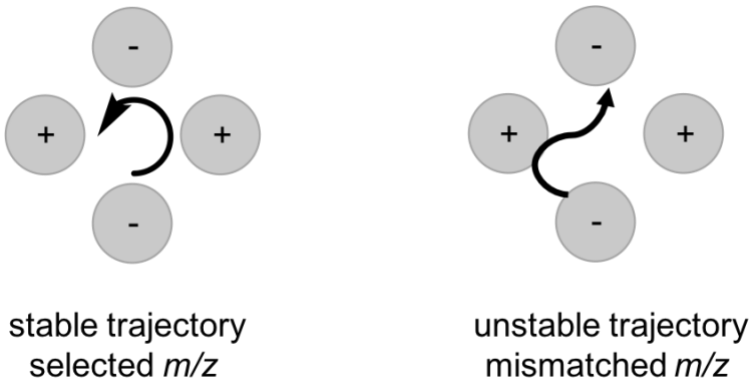

Figure 1-5. Comparison of the ion trajectory from a quadrupole mass analyzer.

A stability diagram in Figure 1-5 illustrates the relationship of the stable region and the DC and RF voltage in U/m and V/m.[47,51] Masses that lies within the stable region display stable trajectories on the x-y plane along the ion path. If either U/m or V/m is greater than the stable region, masses equal to m or lower than m will have an unstable trajectory in the quadrupole. Resolution can be adjusted by the slope and it should lie within the stable region, hence both DC and RF voltage are ramped together at a particular ratio to give the slope A and B.[46] Slope A has a higher resolution but it has a smaller mass range window which results in lower sensitivity whereas slope B has a lower resolution but it covers a larger mass range window.

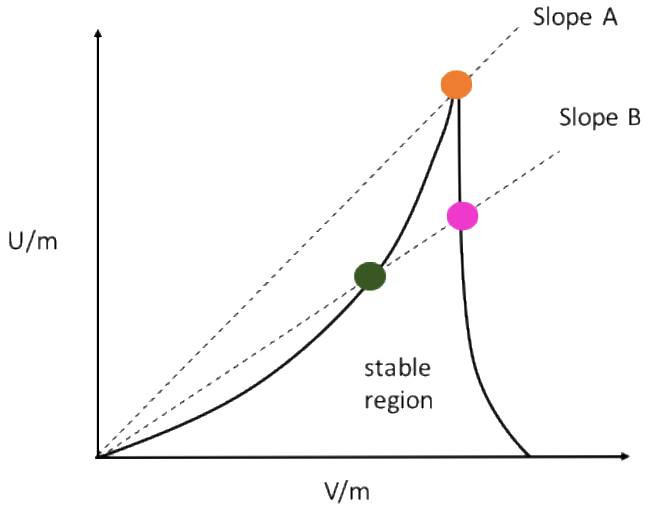

Figure 1-6. Stability diagram demonstrating the Mathieu equation.

Quadrupole can also act as an ion guide by applying an RF-only voltage. The DC voltage is set to zero and ions of a broad range of *m/z* are able to pass through. Hexapole and octapole are also employed as ion guides and can take part in a triple quadrupole mass analyzer as a collision cell with another quadrupole to carry out tandem mass spectrometry.

Mass spectrum, Mass Accuracy, and Resolution

Mass accuracy and resolution are parameters that measure the performance of a mass analyzer. Mass accuracy measures the difference of the theoretical *m/z* and the experimental *m/z* and is expressed as follow: [44]

$$Mass\ accuracy\ in\ ppm = \frac{m_{theoretical} - m_{experimental}}{m_{experimental}} \times 10^6$$

The resolution in mass spectrometry measures the ability to separate two mass peaks. There are various methods to define mass resolution, therefore it is crucial to state the selected method before drawing a comparison. Resolving power measures the ability of a mass spectrometer to give a specific mass resolution of a single mass peak. It is expressed as

$$Resolving\ power = \frac{\mathrm{m}}{\Delta m_{\mathrm{x\%}}}$$

where m is the average mass of the two neighbouring peaks and $\Delta m_{x\%}$ is the difference of the two peaks and x% is the overlapping valley that must be stated for the calculation. Figure 1-6 illustrates an example of resolution and resolving power with 10% and 50% valley. The resolving power using with 10% valley of overlapping peak tails is 1000/0.208 = 4800, where m = 1000 and Δm = 0.208.[44] The same equation can be used to defined another method, known as the full width of a single mass peak at half of its maximum height (FWHM) where m is the *m/z* of the single peak and $\Delta m_{50\%}$ is the width of the peak at 50% of the peak height.[44,47] Using this method, the resolution of the first peak would be 1000/0.1 = 10, 000. Another variation of the equation using full width at 5% maximum is

also common. The FWHM is applicable to low resolution mass analyzers, such as quadrupole instrument which has an FWHM resolution of 2000 and a mass accuracy of 100 ppm.

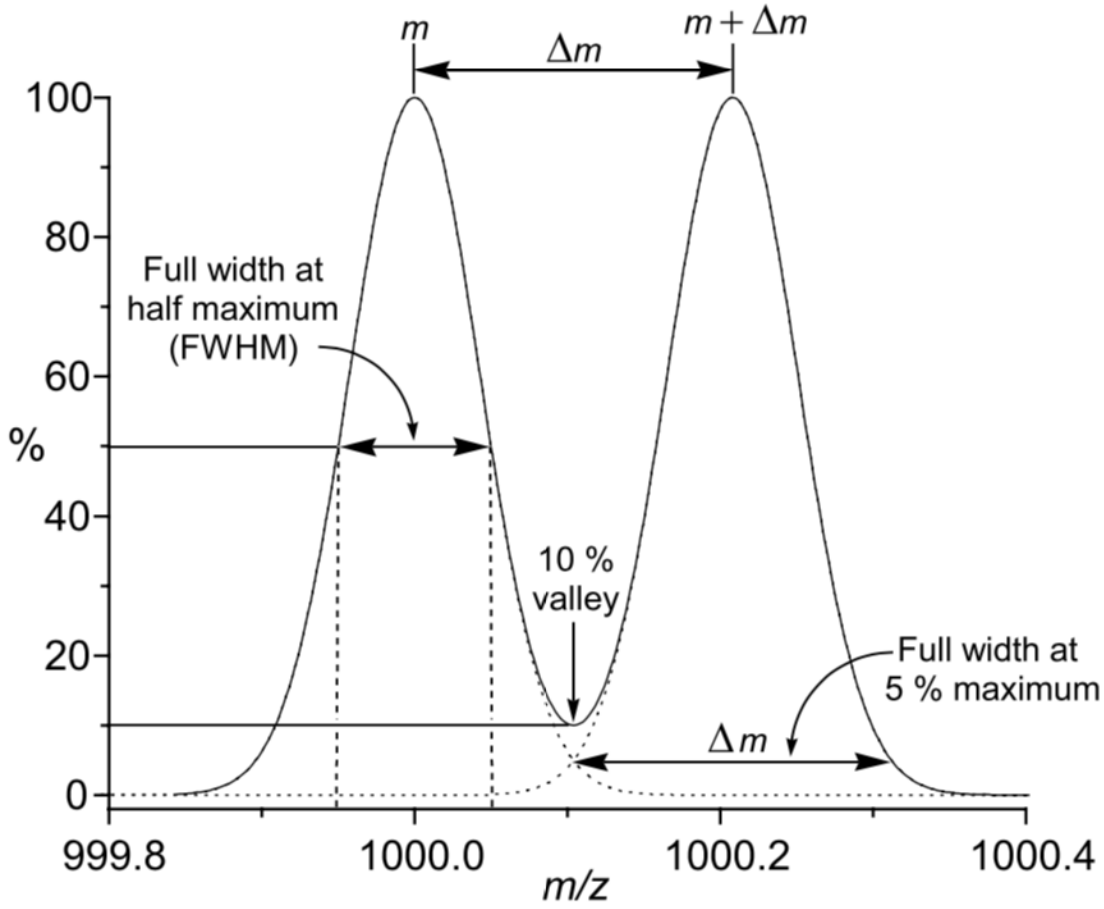

Figure 1-7. Two methods that describes resolution.[44]

Despite the low resolution, quadrupole is still a popular option as mass analyzer because its benefits weigh out the drawbacks, for instance, it is low cost, robust and has high scanning speed and a mass range of *m/z* 3000. It can be a stand-alone mass analyzer or a hybrid mass analyzer when it is coupled with a time-of-flight (Q-TOF), ion trap (QIT) or two other quadrupoles to be a triple quadrupole (QqQ).

Triple Quadrupole Mass Analyzer

Triple quadrupole mass spectrometers (QqQ/QhQ) employ two quadrupole mass analyzers (Q1 and Q3 or MS1 and MS2) separated by a collision cell (more often a hexapole or an octapole, thanks to their superior ion confinement properties, but "triple quad" has stuck as the encompassing term for these instruments).[7,46,50] The Q1 and Q3 serve as mass filters and the second quadrupole is a radio frequency only quadrupole that serves a different function, hence the lower-case q in the acronym. At the second quadrupole, the collision cell is where the fragmentation process occurs. The collision cell facilitates single or multiple ion fragmentations unlike the scanning function in Q1 and Q3. A modern collision cell is usually made of hexapoles or octapoles for better ion confinement instead of a quadrupole. One can think of a triple quadrupole mass analyzer as two quadrupoles "sandwiching" a collision cell. With this arrangement, various type of ion transition experiments can be achieved through tandem mass spectrometry (MS/MS).[7]

In the QqQ mass analyzer, MS operation can be divided into two categories, scan modes with and without the use of CID, full scan and selected ion monitoring, while scan modes with the use of CID (MS/MS) are product ion scan, precursor ion scan, neutral loss scan, and multiple reaction monitoring. Both are equally useful in quantitative and qualitative analysis.[7,45,46,51] Full scan mode is the most general scan mode because it provides a "big picture" of the sample of interest (See Figure 1-8a). A mass range is selected and only ions with a specific DC and RF ratio are able to pass through Q1 then enter the collision cell, move to Q3, and finally to the detector. In this case, Q1 is scanning ions and the collision cell and Q3 are acting as RF-only ion guides. A typical problem with full scan experiment is that at a given *m/z* ratio one mass peak can represent more than one species because

different species can have the same *m/z* ratio. To solve this problem, mass spectrometry users often run the following scan modes when appropriate. Selected ion recording (SIR) is a selective single stage MS scan where one or more ions of interest are selected instead of a mass range are allowed to pass through Q1, q and Q3. This scan mode is useful in screening target compounds with known *m/z*. However, the entire mass spectrum of a SIR experiment is not recorded and rather the individual m/z relative intensity is shown.

Product ion scan allows for direct structural analysis of a particular ion through CID. In Figure 1-8b, a precursor ion is selected and only ions of this *m/z* can pass through Q1 to the q to undergo CID. The precursor ion and its fragments are detected in Q3. This scan mode is important in identifying unknown compounds because compounds that have the same *m/z* may have different ion fragments and isotopic pattern at different collision voltage, which can be characterized through product ion scan.

In neutral loss scan (NLS), all ions undergo CID in q, meaning both Q1 and Q3 are scanning together, with the latter also scanning an offset of a common neutral fragment loss (see Figure 1-8c). In order to run a neutral loss scan, both full scan and product ion scan experiments should be carried out to determine the common neutral fragment *m/z* and the optimal collision voltage.

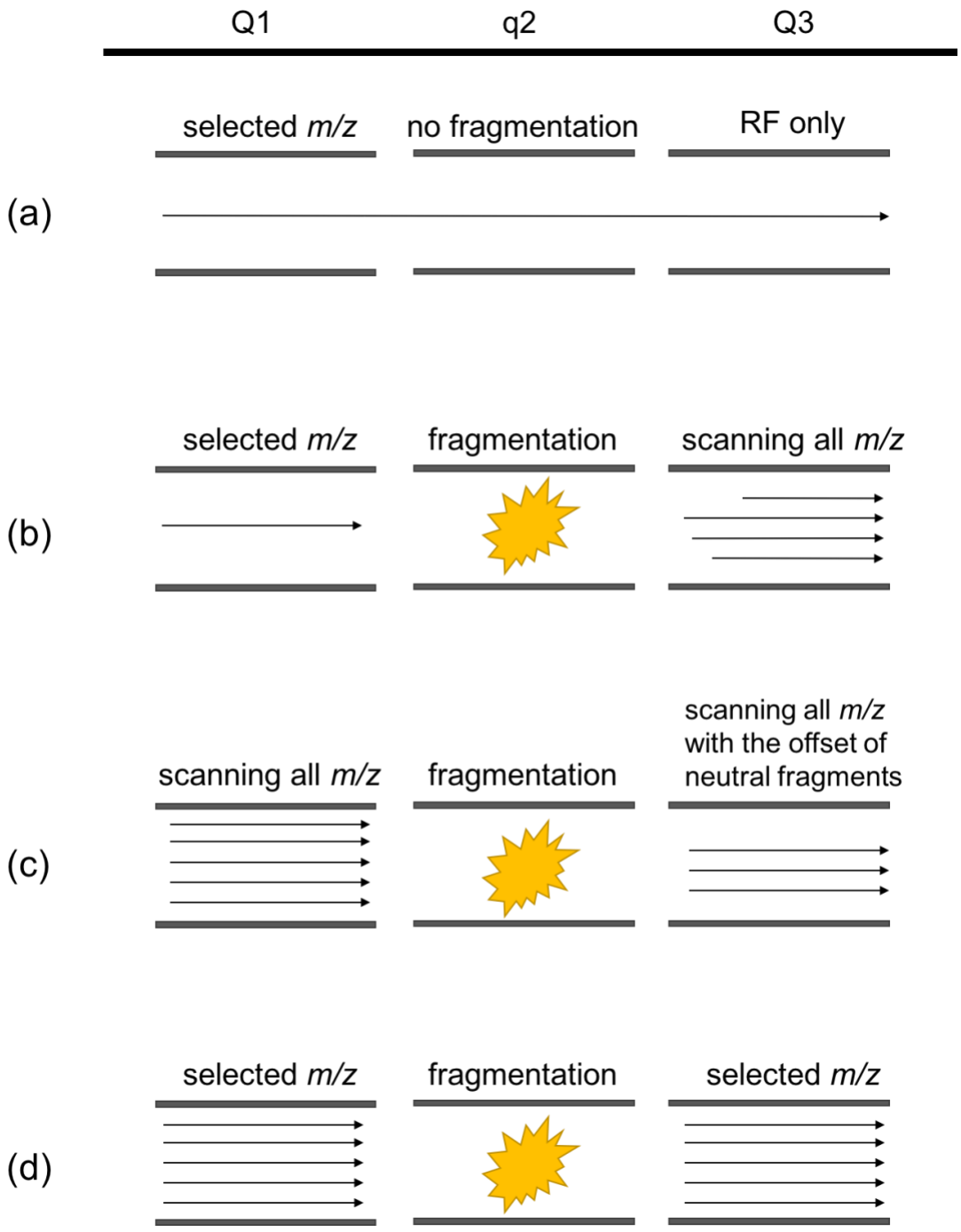

Figure 1-8. Tandem mass spectrometric scan modes on a triple quadruople mass analyzer: (a) full scan mode, (b) product ion scan, (c) neutral loss scan, and (d) multiple reaction montioring.

Multiple reaction monitoring (MRM) is both highly sensitive and selective, and therefore is used for monitoring a one or multiple specific ion transition(s). As seen in Figure 1-8d, the precursor ion is selected in Q1 then undergo CID in the collision cell and only the product ion (of the precursor ion) is selected in Q2 for detection. The requirements to run an MRM experiment are the *m/z* of the precursor ion, *m/z* of the product ion and the collision voltage, which are all essential information to produce a diagnostic charged fragment of that ion. Both SIR and MRM increase sensitivity by scanning selected *m/z* ratio rather than a mass range, so the mass analyzer can spend more time on each ion. However, ions in SIR do not undergo CID, therefore it is not as selective as MRM because MRM only analyze a selected precursor/product ion combination at a specific collision voltage. This property greatly eliminates species that share the same *m/z* ratio. NLS and MRM are effective in differentiating species that share the same *m/z* ratio but in terms of sensitivity and selectivity, MRM is a much better candidate. MRM scans can be looped together into one experiment to detect the presence of many specific ions in a complex mixture and is a remarkable way to improve the signal-to-noise ratio by filtering out chemical noise.

The type of scan mode is also closely related to the type of mass analyzer. While MS/MS is an essential feature on a mass spectrometer, only triple quadrupole mass analyzer can carry out all the target scan modes described above, which allows for enhanced selectivity and sensitivity as ions have the chance to go through stages of transition.

Reaction Monitoring by Mass Spectrometry

Online-reaction monitoring allows real time data to be collected by mass spectrometry while the reaction is in progress and is of great significance in elucidating short-lived

reaction intermediates.[31,34,57,36,41,42,44,53–56] The first online study using mass spectrometry was reported by Heitbaum and coworkers for studying electrochemical reactions using a thermal spray quadrupole mass spectrometer in 1986.[5,53] Covey and coworkers came up with another way to monitor reaction continuously by directly infused sample to the ion source.[56] They were able to monitor the hydrolysis of methandrostenolone sulfate by dissolving the reactants in methanol in a reaction flask and transferred an aliquot of the reaction mixture with a syringe that can be directly injected into the ESI inlet. Since then, different methods have been developed to study reaction mechanisms,[18,34,54] for instance, the use of microreactors and mixing tees.

In offline-reaction monitoring, the entire reaction process is not recorded, rather a small aliquot of the reaction sample is first diluted before it is introduced into the mass spectrometry and the chemical composition of the reaction mixture is analyzed. The pre-diluted sample can also be subjected to other analytical instruments, such as NMR, infra-red spectroscopy (IR) or ultraviolet–visible spectroscopy (UV-VIS). This traditional approach is flexible in analyzing reaction sample at different stages over the course of a reaction but fail to detect unstable or transient intermediates. One can think of online monitoring as a video recording of series of events over time and offline reaction monitoring as a snapshot of each event at a specific time frame.

Recent development has also allowed chemists to study air or moisture sensitive reactions with mass spectrometry, for instance setting up a glove box next to matrix-assisted laser desorption ionization (MALDI)-MS or ESI-MS.[57–59] In the article, "Insight into Solution Chemistry from Gas-Phase Experiments",[60] Schröder highlighted the difficulties in studying reaction mechanisms and suggested that the features of ESI-MS

makes it a great tool in synthetic research. The limitation in using ESI-MS to study reaction mechanism has been addressed in the past, the use of charge-tags make the sample visible to MS.[55] Schröder raised a fair point that ESI-MS still met with questions whether mass spectrometry result is "real and legitimate" because of the lack of a lingua franca between synthetic chemists and mass spectrometrists. Our group has studied numerous inorganic reactions using ESI-MS along with orthogonal and traditional techniques and the results were often in agreement.[39,61–69] However, it is still cumbersome to study catalysis where there are pre-catalytic species, reactants, resting state species, intermediates and products are involved and because the addition of each species to the reaction mixture reveals valuable information of each catalytic step. PSI-ESI-MS offers a cost-effective and simple setup to study reactions solution continuously to solve this problem and bridge the gap between organometallic chemist and an analytical instrument.

Chapter 2 Suzuki Polycondensation

Introduction

Cross-coupling reaction using organometallic reagents and transition metal catalyst was a breakthrough in synthesizing new carbon-carbon bonds. The discovery of cross-coupling reactions can be dated back to the 1900s and is divided into three aspects: the discovery of metal catalysts, the use of organometal coupling partners, and the tuning and optimization of reaction parameters.[70–75] Palladium catalyzed cross-coupling reaction has gained a lot of attention due to the contribution of its wide applications in technological and economic growth such as the making of polymer, bulk materials, and pharmaceutical compounds.[76] The 2010 Nobel prize in Chemistry was awarded to Richard Heck,[77] Akira Suzuki,[78] and Ei-ichi Negishi[79] because of their contribution in discovering palladium catalyzed cross-coupling reaction.[80–82] The general equation of palladium cross-coupling reaction is shown in Scheme 1, where an organohalide reacts with an organometal coupling partner and the reaction proceed with the aid of a palladium catalyst.

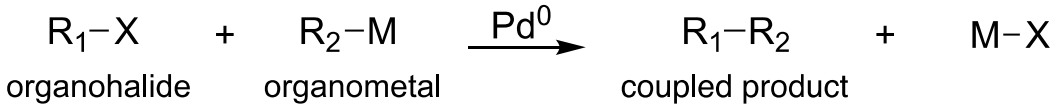

Scheme 1. Palladium cross-coupling genearl equation.

Historically, there are several copper and nickel-catalyzed cross-coupling reactions that were discovered prior to the rise of palladium complexes as catalyst. The Ullmann reaction is a copper-mediated dimerization where the coupling process happens at the aryl halide under harsh thermal conditions.[83] The Heck reaction is a palladium catalyzed coupling reaction of olefin and organohalide and is also considered to be the palladium cross-

coupling reaction that initiated the wide spread of research study in the field. Thereafter, notable palladium coupling reactions were reported using different coupling partners, Negishi, Stille[84] , and Suzuki and Miyaura discovered the use of organozinc, organotin and organoboron, respectively. The Negishi and the Suzuki-Miyarua reaction share a similar mechanism with the latter requires a base to facilitate the catalytic cycle. The apparent disadvantage of the Stille reaction is the toxicity of organotin reagent.[85,86] Among the variety of palladium cross-coupling reactions, the Suzuki-Miyaura cross-coupling reaction is shown to have a leading number in research publications and patents in the 2000s. This trend is largely related to the reaction parameters,[82,87] mild reaction conditions; the commercially available and stable starting materials; the compatibility of functional groups; the easily removal of by-products and high yield of products. It is referred as a green reaction due to the use of water as solvent and non-toxic reaction mixture, as well as relatively low catalyst loading and the application in one-pot synthesis.[88]

Synthesis of biaryl moieties has always been a subject of interest and is of great importance in industrial chemistry of developing complex aryl compounds. The Suzuki-Miyaura cross-coupling reaction (SMC) makes new sp^2 hybridized C–C bond using an aryl halides or triflates and an arylboronic acid with a palladium catalyst. Scheme 2 shows the general equation for SMC, Ar_1 and Ar_2 can be an alkenyl, alkynl, aryl or benzyl group with a halide. Aryl iodide and aryl bromide can easily react with the aryl boronic acid to give coupled products.[89–91] Aryl chloride is rarely used in the reaction due to its low reactivity as it has the highest bond strength, but recent reports from the Buchwald group show examples with the use of aryl chloride with amines and boronic acids.[92,93] Arylboronic acids and derivatives (boronate ester and borate) are often non-toxic and stable in air, water,

and thermal conditions. Palladium with tertiary phosphine ligands is the most frequently used catalyst in SMC, along with $Pd(dba)_2$ and $PdCl_2$.

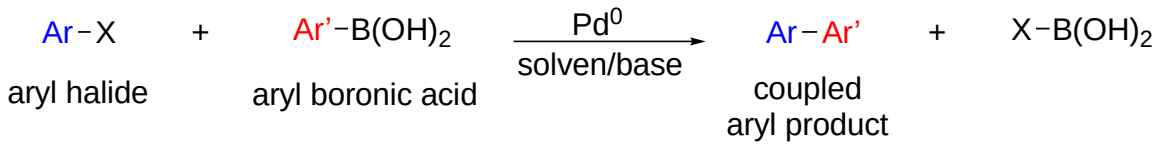

Scheme 2. General equation of SMC, where Ar and Ar' are both aromatic unit.

Catalytic Cycle

The generally accepted SMC catalytic cycle is shown in Scheme 3, the cycle proceeds in three fundamental reactions: oxidative addition of the organohalide to the palladium catalyst, transmetalation of the organoboron coupling partner to the palladium complex, and reductive elimination of the two coupling partners to form new C–C bond along with the regeneration of the palladium catalyst.[80,89]

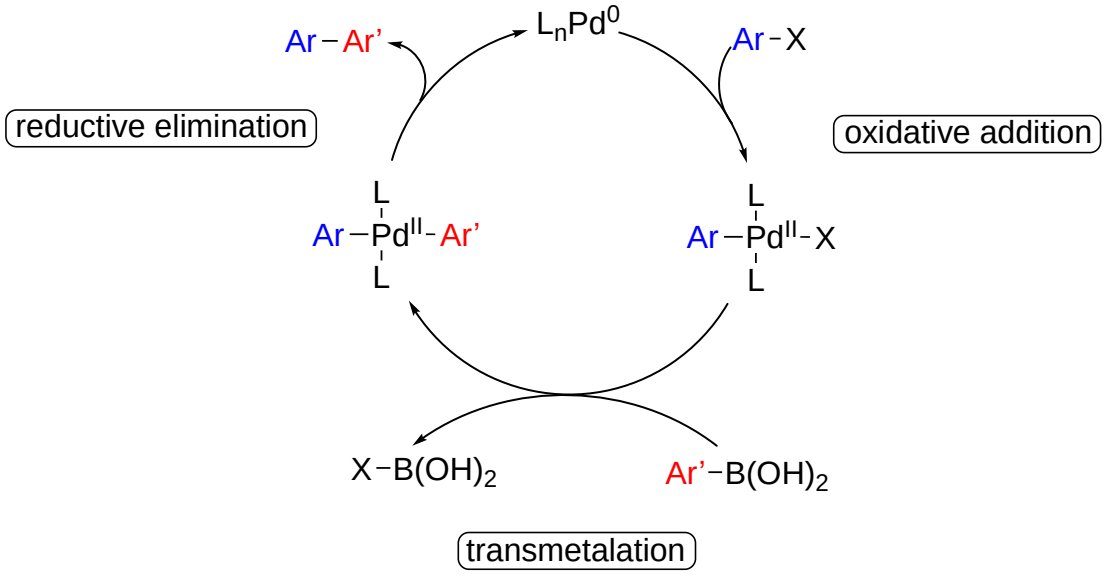

Scheme 3. Genearlly accepted mechanism of the SMC, where L is usaually tertiary phosphine.

The mechanism of oxidative addition and reductive elimination have been extensively studied and well understood over the years.[89] Oxidative addition with aryl halide involves the breaking of the sigma bond of the C–X group to form two new sigma bonds with the $L_nPd(0)$. The oxidation states of the Pd metal is increased by two along with an increase in the total electron count depending on the ligand. Hence, the metal complex is required to have a low oxidation state. The mechanism of reductive elimination can be considered the reverse of oxidative addition step where the catalyst is regenerated and its oxidation state of the Pd(II) is reduced back to Pd(0) and the coupled biaryl product is eliminated.[94]

Oxidative addition of Pd cross-coupling reaction typically proceeds in two mechanisms as shown in Scheme 4,[95,96] the concerted or three-centred mechanism and the S_N2 mechanism depending on the catalyst, substrates and solvent. In the concerted mechanism, X-Y binds to the metal centre through one bond forming a three-centred species in a transition state, then this bond breaks to form two new bonds, M–X and M–Y at the same time. The oxidative addition proceed in the concerted pathway where aryl halide is the coupling partner. The S_N2 mechanism proceeds in two steps, the electron rich metal first attacks ligand X to form $[L_n–M–X]^+$ causing ligand Y to leave, then recombine with Y to form a $[L_n–M–XY]^+$, a S_N2 transition state like species and forming the final product $L_nM(X)(Y)$. This mechanism is observed in SMC with polar reagents and notably alkyl halides.[96] The bond strength of aryl halide bond is as follow: iodide > triflate > bromide >> chloride, therefore oxidative addition is unlikely to be the turnover limiting step for aryl chlorides.[95] Aryl iodides, bromide, and triflates are often employed in SMC.[97,98]

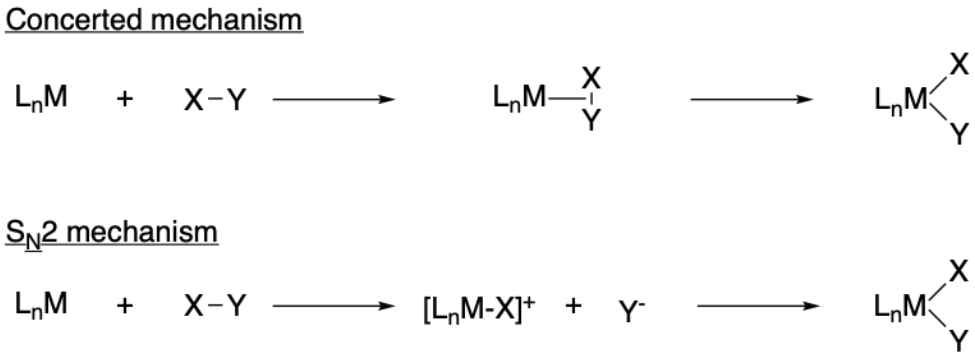

Scheme 4. Mechansim of the oxidative addition step in the concerted and SN2 pathway.[96]

The transmetalation step in cross-coupling reactions starts with the transfer of the arylboronic acid onto the arylpalladium halide complex and follow by the dissociation of the halide, however the mechanism is not well-established to this day.[96,99,100] This step is aided by the addition of a base and common bases employ for this step includes hydroxides, carbonates, and phosphates of alkali metals (Na, K, Cs).[70,78] The presence of base is vital to the catalytic cycles as boronic acid does not react directly with the oxidative addition complex,[70] which sparks a discussion of two proposed mechanisms by Buchwald is shown in Scheme 5.[99] The first mechanism suggested that the arylboronic acid reacts with a base to form a nucleophilic borate that attacks the arylpalladium(II) halide complex causing the halide to leave, forming the transmetalation intermediate. [101–103]

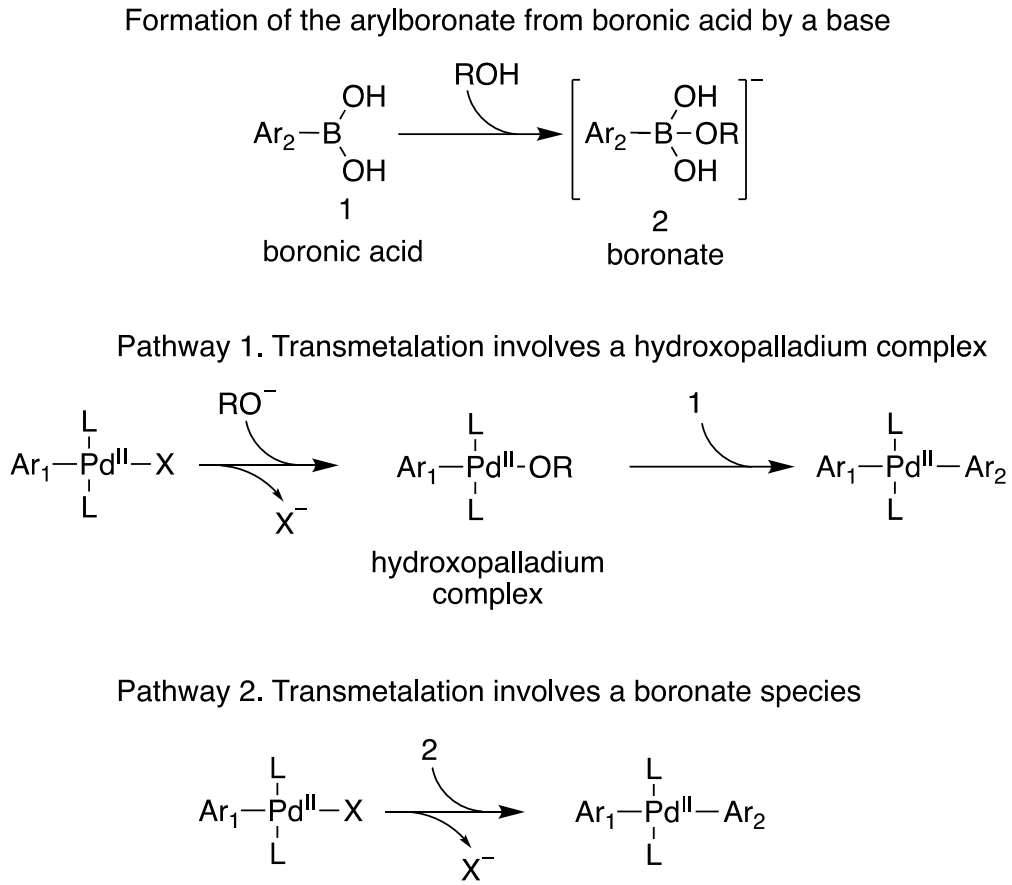

Scheme 5. Proposed transmetalation mechanisms is shown in two pathways, the first requires the formation of an hydroxopalladium complex and the other requires the activation of the boronate species.

The second proposed mechanism suggests that the base induces nucleophilic attack on the arylpalladium (II) halide complex rather than the boronic acid to make a hydroxopalladium(II) complex.[104] Then, this complex reacts with the arylboronic acid to form the transmetalation intermediate. The exact mechanism appears to be dependent on the reaction conditions and the starting materials and each mechanism involves multiple steps to generate a number of intermediates. This proposed mechanism is supported by the fact that the hydroxopalladium(II) complex intermediate is also observed using nuclear

magnetic resonance (NMR) by the Denmark group.[105] Transmetalation step typically is considered to be the turnover limiting step in palladium cross-coupling reaction but it can vary with oxidative addition depending on substrates and reaction conditions.[99]

Suzuki Polycondensation

The Suzuki polycondensation (SPC) is a reaction that was derived from the SMC and it took about ten years for the SPC to make its way to polymer synthesis by Gerhard Wegner at the Max Planck Institute in 1989.[106] Similar to the applications of SMC, the SPC is a broadly efficient reaction to make polyarylenes (PPP) and other conjugated polymers. Polymer is made up of many monomer units called repeating units. The length of a polymer is defined by the average number of monomer units link together in a polymer, degree of polymerization (D_p). Typical length of a polymer ranges from 100s – 1000s repeating units or 15,000 Dalton. Polymers with two to fifty repeating units are referred as oligomers.

Conjugated polymer made from SPC is regiospecific, has great functional group compatibility, and high molecular weights are observed under optimized conditions.[107–109] While it is used extensively in the pharmaceutical industry for the purpose of directly coupling aromatic units, its potential is seen best in the synthesis of organic light emitting diodes (OLEDs).[110–112] OLEDs are a recent display technology which are quickly taking over cell phones and electronic companies as the favoured components of screens. These screens contain an electron transport layer made up of organic polymers which are heavily conjugated to create inherent electronic properties.[113] This gives them the potential to be applied to electroluminescent devices due to the wide HOMO/LUMO gap.[114,115] When excited, the electrons will emit colours of red, green, and blue to create the overall expected

visual for the observer. Attractive features of OLEDs include higher contrast and resolution, and the flexibility into the making of curved displays.

SPC pathways: AA/BB and AB methods

The SPC can proceed via two approaches, the AA/BB method and the AB method (Scheme 6).[108,116–118] The AA/BB method is where two monomers with difunctional groups combine to make a polyarylene backbone. Each monomer will contain either two aryl boronic acids or derivatives or two aryl halides. Aryl bromides are the most commonly employed functional group counterparts in SPC, followed by iodo and triflates compounds unlike in SMC.[119] The alternative route is the AB method in which only requires one monomer unit that has both of the functional groups. Both methods are used in academia and industrial setting with attractive results.[106,113,117,120–124]

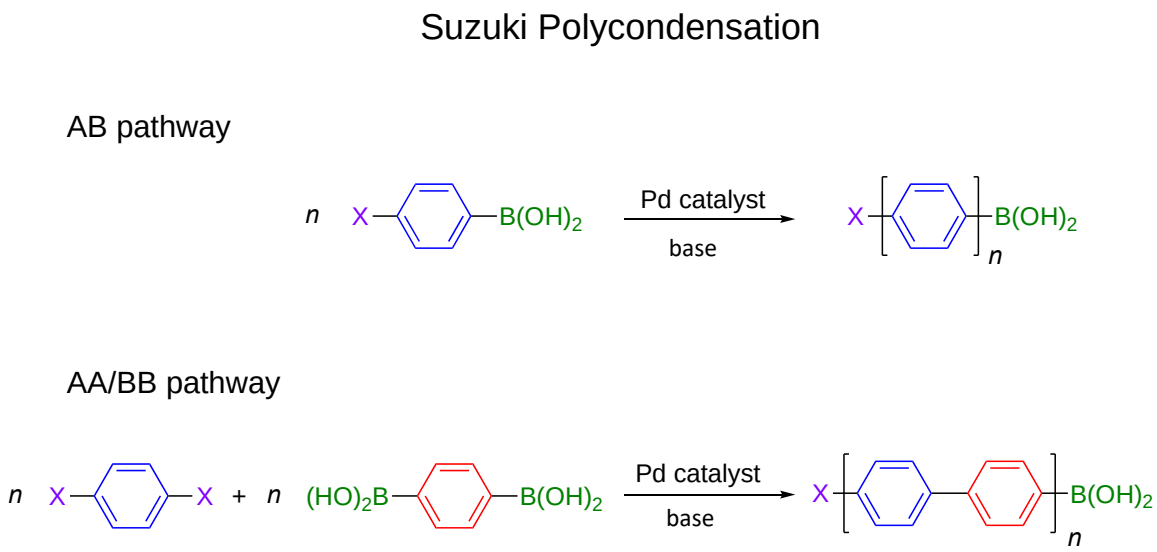

Scheme 6. Two approaches to Suzuki polycondensation for the AB and AA/BB pathway. X = halide, C_6H_4 rings are shown, but these could be other aromatic rings.

The AA/BB pathway can provide more structural variability than the AB pathway as the formation of the polymer is in an alternating fashion, and the AA/BB monomers are easy to synthesize because each monomers has the same functional group (Figure 2-9). Although the synthesis of AB monomers is often tedious due to its non-symmetric nature, the formation of the polycondensation polymer from the AB pathway can provide chain directionality that is not seen in the AA/BB pathway, i.e. the monomers are incorporated in a "head to tail" fashion, meaning every AB monomer can reaction with each other for form a polymer.[116] Unlike the AB pathway, the AA/BB monomers has the downside of lacking a built in 1:1 stoichiometric ratio which contributes to incomplete polymer conversion.[108,109] This exact stoichiometry is needed to obtain high molecular weight polymers. Both methods are susceptible to side reactions that are seen in SMC.

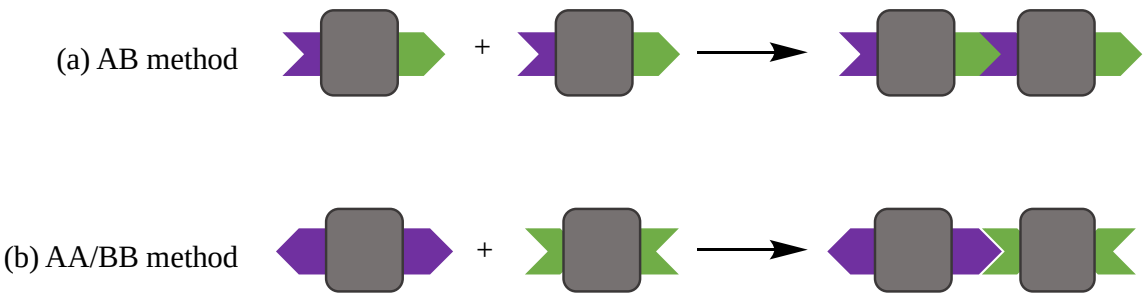

Figure 2-9. Illustration showing the difference in the product from the AB method and the AA/BB method.

The AB method in SPC is considered a step-growth polymerization based on the fact that it does not require an initiation and a termination step.[108,121,125] Additionally, a series of oligomers is observed and the molar masses continuously and consistently shift to higher values during the early stages of polymerization. This indicates that a dimer formed from

the first coupling reaction can re-enter the catalytic cycle to react with either another monomer, dimer or oligomers unlike in chain growth polymerization where the monomer is added onto the on-going chain. However, it has been proven that palladium can rest on π- systems and so for the AA/BB method, this may not be the case.[108] The palladium metal, stabilized by ligands, is capable of moving from the last reaction site and across the newly added terminal aromatic unit, to add oxidatively into its carbon-halogen bond to begin the next cycle of the catalysis. All of this happens without the palladium ever leaving the polymer. This would mean that the mechanism would be chain growth rather than step growth and that the two methods would polymerize in different ways.[126,127]

Side Reactions in SPC and SMC

Side reactions or off-cycle reactions in SMC do not only affect the product yield but also plague the polymer conversion that is reflected in the molecular weight in SPC.[108,109,123] Figure 2-10 illustrates the common side reactions of SMC, protodeboronation is a well-documented problem in which the carbon-boron bond is replaced by a carbon-hydrogen bond from a proton source, often water.[128–130] Boronic acids can be substituted with boronate esters as they are less susceptible to protodeboronation.

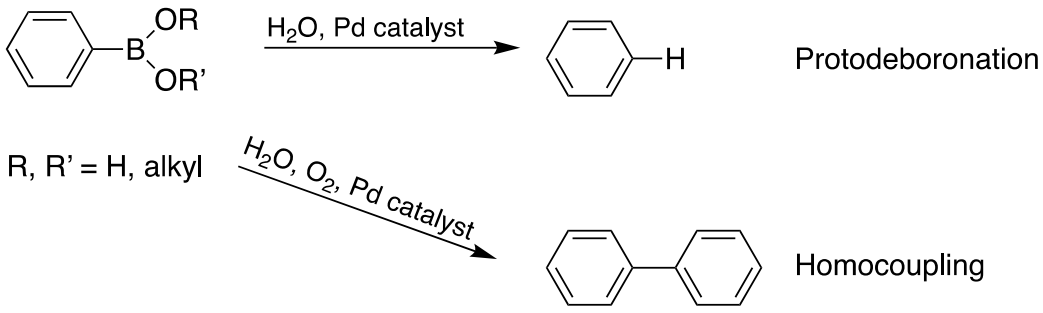

Figure 2-10. Protodeboronation and homocoupling of aryl boronic acid.

Homocoupling of arylboronic acid is usually a result of the presence of oxygen in the reaction, and the process is accelerated in the presence of water.[96,120] The formation of homocoupling product is often negligible and can be avoided by vigorous purging of air and the use of a degassed solvent. Another competing side reaction is the hydrodehalogenation of the aryl halide,[96,107] which the carbon-halide bond is replaced by a carbon-hydrogen bond, not only decreases product yield but also synthesizes unwanted side products. Alkyl halides or secondary alcohols can also participate in B-hydrogen elimination after the oxidative addition step to lower final product yield. In general, these are not worried about as they are minor contributors and can be easily removed from the desired products.

With Suzuki polycondensation, these side reactions impose defects in the polymer chain and its optical and electronic properties as a result of the loss of the terminal functional group which defeats the possibility of further polymerization. Ligand scrambling is a notable intramolecular side reaction in palladium cross-coupling reaction where phosphine ligand is employed (Scheme 7).[107,108] Instead of forming the bifunctional aryl product from the reductive elimination step, the phosphine ligand on the aryl halide palladium(II) intermediate ($ArPdL_nI$) can participate in the aryl-aryl coupling to generate phosphine

bound aryl byproducts. Aside from the first phosphine scrambling a second phosphine scrambling can occur where two phosphine ligands are participating in the exchange which leads to a phosphine-incorporated polymer chain.

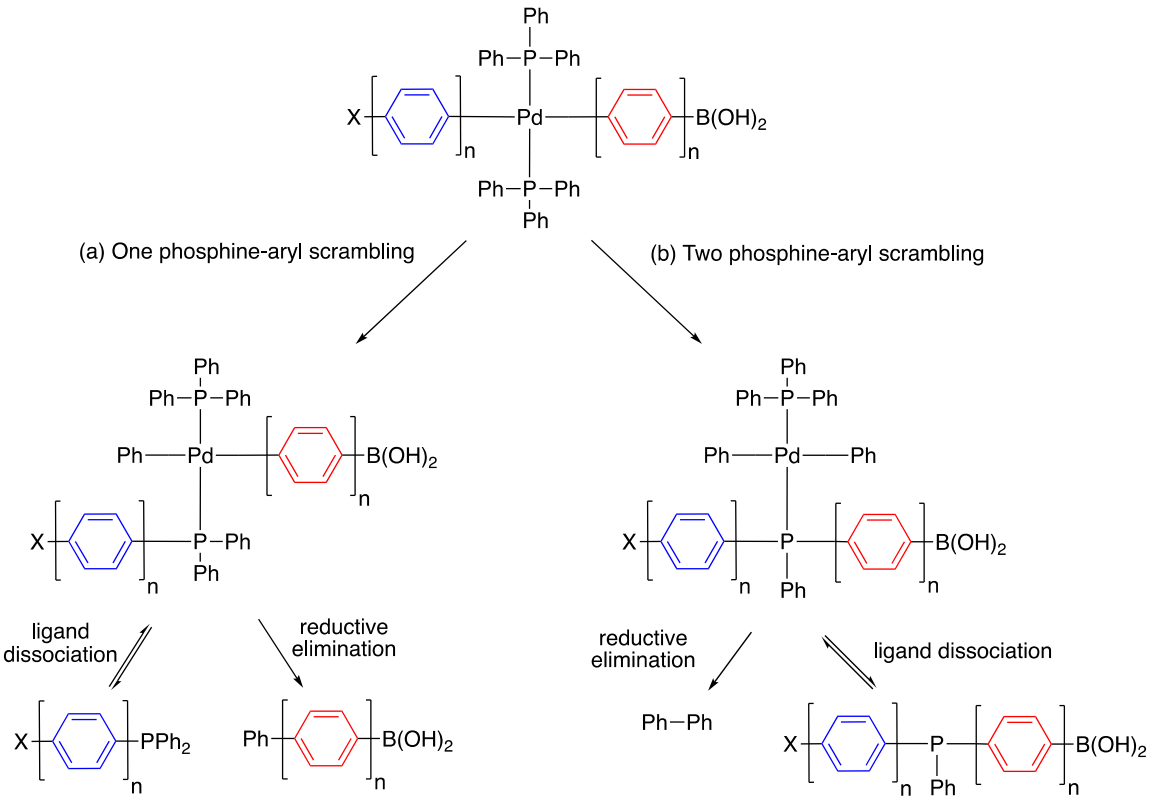

Scheme 7. Proposed aryl phosphine scrambling pathway.

According to the Novak group, the phosphine aryl scrambling of the Pd-complex is observable through hydrogen and phosphorous NMR when a triphenylphosphine-base catalyst is employed in the synthesis but the results were inconclusive due to the overlapping region of the starting material and the product.[131–133] The mechanism of this side reaction is not well understood but it is important to optimize reaction conditions to avoid the formation of these phosphorous-incorporated polymer. Because the problem is the involvement of the triarylphosphine ligand, effective solutions include switching to a

phosphine-free catalyst system, e.g. $Pd(OAc)_2$ or to use bulkier ligands such as P(*o*-tolyl)$_3$ and PCy_3.[134,135]

Aim of the Project

Mechanistic interest in the reaction stems from the importance of side reactions becoming magnified by their effect on polymer chain length and identity of end groups. Methods for analyzing the products of the Suzuki polycondensation are well-developed, as they are amenable to all the tools of the polymer chemist. However, following the reaction on a molecular level is hard, because the growing polymer chain repeatedly interacts with the metal catalyst, making the identity of the intermediates and resting states in the reaction change with every turnover.[53]

The SPC mechanism follows closely to the SMC catalytic cycle, which starts with the oxidative addition of the aryl halide Ar–X, to the palladium(0) catalyst to form an aryl palladium(II) halide complex Ar_1–Pd–X. Transmetalation occurs between the aryl boronic acid Ar_2–$B(OH)_2$ and the Ar_1–Pd–X complex in the presence of a base to form an Ar_1–Pd(II) –Ar_2 intermediate, then followed by reductive elimination where the two aryl units leave the intermediate to form product Ar_1–Ar_2 and the palladium catalyst is regenerated in the catalytic cycle. In the case of SPC, the biaryl reductive elimination product can re-enter the catalytic cycle as additional monomers are added to the reaction to generate a conjugated polymer.

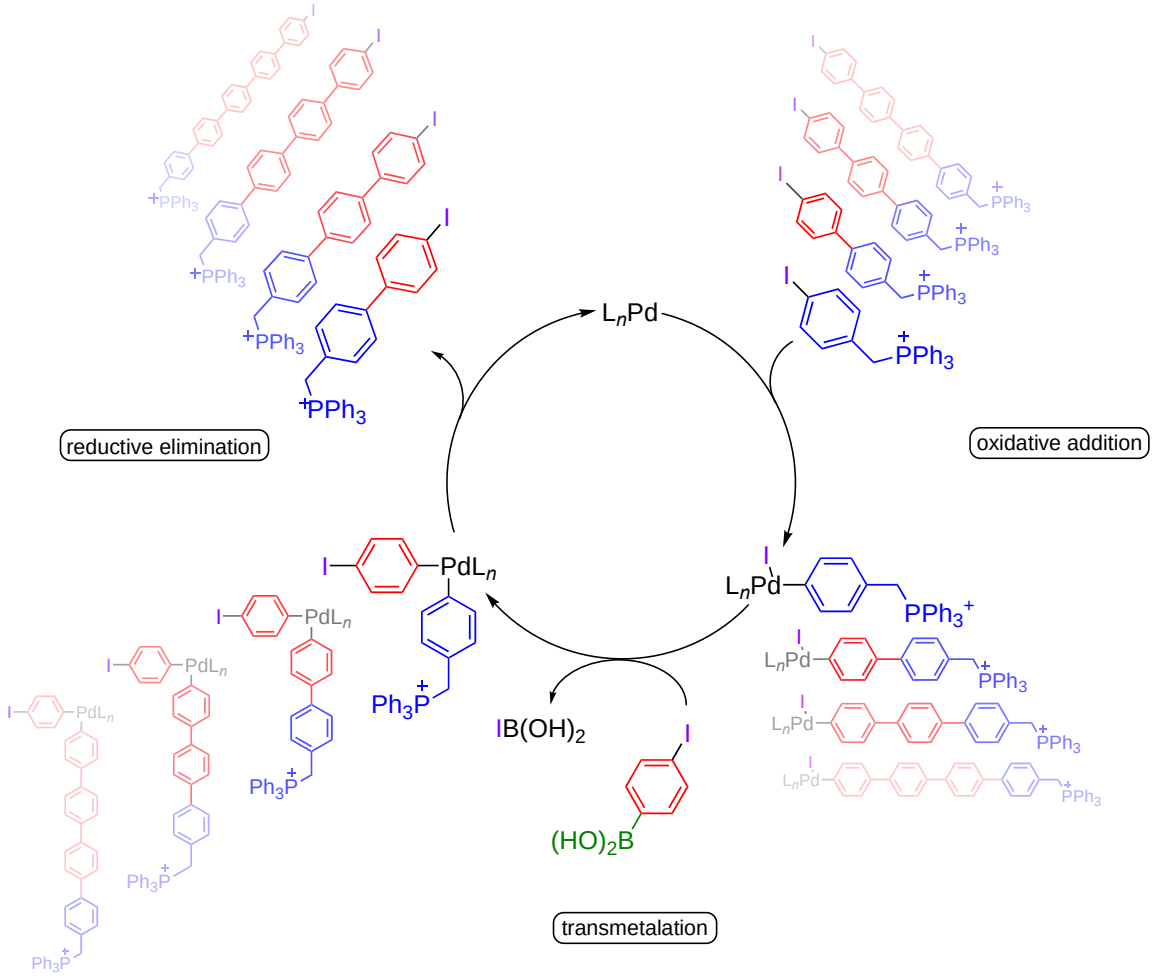

Scheme 8. Proposed SPC catalytic cycle where L = PPh_3, a phosphonium charged iodide tag, and an AB-type monomer *p*-iodophenylboronic acid were employed.

We have previously used real-time mass spectrometric methods to study the SMC and related transformations.[32,36,37,39,136–138] This work aimed to develop a stepwise tandem mass spectrometry strategy to study short-lived catalytic intermediates and make reaction monitoring more efficient and practical. Therefore, we chose to monitor the SPC reaction using simple reagents. Mass spectrometry has been proven to be an effective technique to study multi-components reaction which makes Suzuki polycondensation an excellent reaction candidate because the catalytic cycle involves some many reactive species and

side reaction byproducts. Although mass spectrometry is famously fast and extremely sensitive, studying the SPC poses challenges: no two products or intermediates have the same molecular weight, and so whatever ion intensity one has to deal with at the start of the reaction is dispersed across many new ions over the course of the reaction. Given the complexity of the reaction, a thorough understanding of mass spectrometry instrumentation is critical to developing a strategy that can differentiate reaction species and study reaction dynamics.

Method Development

Our standard method of analysis involves transporting a solution from the reaction flask using PSI-ESI-MS to monitor reaction progress continuously. Since ESI-MS can observe only ions, not neutrals, the entities of interest need to carry a charge (inherent, or appended synthetically in a location that does not affect the chemistry under investigation). So far, we have applied the technique using a hybrid quadrupole-time of flight instrument, which can operate in one of two modes: TOF-only MS mode, or an MS/MS mode wherein a particular ion is selected in the quadrupole and fragmented by CID in a collision cell filled with argon. We aim to explore the Suzuki polycondensation reaction using other instrument configurations exist with different capabilities, and the scan modes that a triple quadrupole mass spectrometer offers is up for the challenge.

Chapter 3 Results and Discussion

For easy reference, SPC catalytic species are labelled as $\mathbf{1_n}$ for aryl iodide species $[Ph_3PCH_2C_6H_4(C_6H_4)_nI]^+$, $\mathbf{2_n}$ for palladium-containing intermediates $[Ph_3PCH_2C_6H_4(C_6H_4)_n–Pd–(PPh_3)_2(I)]^+$ or $[Ph_3PCH_2C_6H_4–Pd–(PPh_3)_2(C_6H_4\ I)_n]^+$, and $\mathbf{3_n}$ for capped aryl oligomers $[Ph_3PCH_2C_6H_4(C_6H_4)_n]^+$. We will refer the charged phosphonium aryl group, $(Ph_3P^+CH_2C_6H_4–)$ from $\mathbf{1_0}$ as Ar^+ in the section of Tandem Mass Spectrometry Experiments.

Table 1. Numbering system of catalytic species in SPC and the *m/z* ratio of each species.

Species #	n	Species	*m/z*
$\mathbf{1_n}$	0	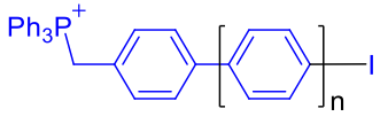	479
	1		555
	2		631
	3		707
	4		783
	5		859
	6		935
$\mathbf{2_n}$	0	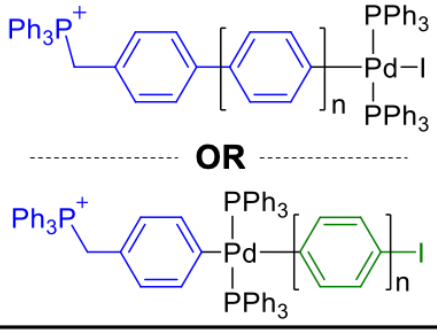	1109
	1		1185
	2		1261
	3		1337
	4		1413
	5		1489
	6		1565
$\mathbf{3_n}$	0	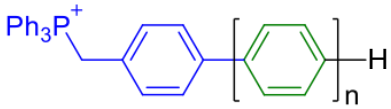	429
	1		506
	2		583
	3		660
	4		737
	5		814
	6		890

Initial Experiments: Suzuki polycondensation Monitoring in Full Scan

Applying the full scan mode to the SPC, we used conditions analogous to those we previously employed to examine the SMC reaction,[65,136] but instead of using a simple boronic acid as a cross-coupling partner, we used an AB-type monomer *p*-iodophenylboronic acid, $IC_6H_4B(OH)_2$, tetrakistriphenylphosphine palladium(0) catalyst, $Pd(PPh_3)$ and a capping agent phenylboronic acid, $PhB(OH)_2$. We tracked the reaction using PSI-ESI-MS in the positive ion mode, methanol and caesium carbonate were pre-mixed in the PSI flask sealed with a rubber septum and warm in an oil bath at 40 ℃. Reagents were added into the in the following order: charge-tagged aryl phosphonium iodide $\mathbf{1_0}$, $Pd(PPh_3)_4$ catalyst, the AB monomer, and the end-capping agent. Data was collected for 80 minutes.

All traces are normalized to the total ion current (TIC) presented in a chronogram in Figure 3-11. At 0 minutes, $\mathbf{1_0}$ was observed and the $Pd(PPh_3)_4$ catalyst was added to the solution at 2 minutes causing a decrease in the intensity of $\mathbf{1_0}$, accompanied by an increase in intensity of $\mathbf{2_0}$. When the AB monomer substrate was added at 20 minutes, a decrease in intensity of $\mathbf{2_0}$, was observed and species corresponding to $\mathbf{1_{1\text{-}6}}$ and $\mathbf{2_{2\text{-}4}}$ appeared sequentially, indicating that reaction turnover had occurred. Little change to the speciation occurred after the 40 minutes' mark, and a capping agent, $PhB(OH)_2$, was added at 44 minutes and $\mathbf{3_{0\text{-}4}}$ were observed.

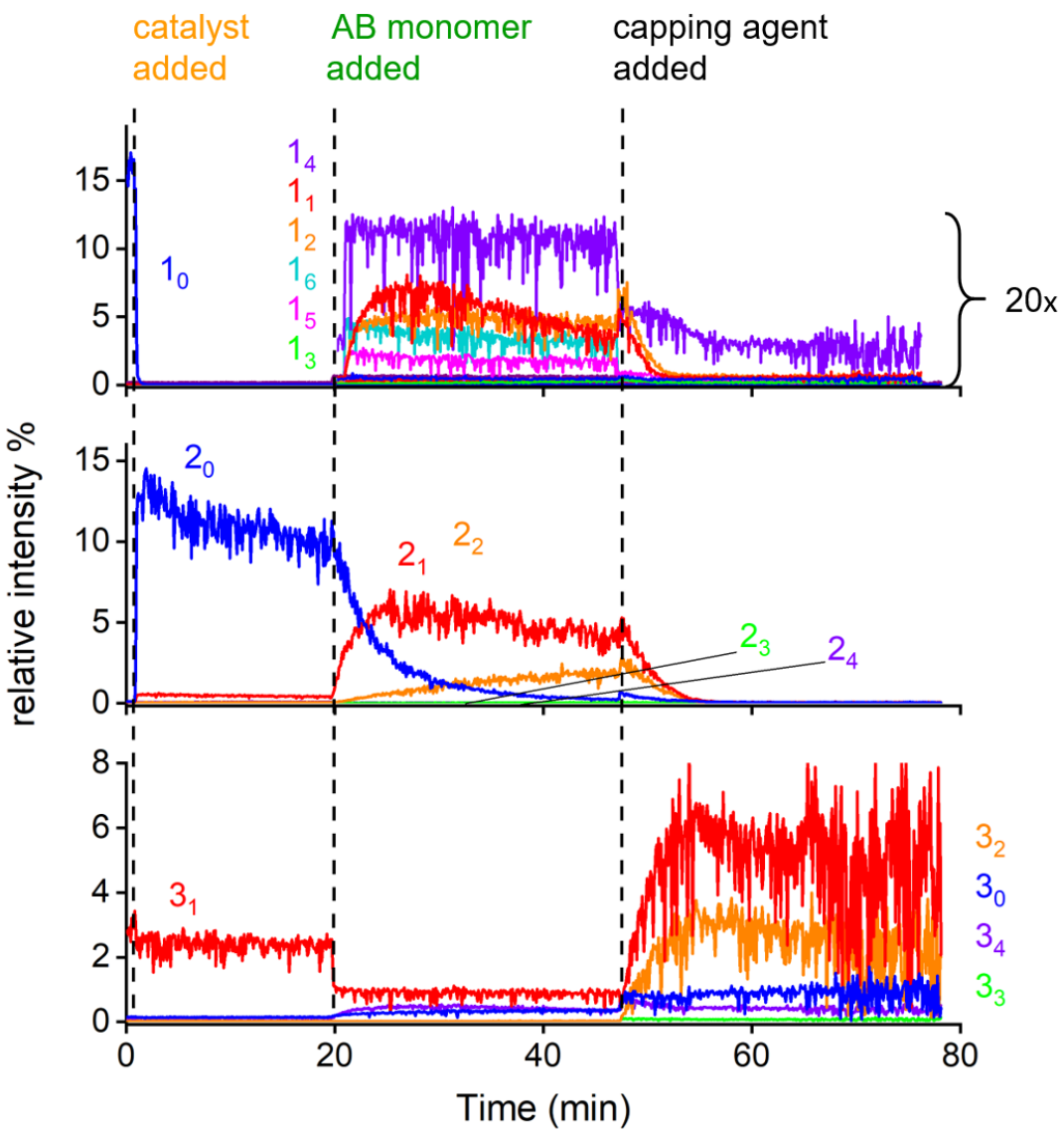

Figure 3-11 The normalized PSI-ESI-MS full scan chronogram of the SPC. Aryl iodide species are label as 1_n, intermediates as 2_n, and capped oligomer products as 3_n (n = 1– 6). The $Pd(PPh_3)_4$ catalyst, AB monomer *p*-$(OH)_2BC_6H_4I$ and the end-capping agent $PhB(OH)_2$ was added to the reaction solution at 2 minutes, 20 minutes, and 44 minutes indicated with dotted lines.

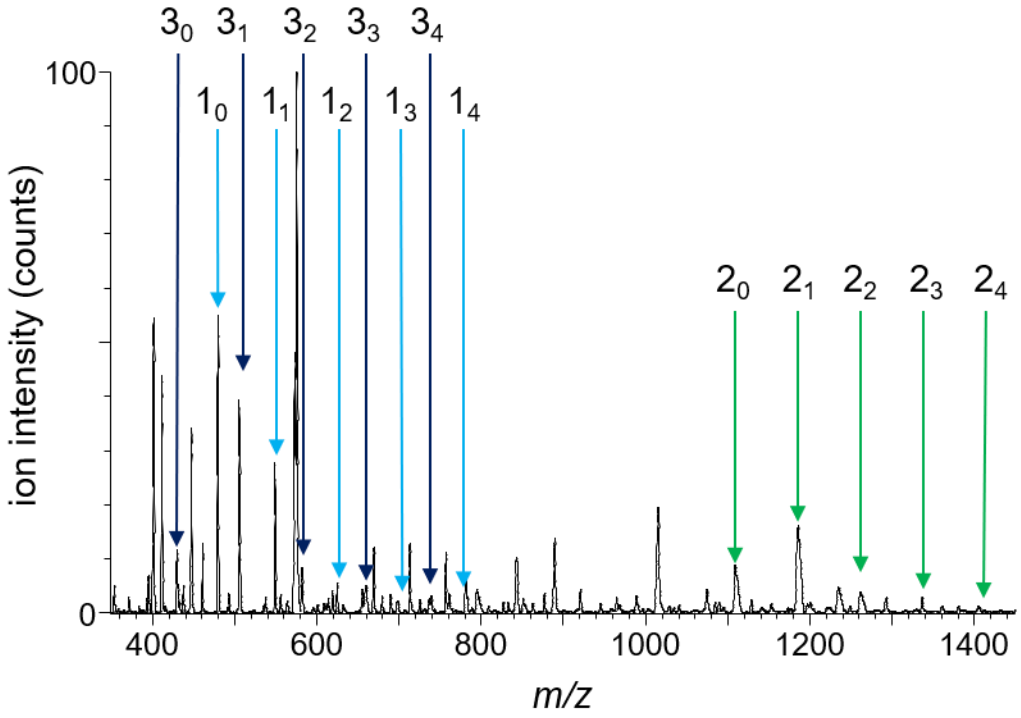

Figure 3-12. The summed ESI mass spectrum for the SPC species 1_n, 2_n, and 3_n (n = 0 – 4) in methanol in the presence of $Pd(PPh_3)_4$ and Cs_2CO_3. The end-capping reagent $PhB(OH)_2$ was added late in the reaction.

The reaction profile (Figure 3-12) showed evidence of the reaction we were trying to study but the data were also badly flawed. We had hope to observe up to (12 × 3 =) 36 species from the SPC since we used 12 mole equivalents of the AB monomer but only observe species up to n = 6 in the summed mass spectrum and the rest (n > 6) are lost in the baseline. SMC and SPC reactions typically take hours or overnight to react and that the concentration of the reaction used in this reaction was in the micromolar range. The SPC shown in Figure 3-12 and 3-13 may not have turned over as many times as it could have in

80 minutes. The aryl iodide series $\mathbf{1_{1\text{-}6}}$ were multiplied by a factor of 20. Since $\mathbf{1_{1\text{-}6}}$ was observed for the oxidative addition species $[Ph_3PCH_2(C_6H_4)_nI]^+$, we expected the same for the Pd-containing intermediates $[(Ph_3P)_2Pd\{Ph_3PCH_2(C_6H_4)_nI\}]^+$, $\mathbf{2_{1\text{-}6}}$ and the capped oligomers $[Ph_3PCH_2(C_6H_4)_n]^+$, $\mathbf{3_{1\text{-}6}}$. Some species appeared to be present before it was physically possible for them to be there as the corresponding reagent was not inject into the reaction mixture until later on in the reaction time. This phenomenon is observed in Figure 3-11, where $\mathbf{2_{1\text{-}2}}$ showed a low intensity before the AB monomer was added and is more prominent where $\mathbf{3_1}$ appeared at the beginning of the reaction at 0 minutes. It was speculated such behavior was due to the presence of conflating species and contaminants with the same *m/z* as the catalytic species of interest. However, some species were not observed at all, $\mathbf{2_{5\text{-}6}}$ and $\mathbf{3_{5\text{-}6}}$ could be seen in the summed spectrum but were insufficiently abundant to show up in the chronogram. It is noted that there are a number of unassigned mass peaks in the mass spectrum, which are likely to be caesium carbonate aggregates, species formed from methanolysis and contaminants from the septa when reagents were injected into the reaction mixture.[139]

Overall, signal-to-noise ratio was a problem but additionally, there were all manner of complications arising from the overlap of signals, such that chemically nonsensical results were obtained. Nonetheless, the preliminary results were encouraging. It was clear that the chemistry could be studied despite the fact the key intermediate changed in *m/z* with every turnover, as did the *m/z* of the product but the methodology needed improvement.

Selected Ion Recording Experiments

With the known target species in hand, we could start applying different methods to get more reliable, selective and sensitive chronograms of the catalytic reaction. The first method we tried was selected ion recording (SIR), an approach that can be employed by any scanning MS instrument. Instead of scanning the entire mass range, only the ions of interest are targeted. The most intense peak of a particular isotope envelope can be selected (or the most intense one unaffected by overlap with another species), and the amount of time each species is dwelled upon can be customized. The *m/z* ratio of each catalytic species was calculated and input into the mass spectrometer. The dwell time of the Pd-containing species was set to be longer than that of the aryl iodide and oligomeric product species to increase the S:N ratio. The mole ratio of the AB monomer was adjusted to 6 mole instead of 12 mole equivalent since species with $n > 5$ were not observed and it was noted that the TIC of the SIR was lower by a magnitude of 10^3 compared to the TIC of the full scan experiment. All other reaction conditions and mass spectrometer settings remained the same in order to compare results with the full scan chronogram. The mass spectrum of SIR experiment does not show the isotopic pattern but selected mass peak(s) and their intensity (Figure 3-13).

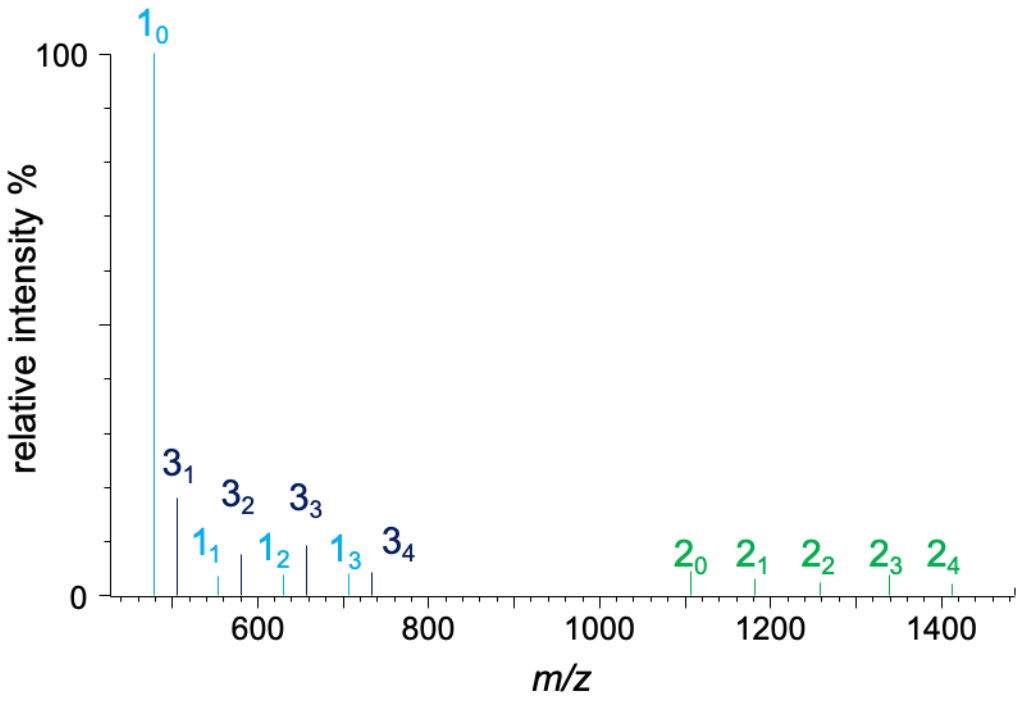

Figure 3-13. The summed SIR mass spectrum with labelled aryl iodide species as 1_n, intermediates as 2_n and capped oligomer products as 3_n where $n = 0 - 4$).

The normalized chronogram of each set of species is shown in Figure 3-14. At 0 minutes, **1₀** was observed and its intensity decreases around the same time of the appearance of **2₀** upon catalyst addition at 5 minutes. At 14 minutes, AB monomer was added and the intensity of **2₀** decreases which correspond with the increase of **1₁-₃** and **2₁-₄**. At 57 minutes, the capping agent was added and **3₀-₄** were observed. The SIR chronogram showed significant improvements in the traces of all species and appeared visually intelligible. A lower multiplier of 7× was used on species **1₁-₃** instead of a multiplier of 20× in the full scan chromatogram and is likely due to the fact that SIR does not scan the full mass range but only the targeted ion interest. Low intensity species observed in a full scan chromatogram can be amplified in an SIR chromatogram by adjustment of the dwell time. Upon AB monomer addition, **2₁-₄** species showed a significant increase in relative intensity

and decrease when the capping agent was added to the reaction mixture in Figure 3-14. Why the Pd-containing species $\mathbf{2_n}$ behave better than the aryl iodides $\mathbf{1_n}$ in this respect may be to do with their relative *m/z* values – low mass ions are more likely to experience adventitious overlap than higher mass ions. Aside from the $\mathbf{2_n}$ intermediates, we were also able to observe the capped oligomers $\mathbf{3_{0\text{-}4}}$ when the capping agent was added at 57 minutes (they were of very low intensity in the full scan chromatogram). However, their behavior is clearly non-physical: they seem to appear long before the capping reagent itself is added and this is also observed in the $\mathbf{2_n}$ species prior to AB monomer addition. How can we differentiate when a trace is coming from background noise or overlapping species or part of the catalytic cycle?

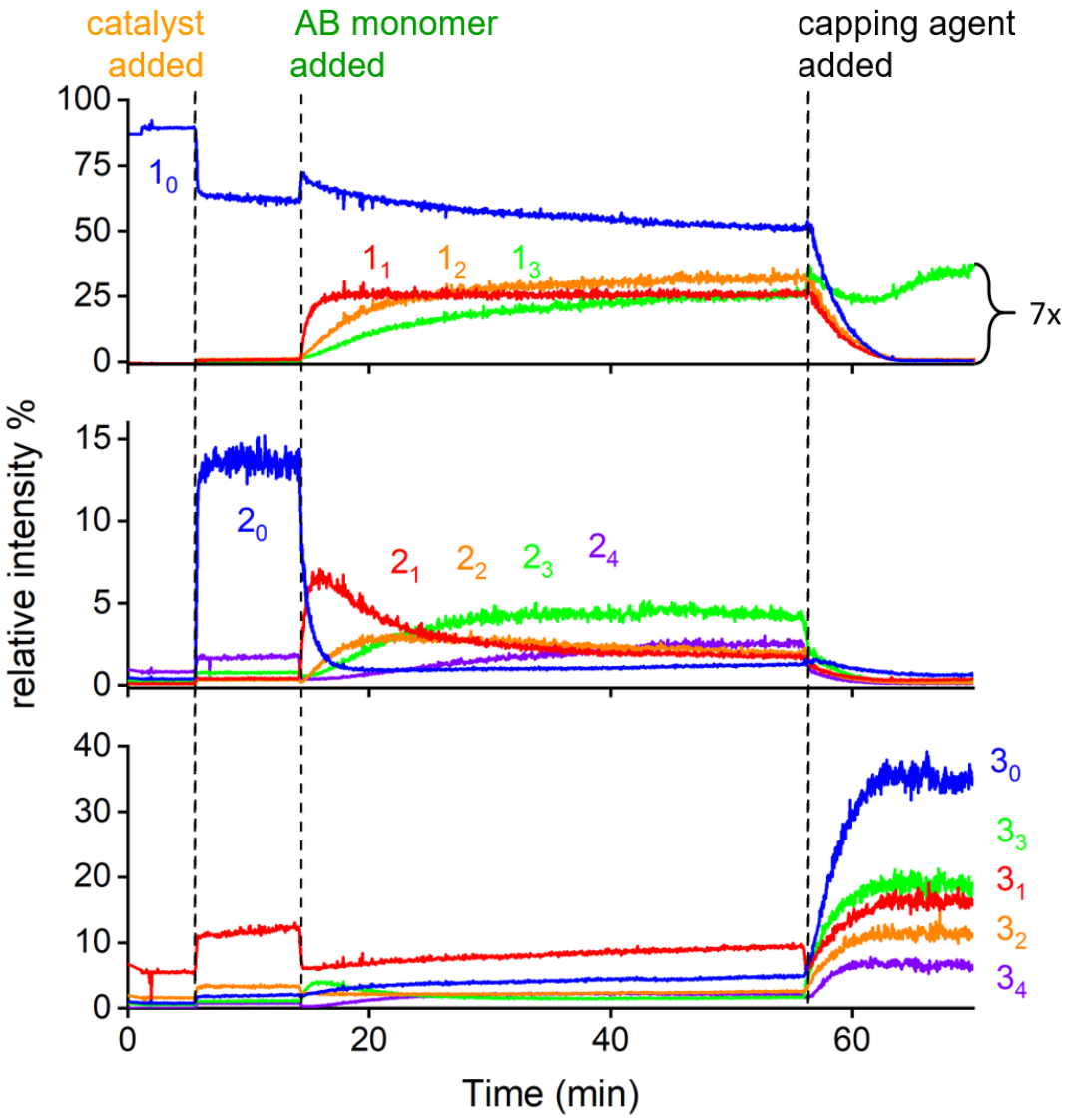

Figure 3-14. Normalized ESI-MS SIR chronogram of the SPC showing the relative intensity of aryl iodide species label as 1_n, intermediates as 2_n, and the new end-capped oligomer products as 3_n (n = 0 – 4). The $Pd(PPh_3)_4$ catalyst, AB monomer *p*-$(OH)_2BC_6H_4I$, and the end-capping agent $C_6H_4B(OH)_2$ was added to the reaction solution at 5 minutes, 14 minutes, and 57 minutes indicated in dotted lines respectively.

Tandem Mass Spectrometric Experiments: Product Ion Scan

We then turned to MS/MS methods. Product ion scan is the most common MS/MS experiment to study the fragments of an ion of interest. A precursor ion is selected in the MS1 and undergoes collision-induced dissociation to produce a product ion, and a neutral fragment and the product ion is detected in MS2. Product ion scans were performed on $\mathbf{1}_{0\text{-}4}$, $\mathbf{2}_{0\text{-}4}$, and $\mathbf{3}_{0\text{-}4}$ and revealed that all ions under study decompose in the gas phase under CID conditions to lose triphenylphosphine (PPh_3), an L-type ligand. L-type ligands tend to dissociate first because they are stable as free entities, while X-type ligands take more energy for dissociation since it involves the formation of a radical.[37,39,44,136] A change in isotope between separate product ions will also indicate when a particular atom has been fragmented from the precursor ion. In Figure 3-15 and 3-16, $\mathbf{1}_{0\text{-}4}$ and $\mathbf{3}_{0\text{-}4}$ showed a constant loss of 262 Da, which corresponded to the mass of a PPh_3 ligand. The product ion scan of $\mathbf{2}_{0\text{-}3}$ displayed a more complex fragmentation pattern than $\mathbf{1}_n$ and $\mathbf{3}_n$. We were able to observe this consistent fragmentation pattern in species that partook in the catalytic cycle up to $n = 4$ using real time reaction monitoring with the PSI method and optimized the collision energy to maximize the abundance of the product ions.

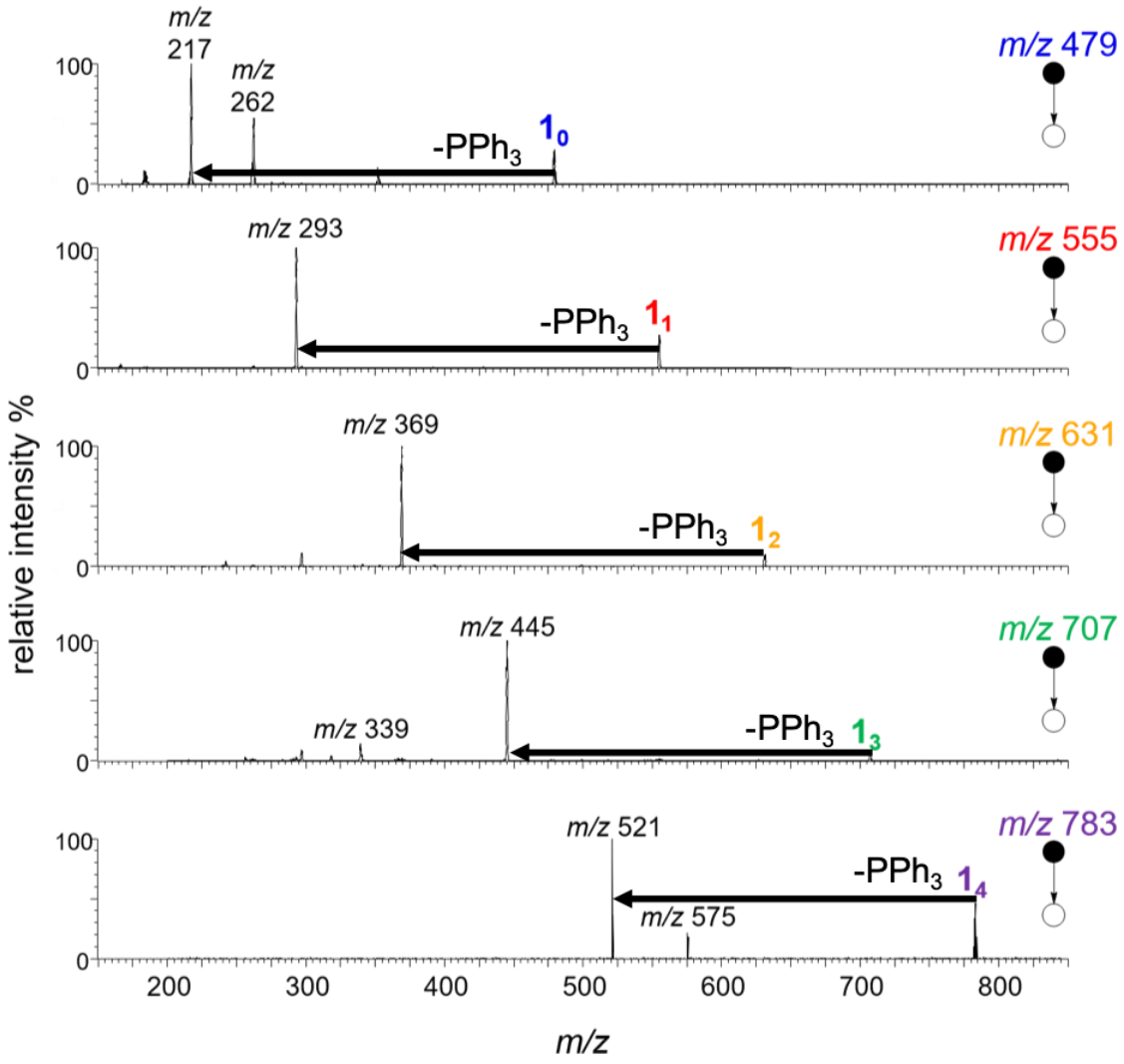

Figure 3-15. CID spectra of the aryl iodide species $1_{0\text{-}4}$ labelled as the precursor ion. The major fragmented ions were shown in the form of $[H_2CC_6H_4Ar_nI]^+$ and were indicated with a dotted arrow showing the fragment as triphenylphosphine (PPh_3).

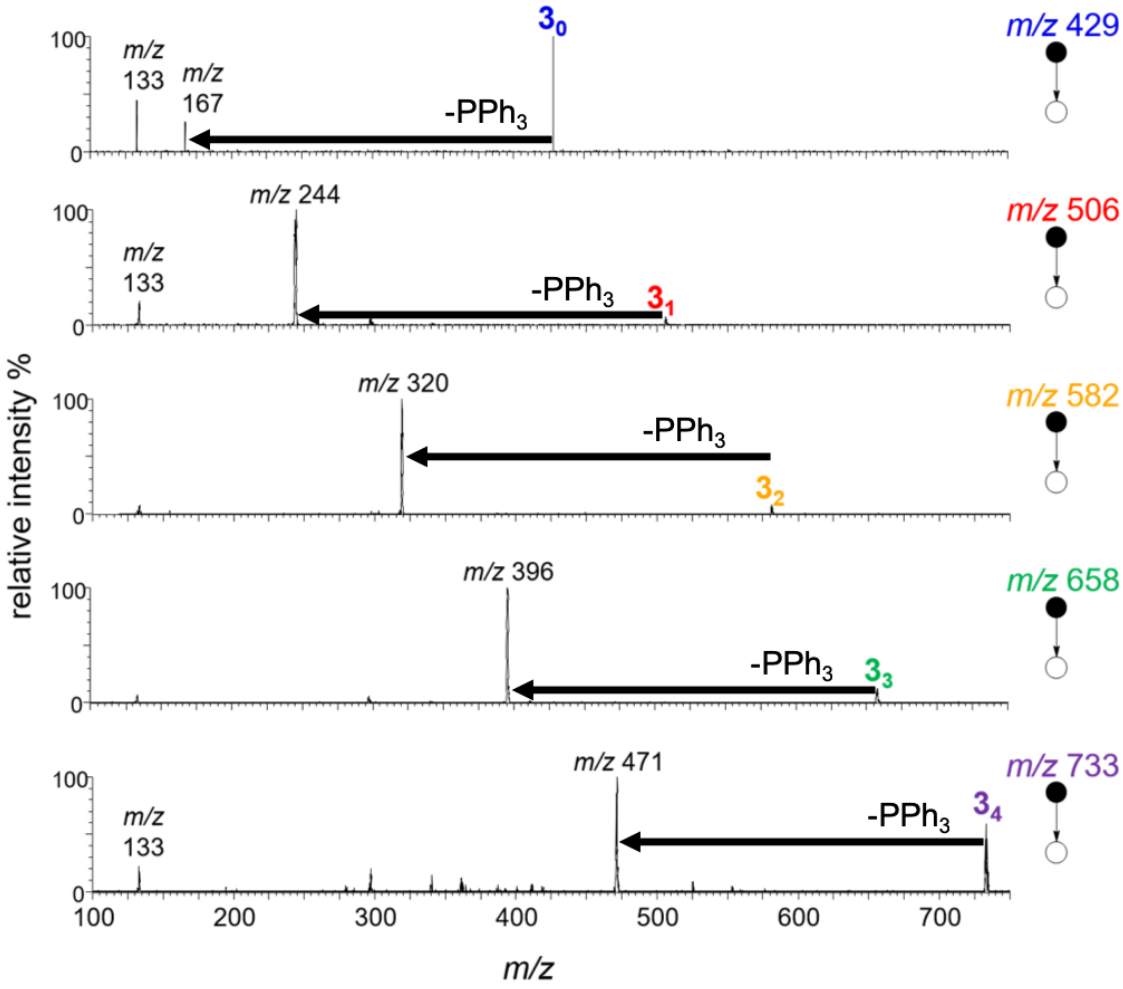

Figure 3-16. CID spectra of the capped oligomer products $3_{0\text{-}4}$ labelled as the precursor ion. The major fragmented ions were shown in the form of $[H_2CAr_nC_6H_5]^+$ and were indicated with a dotted arrow showing the fragment as triphenylphosphine (PPh_3).

The mechanisms of PPh_3 loss are probably different in each case; the aryl iodides, $\mathbf{1_n}$ and capped aryl oligomers, $\mathbf{3_n}$ by the elimination of PPh3 from the charged tag and the Pd intermediates $\mathbf{2_n}$ by the loss of PPh_3 ligands from the catalyst. This suspicion is borne out by the relative energies at which each occurs (Figure 3-17 to 3-21) and the number of signals in the spectra. The collision energy required for $\mathbf{2_n}$ series ranges from 15 – 20 V, lower than required for $\mathbf{1_1}$ and $\mathbf{3_1}$ (30 – 35 V). It appears that the $\mathbf{1_n}$ and $\mathbf{3_n}$ species showed one major signal in each CID spectrum which is a firm indication of a single reaction pathway. Unlike the results of the $\mathbf{1_n}$ and $\mathbf{3_n}$ species, each $\mathbf{2_n}$ species spectrum exhibited multiple signals indicating more than one fragmentation pathway may be at work.

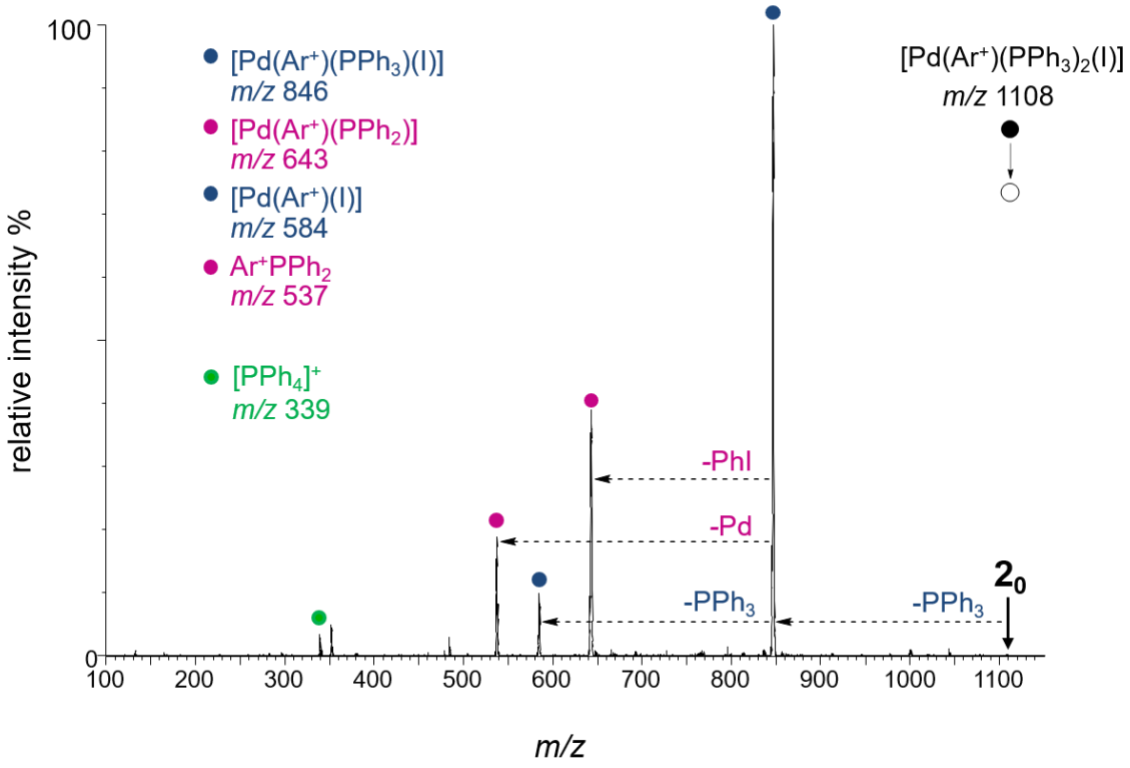

Figure 3-17 CID spectrum of 2_0 showing the fragmentation pattern and $Ar^+ = Ph_3P^+CH_2C_6H_4$.

In Figure 3-17, the CID spectrum of the product ion scan of $\mathbf{2_0}$ displayed multiple fragments upon CID at 15 V. The most prominent peak at *m/z* 846 corresponded to the loss of one PPh_3 and was assigned as $[Pd(Ar^+)(PPh_3)(I)]^+$. A weaker signal at *m/z* 584 was shown to have lost two PPh_3. Product ions involving 262 Da loss are labelled with blue dots. We also observed species that are highlighted with pink dots to indicate that $\mathbf{2_0}$ has undergone phosphine scrambling pathway. Ions at *m/z* 643 and m/s 537 were assigned as $[Pd(Ar^+)(PPh_2)]$ and Ar^+PPh_2, having lost an iodobenzene and a palladium from $[Pd(Ar^+)(PPh_3)(I)]$. Phosphine scrambling is a notable side reaction in palladium-cross coupling reaction as mentioned in Chapter 2. We found products that may have arisen from phosphine scrambling and further investigated this phenomenon with $\mathbf{2_{1\text{-}3}}$.

Phosphine Scrambling

Recalling the results from the full scan and the SIR chromatograms, the appearance and disappearance of $\mathbf{2_0}$ followed a sequential order. The appearance of $\mathbf{1_1}$ and $\mathbf{2_1}$ after AB monomer addition indicates that the 1st catalytic cycle has turned-over. It would be straight-forward to refer to the $\mathbf{2_1}$ species as transmetalation intermediates, but we found the results of the product ion MS/MS studies of $\mathbf{2_{1\text{-}3}}$ do not support this claim. Further analysis of the catalytic cycle (Scheme 8 in Chapter 2) shows that the transmetalation intermediate $\mathbf{2_0}$ from the first cycle has the same *m/z* as the oxidative addition product in the second cycle.

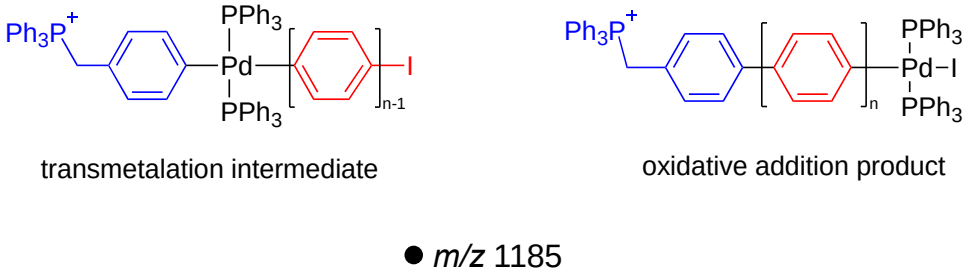

Figure 3-18. Proposed structures of $[Pd(PPh_3)_2(Ar^+)(C_6H_4)_n(I)]$ with *m/z* 1185 where $n = 1$. (Pd^{II} complexes are usually square planar but stereochemistry is omitted in this figure as ESI-MS cannot distinguish trans vs cis isomers).

MS/MS experiments should be able to distinguish the two proposed structures as shown in Figure 3-18. If the transmetalation intermediate is the assignment, we expect to see the formation of the reductive elimination product under CID conditions. However, the results appeared to be interfered with by phosphine scrambling. A proposed phosphine scrambling pathway was summarized in Scheme 9, both possible structures were considered to interpret the MS/MS spectrum of $\mathbf{2_1}$. In the case of the oxidative addition species, it first loses a PPh_3 fragment then the aryl group with a charged phosphonium can swap with a phenyl group on the remaining PPh_3 that is attached to the Pd. This aryl interchanged product may further reductively eliminate to form an iodobenzene product (*m/z* 203) and a Pd-bound phosphine (*m/z* 719). The transmetalation species would have a similar pathway as the oxidative addition species but will lead to different products formation. The swapping takes place on the aryl iodide that bounds to the Pd with the phenyl group of the PPh_3 and reductively eliminate a charged phosphonium aryl product (*m/z* 429) and a $Pd(PPh_2C_6H_5I)$. Since ESI-MS can only detect charged speciation, iodobenzene and $Pd(PPh_2C_6H_5I)$ cannot be observed (labelled with * in Scheme 9).

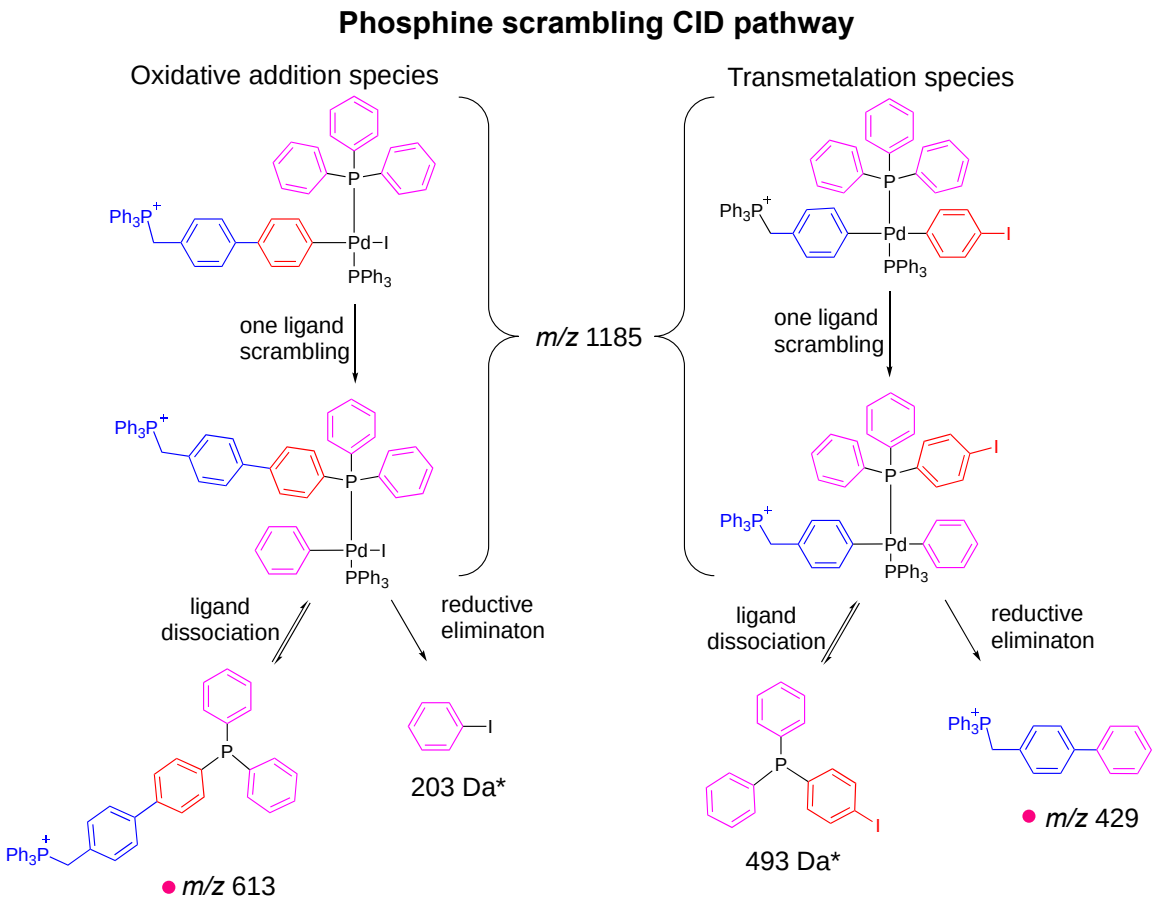

Scheme 9. Comparison of the proposed aryl-phosphine scrambling mechanism as the oxidative addition species and the transmetalation species.

In Figure 3-19, the product ion scan of $\mathbf{2_1}$ showed a prominent peak at *m/z* 922 and was assigned to $[Pd(Ar^+)(C_6H_4)(PPh_3)I]$ as it lost a PPh_3 fragment. This signal could either come from the oxidative addition species or transmetalation species as it is isomers of each other (See Scheme 9). A weaker signal at *m/z* 719 was assigned to $[Pd\{(Ar^+C_6H_4)P(Ph_2)\}]$ as it showed a loss of iodobenzene and a further loss of palladium (106 Da) at *m/z* 613 as $Ar^+(C_6H_4)I$. This observation suggests that *m/z* 1185 is most likely the oxidative addition species and is consistent with the MS/MS results of $\mathbf{2_0}$. We also noticed a new peak appeared with a weaker signal at *m/z* 429 and was assigned as $Ar^+(C_6H_4)$. This peak

corresponded to a loss of [PdP(Ph_2)(C_6H_4I)] of the phosphine scrambling from the transmetalation species. Another peak at *m/z* 555 was assigned to Ar^+(C_6H_4)I, which corresponds to the aryl iodide species $\mathbf{1_1}$ that can only be explained by the reductive elimination of $\mathbf{2_1}$ to the aryl iodide species $\mathbf{1_1}$ under CID conditions. These two observations would suggest that if *m/z* 1185 is the transmetalation species, it can participate in the phosphine scrambling pathway and the reductive elimination. Piecing all these fragmentation patterns together, the assignment of $\mathbf{2_1}$ is likely to be a combination of the oxidative addition species from the second catalytic cycle and at least a small amount of the transmetalation species from the first catalytic cycle. Other MS/MS experiment examples in which a reductive elimination pathway is possible to include the copper-free Sonogashira reaction of the coupling of aryl halide with a terminal alkyne,[140] and the Buchwald-Hartwig amination of aryl halide with aniline, and these are dominated by reductive elimination vs ligand dissociation. (The latter example is from an on-going research project MS data) Because reductive elimination plays only a minor role here, we suspect the abundance of the precursor is also low.

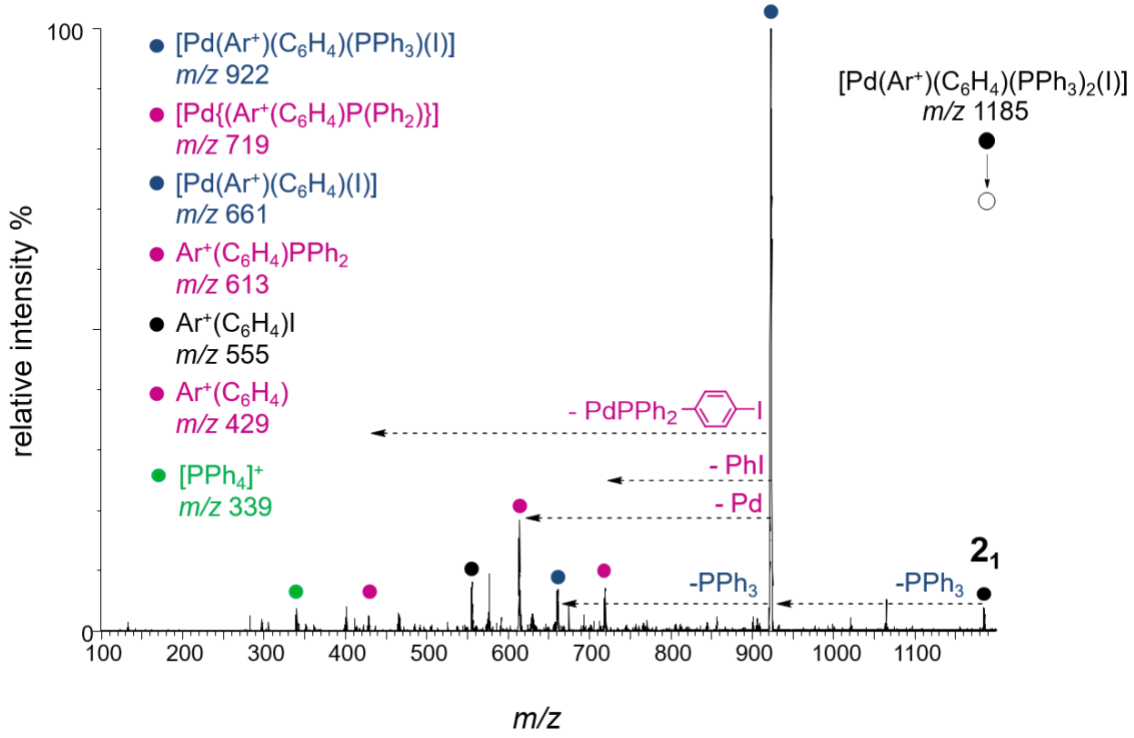

Figure 3-19. CID spectrum of 2_1 showing the fragmentation pattern and $(Ar^+) = Ph_3P^+CH_2C_6H_4$.

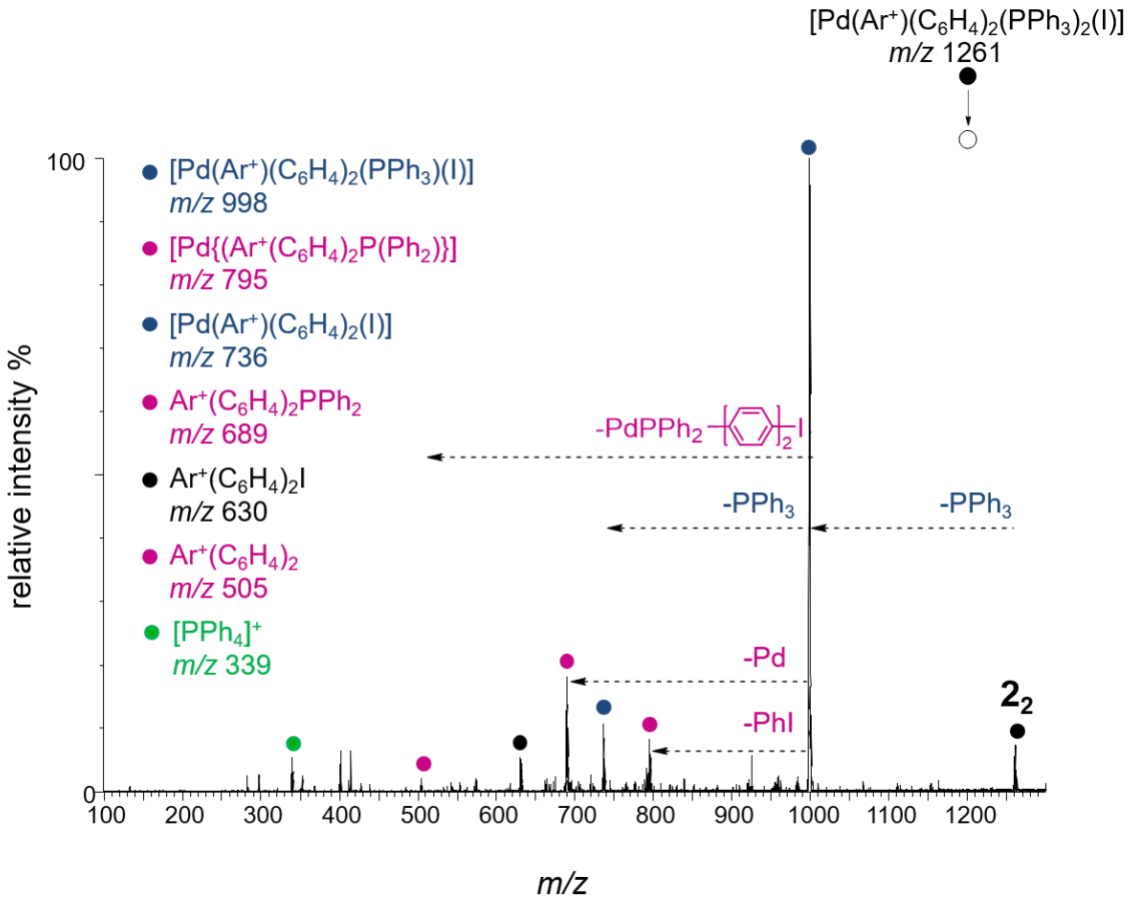

Figure 3-20. CID spectrum of 2_2 showing the fragmentation pattern and $(Ar^+) = Ph_3P^+CH_2C_6H_4$.

MS/MS analysis of $\mathbf{2_2}$ in Figure 3-20 illustrated a similar fragmentation patterns as $\mathbf{2_1}$: *m/z* 795 was assigned as $[Pd\{(Ar^+(C_6H_4)_2P(Ph_2)\}]$, a phosphine scrambling product in the oxidative addition pathway from the precursor ion $\mathbf{2_2}$ had an increase of 76 Da that represented the aryl group in the subsequent catalytic cycle of $\mathbf{2_1}$. The same trend is applied to peaks at *m/z* 998, 795, 736, 689, 630, 505. Tandem mass spectrum of the precursor ion $\mathbf{2_3}$ in Figure 3-21 was found to follow this fragmentation pattern.

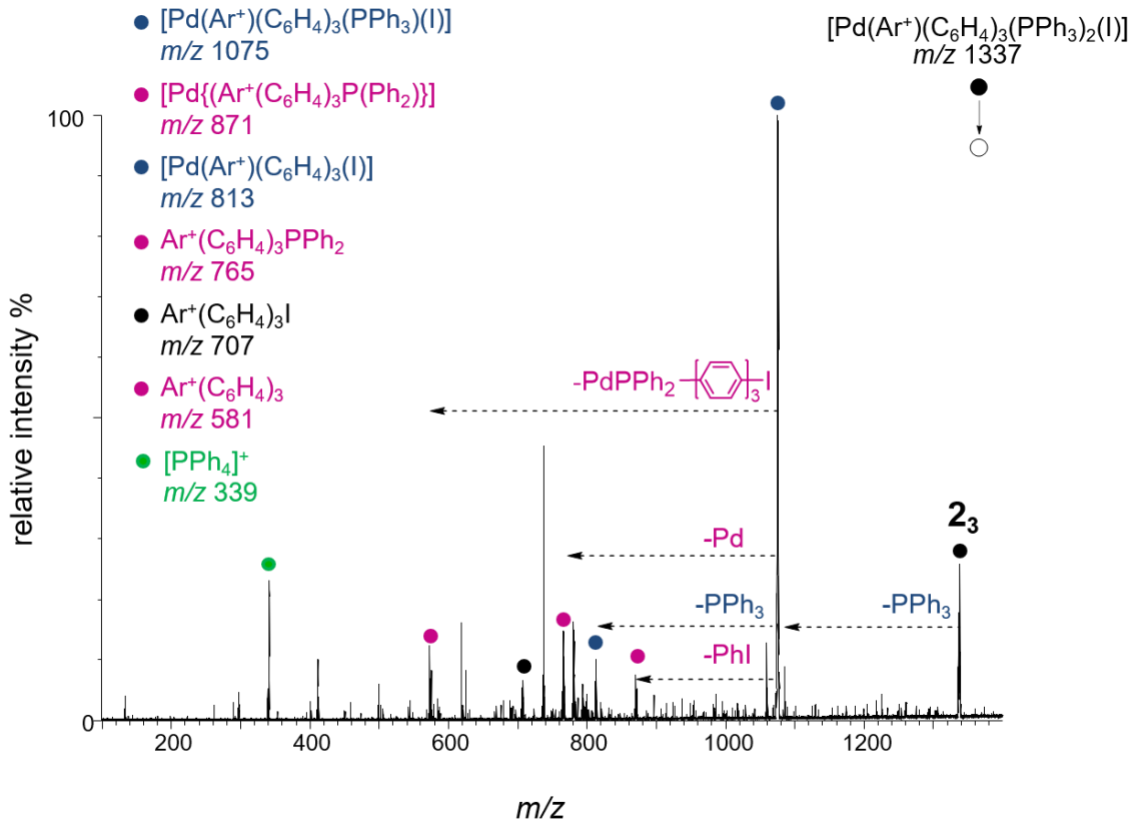

Figure 3-21. CID spectrum of 2_3 showing the fragmentation pattern and (Ar^+) = $Ph_3P^+CH_2C_6H_4$.

In addition, a signal at *m/z* 339 was assigned to tetraphenylphosphonium, PPh_4^+ that is found in all tandem mass spectra of $\mathbf{2_{0\text{-}4}}$. PPh_4^+ is an established sign of the occurrence of phosphine scrambling.[141]

Changing the End-Capping agent: Methoxyphenylboronic acid

Table 2. Numbering system of the capped oligomers using methoxyphenylboronic acid and the m/z ratio of each species.

Species #	n	Species	*m/z*
4_n	0	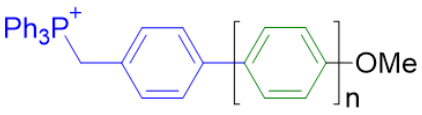	459
	1		535
	2		611
	3		687
	4		763
	5		839

The results of the MS/MS analysis on $\mathbf{2_n}$ species may provide a plausible explanation of the peculiar behavior of the capped oligomers $\mathbf{3_{0\text{-}4}}$ in the full scan and SIR chromatogram. We used phenylboronic acid, $C_6H_4B(OH)_2$ as the capping agent for the SPC and found that the predicted *m/z* ratio of the capped oligomers would have the same *m/z* ratio as the phosphine scrambling products (Table 1). Recalling each tandem mass spectra of $\mathbf{2_{1\text{-}3}}$ showed low abundance signals at *m/z* 429, 505, 581 that are assigned as aryl phosphine scrambling products through the transmetalation species pathway, $Ar^+(C_6H_4)H$, $Ar^+(C_6H_4)_2H$ and $Ar^+(C_6H_4)_3H$. With this in mind, it would be possible to observe the appearance of $\mathbf{3_{0\text{-}4}}$ prior to the addition of the capping agent in the full scan and SIR chronograms. Their appearance would also indicate that there is a substantial amount of phosphine scrambling products in the reaction solution that we should not consider the behaviour of $\mathbf{3_{0\text{-}4}}$ as background noise or adventitious overlapping species. We addressed this complication by switching to a different capping agent, methoxyphenylboronic acid $MeOC_6H_4B(OH)_2$. We hypothesized that a new set of capped products

$[Ph_3PCH_2C_6H_4(C_6H_4)_nOMe]^+$, which will be referred as $\mathbf{4_n}$ species from now on, would enable detection only when the capping agent is added to the reaction solution because it bears different *m/z* ratios than that of the original capped $\mathbf{3_n}$ species.

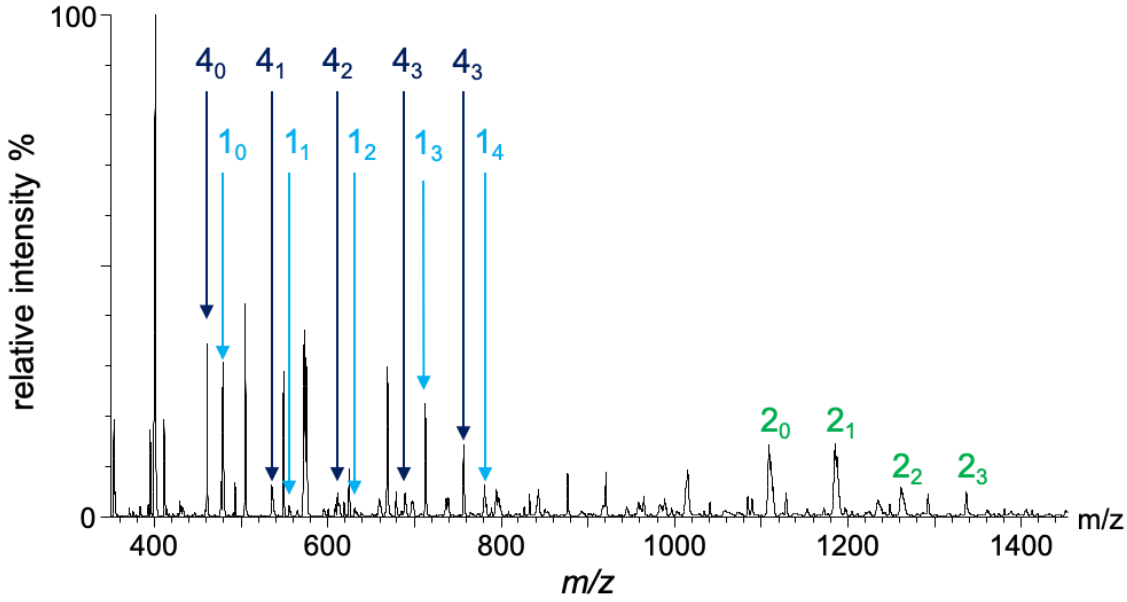

Figure 3-22. The summed ESI mass spectrum for the SPC species 1_n, 2_n, and 4_n (n = 0 – 4) in methanol in the presence of $Pd(PPh_3)_4$ and Cs_2CO_3 with the new end-capping reagent $MeOC_6H_4B(OH)_2$ was added late in the reaction.

With the initial full scan chronogram data in Figure 3-23, the assignment of the new capped oligomeric $\mathbf{4_n}$ species in the mass spectrum was made apparent. We expected to see $\mathbf{4_n}$ species to show traces that is closer to the baseline after AB monomer addition with the use of the new capping agent in the chronogram. In Figure 3-23, the $\mathbf{1_n}$ and $\mathbf{2_n}$ species appeared in a sequential manner, which was consistent with previous results. As in previous chronograms, the relative intensity of $\mathbf{1_{1\text{-}4}}$ was multiplied by a factor of 20 for clarity. The relative intensity of $\mathbf{4_{0\text{-}1}}$ had already appeared at 0 min of the chronogram; $\mathbf{4_2}$ also showed

an increase in intensity when the $\mathbf{1_0}$ was added to the reaction solution at 2 mins and appeared to be resting until the addition of the Pd catalyst addition at 6 mins. Apart from these observations, the $\mathbf{4_{0\text{-}4}}$ species appeared to remain relatively constant after the addition of the AB monomer at 16 minutes and until the new capping agent addition at 43 minutes, which was discerned as a good sign as there were no side products during this period of time that would have the same *m/z* ratio as the capped oligomeric products to the best of our knowledge. This does not mean that aryl-phosphine scrambling is not occurring within the catalytic cycle.

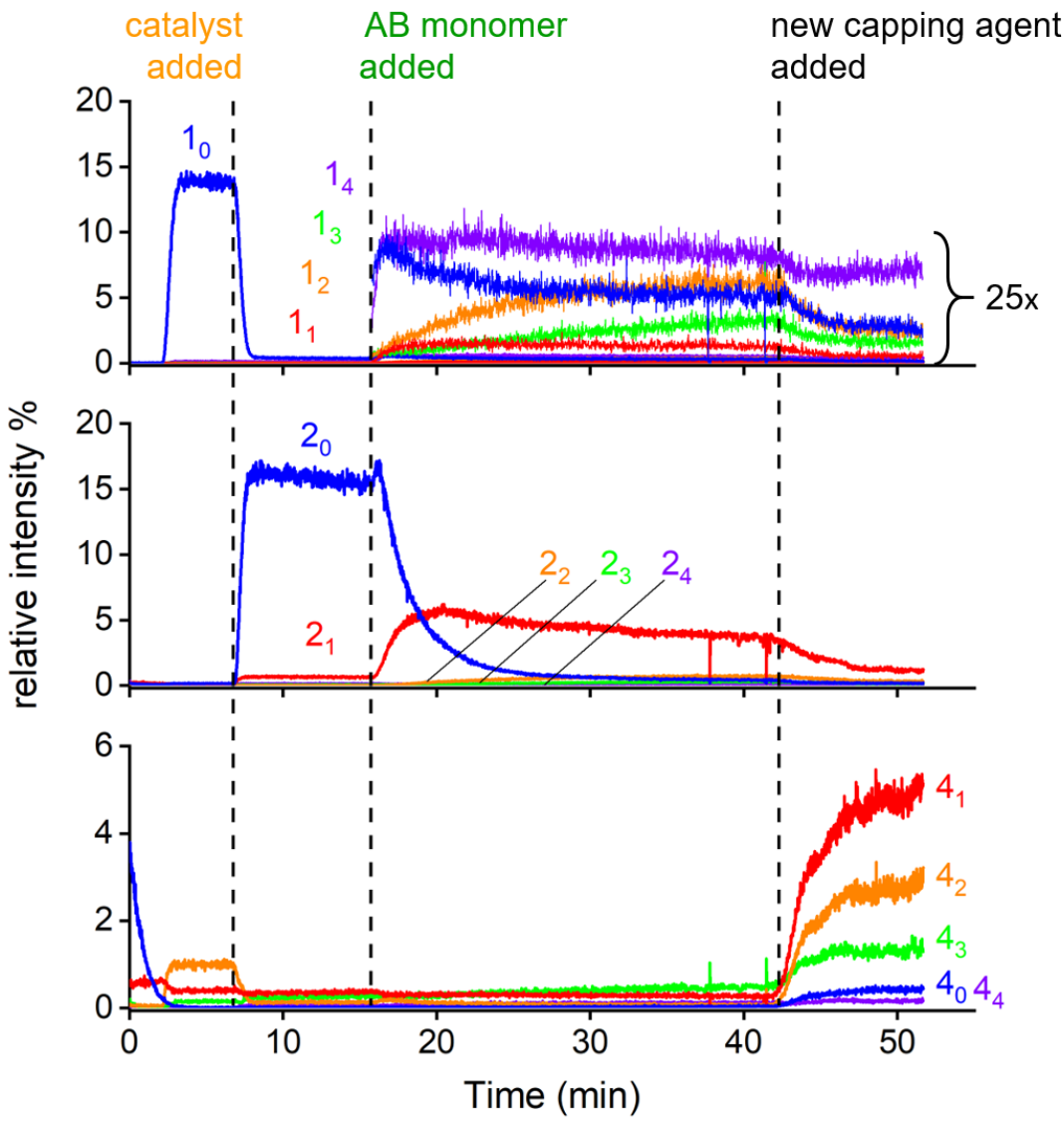

Figure 3-23. The normalized ESI-MS full scan chronogram of the SPC showing the relative intensity of aryl iodide species label as 1_n, intermediates as 2_n, and the new end-capped oligomer products as 4_n (n = 0 – 4).The aryl charge tag 1_0, $Pd(PPh_3)_4$ catalyst, AB monomer *p*-$(OH)_2BC_6H_4I$ and the end-capping agent $MeOC_6H_4B(OH)_2$ was added to the reaction solution at 2 minutes, 6 minutes, 16 minutes, and 43 minutes indicated in dotted lines.

In order to confirm that the $\mathbf{4_n}$ species would undergo the same CID fragmentation pathway as the $\mathbf{1_n}$ and $\mathbf{3_n}$ species losing a PPh_3 ligand from the charged-tag, product ion MS/MS analysis was performed on $\mathbf{4_{0\text{-}4}}$ and shown in Figure 3-24.

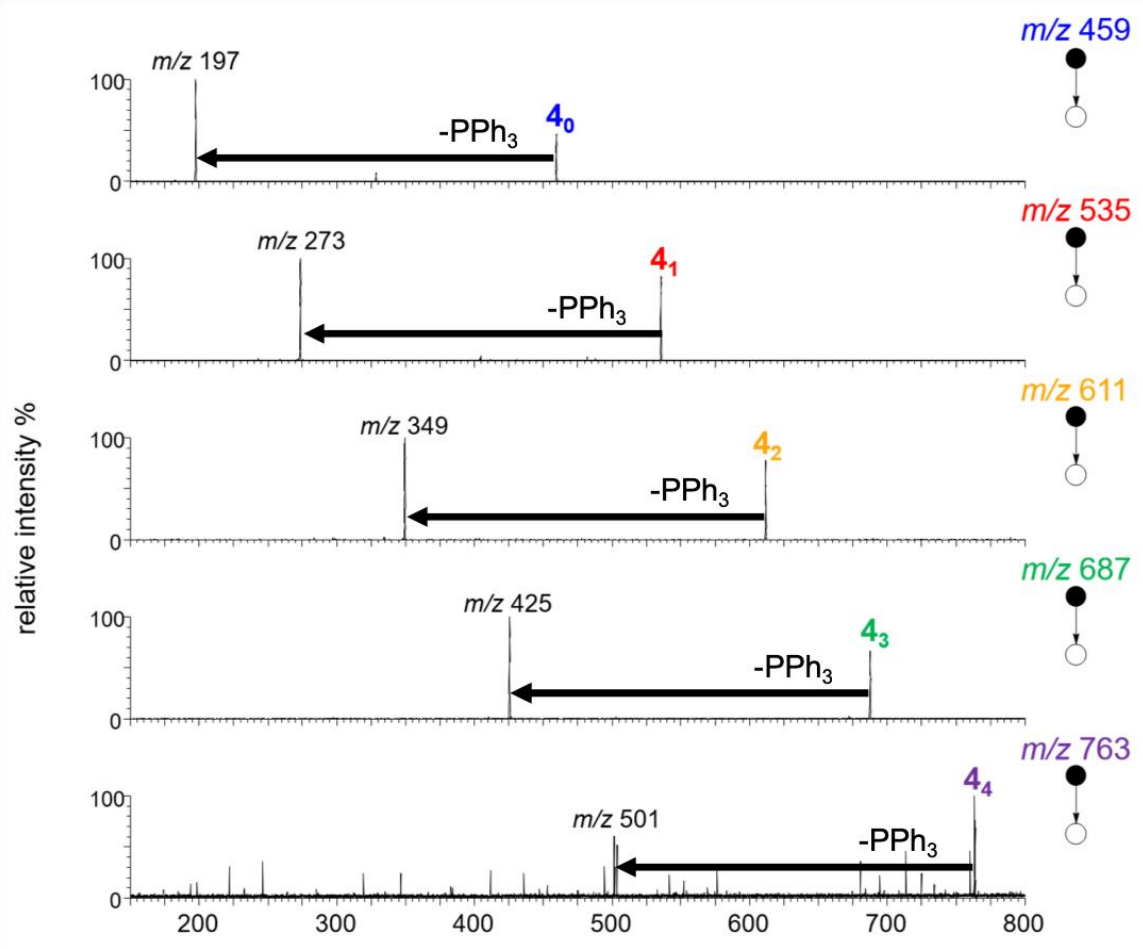

Figure 3-24. CID spectra of the capped oligomer products $4_{0\text{-}4}$ labelled as the precursor ion. The major fragmented ions were shown in the form of $[H_2CAr_nC_6H_5]^+$ and indicated with a dotted arrow showing the fragment as triphenylphosphine (PPh_3).

Neutral Loss Scan Experiments

Because all species decompose by the same fragmentation pathway, PPh_3 elimination, setting up a neutral loss scan was straightforward. In a typical neutral loss scan, both MS1 and MS2 are both scanning together but MS2 scans with a mass offset equivalent to the neutral loss of interest. All ions are allowed to pass through MS1 to undergo the CID process and ions are only detected in MS2 if it loses a common neutral fragment after the CID process. Moreover, neutral loss scan enables two or more functions set up with different collision energy to interweave in the same scan to obtain ions that give out different fragmentation pattern at different collision energy. The data is collected into one single raw file with two (or more) functions with two mass spectra and two chromatograms and each mass spectrum displays ion peak(s) that is detected at the specific collision energy. This scan mode is especially beneficial to study the SPC as it increases the signal-to-noise ratio by excluding ions that bear the same *m/z* ratio as the $\mathbf{1_n}$, $\mathbf{2_n}$ and $\mathbf{4_n}$ species of interests but that do not lose a PPh_3 fragment (262 Da). Since the product ion scan experiments revealed that each series did not exhibit the same fragmentation at the same collision energy, multiple functions of neutral loss scan can be set up to detect ions of all series of interest at its optimal collision energy in one experiment.

The summed mass spectra collected at two collision voltages at 35 V and 15 V are shown in Figure 3-25. The top spectrum displayed signals that corresponded to the $\mathbf{1_n}$ and $\mathbf{4_n}$ aryl iodide and aryl species and the mass spectrum on the bottom displayed signal that corresponded to the $\mathbf{2_n}$ Pd-containing species. The isotopic pattern overlay figures of the $\mathbf{2_n}$ series were also obtained and included in the supporting information to confirm the assignments. One of the apparent improvements in the neutral loss scan spectra was that

the number of peaks was visually less than that in full scan spectrum in Figure 3-11, as expected.

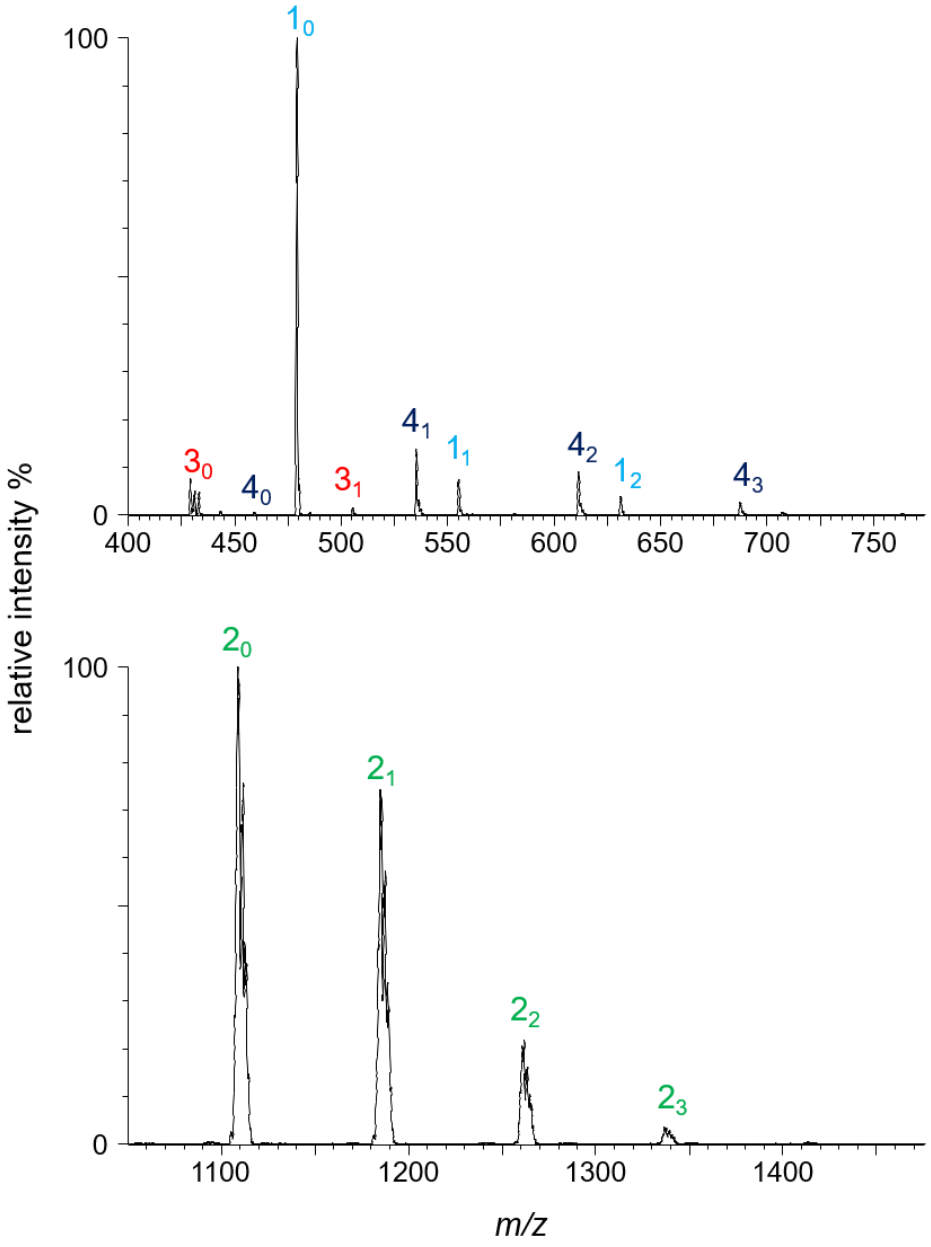

Figure 3-25. Summed ESI neutral loss scan mass spectrum for the SPC of 1_n and 4_n species with CID voltage at 35 V (top) and 2_n species with CID voltage at 15 V (bottom).

The normalized chronogram of the neutral loss scan is shown in Figure 3-26 and all reaction conditions remained the same as full scan and SIR experiments. A multiplier was not necessary given each trace showed an observable relative intensity. The aryl iodide $\mathbf{1_{0\text{-}4}}$ and Pd-containing species $\mathbf{2_{0\text{-}4}}$ exhibited a sequential increase in intensity much like the full scan and the SIR chronogram, a relatively stable sequential increase and decrease during catalyst addition at 12 minutes and AB monomer addition at 18 minutes. The methoxyphenylboronic acid capping agent was added at 36 minutes, both $\mathbf{1_{0\text{-}4}}$ and $\mathbf{2_{0\text{-}4}}$ species were shown to gradually decrease in their relative intensity and $\mathbf{4_{0\text{-}4}}$ showed an increase in their relative intensity.

The neutral loss scan chronogram shows a further reduction of chemical noise in comparison to the full scan and SIR chronograms. It has also eliminated what appears to be a significant problem with the $\mathbf{1_n}$ species, which in SIR mode maintains significant intensity even after the addition of $Pd(PPh_3)_4$. The $\mathbf{1_0}$ species ought to be very reactive towards oxidative addition, and the neutral loss scan confirms this, as it drops in intensity rapidly after addition of the pre-catalyst. Neutral loss scans are useful for reducing noise and overlapping species but do not help in increasing the amount of signal (unlike SIR, which increases signal but does nothing about noise and overlap ion peaks). Signal increases emerge by ensuring the scanning instrument spends its time focused only on the peaks of interest. However, we still cannot completely rule out the possibility of the detection of ions that also have a loss of 262 Da but not are necessarily a species of interest.

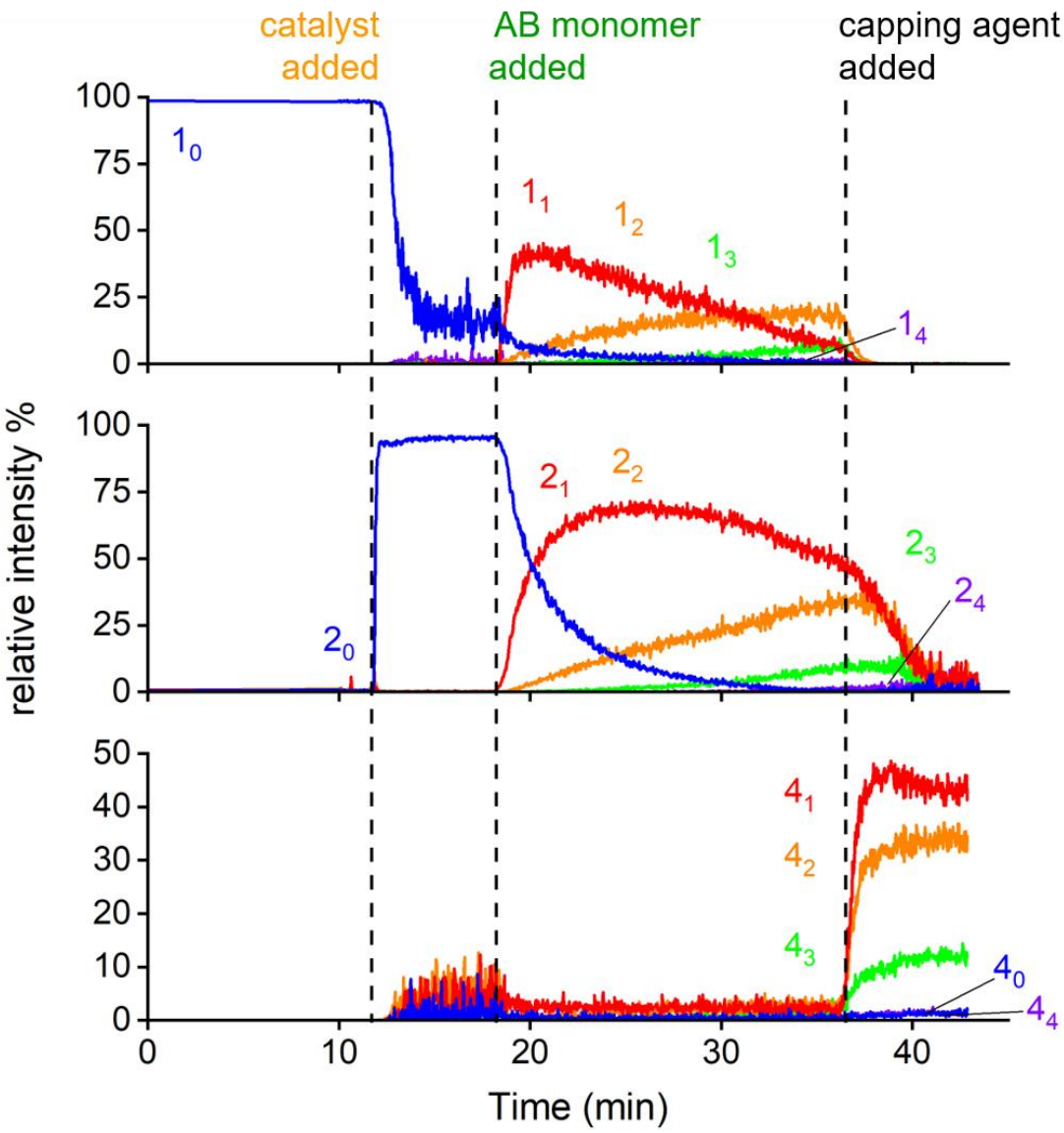

Figure 3-26. The normalized PSI-ESI-MS neutral loss scan chronogram of the SPC showing the relative intensity of aryl iodide species label as 1_n, intermediates as 2_n, and capped oligomer products as 4_n (n = 0 – 4). The catalyst $Pd(PPh_3)_4$, AB monomer *p*-$(OH)_2BC_6H_4I$ and the end-capping agent $MeOC_6H_4B(OH)_2$ was added at 12 minutes, 18 minutes, and 36 minutes indicated with dotted lines.

Multiple Reaction Monitoring Experiments

The experimental results of the neutral loss scan are deemed satisfactory in terms of sensitivity and selectivity of the SPC monitoring but triple quadrupole mass spectrometers still have one more trick up its sleeves: multiple reaction monitoring (MRM). MRM is a rapid, highly sensitive and selective screening method used for monitoring one or multiple specific ion transition(s). The collision energy is optimized to produce a diagnostic charged fragment of that ion (already established from the product ion scan experiments). Many MRM scans can be strung together into one experiment to detect the presence of many specific ions in a complex mixture. It is crucial to obtain precursor ion and product ion information along with ionization and fragmentation parameters prior to an MRM experiment. MRM methods can be easily set up by inputting the precursor ion *m/z*, product ion *m/z*, collision voltage, dwell time and span of the peak. This mode provided by far the best and most chemically sensible data of all the approaches. Similar to an SIR experiment, the mass spectrum of an MRM experiment does not show isotopic patterns but a signal peak at the pre-selected *m/z* ratio (chosen to be the most intense signal in the isotopomer envelope) and the relative intensity of this peak is shown in the extracted ion chromatogram.

The MRM chronogram of SPC was shown in Figure 3-27 and the results appear very comparable to the neutral loss scan chronogram. At time 0, $\mathbf{1_0}$ can be observed and was consumed by the addition of the catalyst, $Pd(PPh_3)_4$ at 8 minutes and accompanied by the appearance of $\mathbf{2_0}$. When the AB monomer was added at 12 minutes, a decrease in intensity of $\mathbf{2_0}$**,** was observed and species corresponding to $\mathbf{1_{1\text{-}4}}$ and $\mathbf{2_{1\text{-}4}}$ appeared sequentially, indicating that reaction turnover had occurred. The capping agent, $MeOC_6H_4B(OH)_2$, was

added at 38 minutes and all the $\mathbf{3_{0\text{-}4}}$ products were produced rapidly. It was also noted that the relative intensity of $\mathbf{4_{3,4}}$ were shown to decrease right after its appearance in this experiment. Overall, the result of the MRM appears to be very clean, species of interest no longer appeared at the beginning of the chronogram, meaning that species (apart from $\mathbf{1_0}$) that appear at 0 mins in the full scan and SIR results were likely to be S:N artefacts or contaminants. The capped oligomer products $\mathbf{4_n}$ did not appear after AB monomer addition in MRM could indicate the use of the methoxyphenylboronic acid was effective in replacing phenylboronic acid to avoid detecting phosphine scrambling products that have the same *m/z* ratio as the capped oligomers $\mathbf{3_n}$.

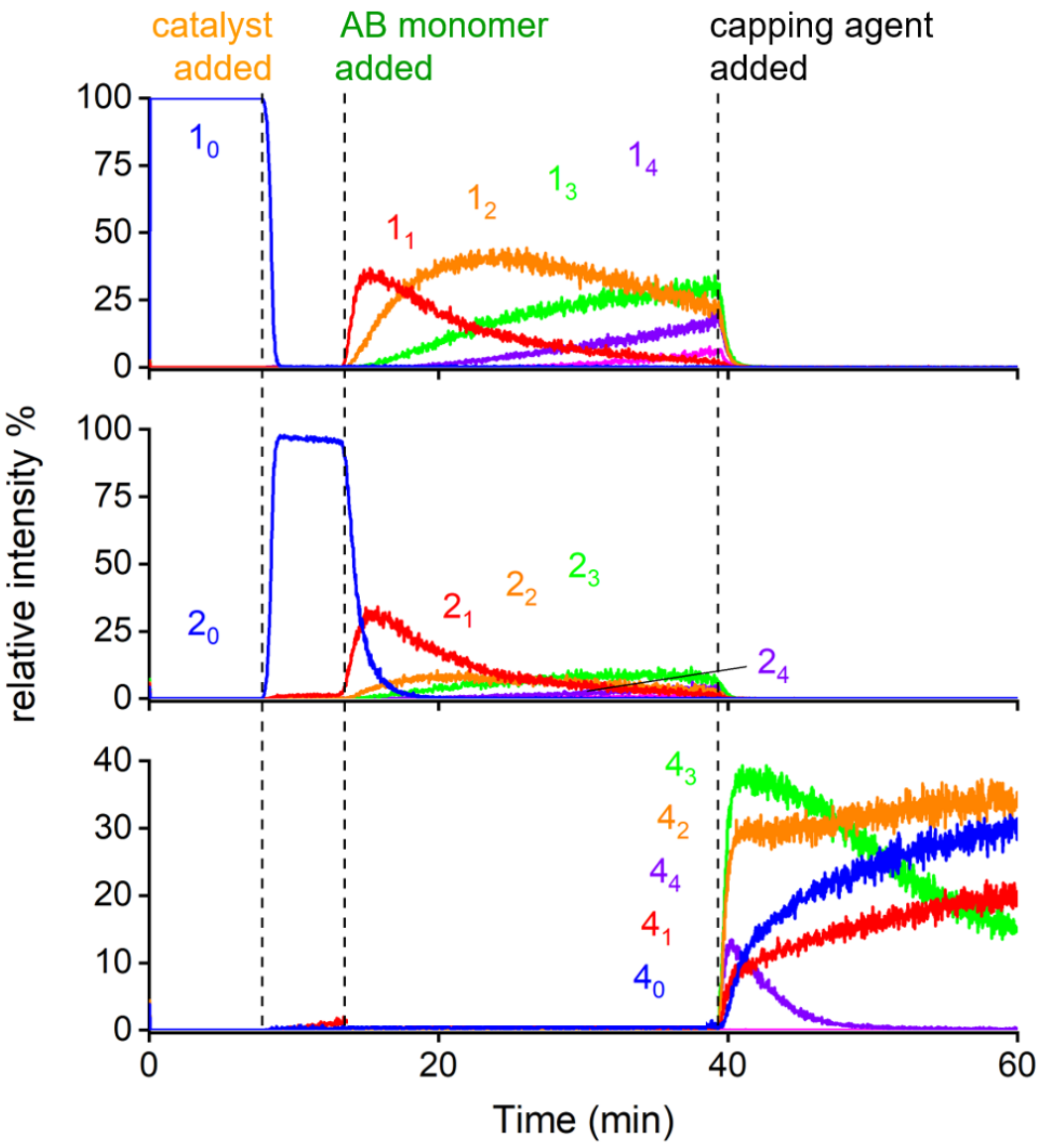

Figure 3-27. The normalized PSI-ESI-MS MRM chronogram of the SPC showing the relative intensity of aryl iodide species label as 1_n, intermediates as 2_n, and capped oligomer products as 4_n (n = 0 – 4). The catalyst $Pd(PPh_3)_4$, AB monomer *p*-$(OH)_2BC_6H_4I$ and the end-capping agent $MeOC_6H_4B(OH)_2$ was added at 8 minutes, 12 minutes, and 38 minutes indicated in dotted lines.

So what does the MRM data tell us about the reaction? First, it needs to be appreciated that the catalytic cycle shown in previous chronograms using full scan, SIR and neutral loss scan is not the complete story because, after reductive elimination of each new biaryl compound, the catalyst has several available options: it can oxidatively add to the charge-tagged polyaryl iodide $\mathbf{1_{n>0}}$, the difunctional AB monomer $IC_6H_4B(OH)_2$, or an untagged difunctional polyaryl iodide, $I(C_6H_4)_nB(OH)_2$. Only one of these is charged, and so an appreciable chunk of the reactive species go undetected. It is also possible that the transmetallation can be between a tagged species and a difunctional polyaryl species of the type $(HO)_2B(C_6H_4)_nI$. A further outstanding question remains concerning the $\mathbf{2_n}$ species. Compositionally, we can be certain they are of the general formula $[(Ph_3P)_2Pd\{(C_6H_4)_nCH_2PPh_3\}I]^+$, but there is some ambiguity in this. There are actually four options: the cis and trans isomers for each of $[[(Ph_3P)_2Pd\{(C_6H_4)_nCH_2PPh_3\}I]^+$, where the ligands are aryl and iodide, and $[(Ph_3P)_2Pd\{(C_6H_4)_nCH_2PPh_3\}(C_6H_4)_nI]^+$, where the ligands are both aryl. MS/MS examination can assist with these options, because bis(aryl) palladium species are prone to reductive elimination of a biaryl species, whereas an aryl palladium iodide is not. However, the product ion scan analysis of each Pd-containing species showed only a low intensity of the biaryls $(Ar^+C_6H_4)_{1\text{-}4}$. The rest of the MS/MS analysis of the gas phase ions revealed a series of fragments suggested that more than one fragmentation pathway was behind the production of these product ions, pointing to the aryl phosphine scrambling reaction. This reaction is a notorious side reaction that takes place in SMC reaction and more so in SPC because the polyaryl chain length can be halted. The fact that the $\mathbf{3_n}$ species appeared right after AB monomer addition observed in the full scan and SIR chronogram is likely an indication of the phosphine scrambling taking place

in the reaction solution. We can be confident about this after switching to a different capping agent and the relative intensity of the $\mathbf{4_n}$ species did not show an increasing trend using MRM. It was not possible to determine the species conformation to be cis or trans using solely mass spectrometry because both would have the same *m/z* ratio and orthogonal spectroscopy methods such as ion mobility spectrometer.

The formation of the oligomer product series $\mathbf{4_n}$ studied in each method were shown to have a dramatic increase as soon as the addition of capping agent terminated the ongoing catalytic cycle and suggested that SPC is a step-growth polymerization. This observation is consistent with the SMC mechanism and the SPC literature as it would be impossible to observe the catalytic species ($\mathbf{1_{2\text{-}4}}$ and $\mathbf{2_{2\text{-}4}}$) at the same time had the reaction proceeded in a chain-growth fashion. The behaviour of $\mathbf{4_3}$ and $\mathbf{4_4}$ were intriguing as the relative intensity rapidly increased and decreased. Because this behavior was more pronounced for $\mathbf{4_4}$ than for $\mathbf{4_3}$, it is most likely due to low solubility of the higher oligomers. Precipitation would result in a decrease in relative intensity of $\mathbf{4_3}$ and especially $\mathbf{4_4}$.

Conclusion

The application of PSI-ESI-MS under our experimental conditions revealed that the palladium intermediates in the Suzuki polycondensation catalytic cycle potentially undergo competing pathway between transmetalation and aryl-phosphine ligand scrambling. We expected to observe a reductive elimination pathway from the Pd intermediates when subjected to MS/MS analysis. Instead, CID data revealed the involvement of aryl-phosphine ligand scrambling pathway in the Pd intermediates to generate aryl, iodobenzene, and Pd-containing phosphine products: $Ph_3P^+CH_2(C_6H_4)_n$, C_6H_4I, $[Pd\{(Ph_3P^+CH_2(C_6H_4)_n)P(Ph_2)\}]$ and $[Pd–P(Ph_2)(C_6H_4I)]$. Product ions with the charged phosphonium tag, $Ph_3P^+CH_2(C_6H_4)_n–$ were well-observed in the CID mass spectra. The ligand scrambling phenomenon may attribute to the incomplete conversion of the observed oligomer products as seen in the chronogram data. We were able to assign the Pd intermediates based on the *m/z* ratio, isotope pattern (from previous work) and CID fragmentation patterns. However, the true identity of palladium intermediates whether it is in the form of a transmetalation intermediate from the n^{th} cycle or in the form of an oxidative addition product in the $(n + 1)^{th}$ cycle remain unsolved in this work since ESI-MS does not differentiate isomers. The CID fragmentation patterns indicated that both species were present in the gas-phase experiments.

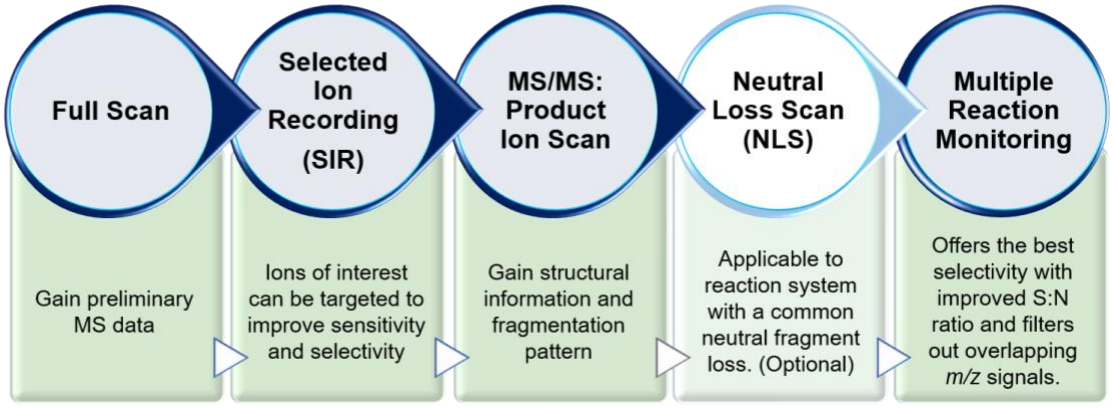

Figure 3-28. Reaction monitoring workflow utilizing MS/MS methods with a triple quadrupole mass analyzer.

Analysis of catalytic reactions is challenging even under ideal conditions. The catalyst is present in low concentration compared to reactants, products and solvent, and can itself manifest in different ways: precatalyst, resting state, intermediates, decomposition products, scrambling products, and more. This problem is further compounded in the case of the Suzuki polycondensation where the intermediates change identity with every turnover. Three significant intermediate types were observed and assigned in each stage of the catalysis, oxidative addition, transmetalation, and reductive elimination in the mass spectrum and their behaviour were observed in the chronogram normalized to the TIC. MRM has proven to be up to the task of establishing the dynamics of these species, though the usual caveats still apply: compositional information is very useful but still leaves structural ambiguity. Nonetheless, we have shown how tandem mass spectrometric methods are up to the challenge when used in the following workflow: selected ion recording (SIR) and neutral loss scan (NLS) dramatically improved the signal-to-noise ratio. Product ion scan revealed all the intermediate oligomers lose a triphenylphosphine

fragment (*m/z* 262) which would either come from the ligand on the Pd-complex or the charged tag.. Ultimately, the extraordinary signal-to-noise ratio and sensitivity of MRM methods are capable of obtaining beautiful real-time data even on extraordinarily small amounts of material. MS/MS methods are promising for improving data quality, selectivity and sensitivity in real time reaction monitoring. The principle is broadly applicable to other systems, from an intricate catalytic reaction with short-lived ionic intermediates to a reaction with only a single product generated.

Experimental Procedure

All experiments and reagents were performed under nitrogen atmosphere using standard Schlenk and glovebox techniques. Reagents were purchased from Sigma-Aldrich and were used without further purification. Methanol (HPLC grade) was distilled from calcium hydride before every use. Gases were purchased from Airgas.

Preparation of solutions for Suzuki polycondensation

Synthesis of the charge tag was previously reported.[39] A stock solution of the charge tag $[Ph_3PCH_2C_6H_4I]^+[PF_6]^-$ (**1₀**, 0.1253 g) was prepared in 30 mL of dry MeOH. Stock solutions of 4-iodophenylboronic acid (52 mg) and 4-methoxyphenylboronic acid (15 mg) was prepared in 10 mL and 20 mL of dry MeOH, respectively. Methoxyboronic acid (50 mg, in 20 mL MeOH) was used instead of 4-methoxyphenylboronic acid in later experiments. Tetrakistriphenylphosphine palladium(0) (11 mg) was prepared in 4 mL of dry THF in a glovebox and stored in a freezer.

General procedure for PSI-ESI-MS monitoring

Suzuki polycondensation was monitored in real time using PSI-ESI-MS in the positive ion mode in the following way. First, methanol solvent (20 mL), stirrer bar and base (9 mg, 10 μmol) were added to the Schlenk flask at an oil bath temperature of 40℃. **1₀**, (1 μmol) was added to the flask by rubber-free syringe through a septum. An aliquot of each stock solutions were added to the reaction mixture in the following sequential order and was left to react for a period of time in between reagent additions: $Pd(PPh_3)_4$ catalyst (0.05 μmol in 4 ml of THF), the AB monomer, $IC_6H_4B(OH)_2$ (12 μmol) and the capping agent $PhC_6H_4B(OH)_2$ (1 μmol). The reaction was allowed to proceed for some time before halting. (See Chronogram data for time points)

General conditions of the mass spectrometer

All mass spectra were collected by a Waters Acquity Triple Quadrupole Mass spectrometer equipped with a Z-Spray pneumatically assisted electrospray ionization in the positive ion mode.

Full scan – MS Tuning parameters

The capillary voltage was held at 3.00 kV, cone voltage at 14.00 V, extraction cone voltage at 3.00 V, and RF lens at 0.30 V. The desolvation settings were optimized: desolvation gas flow rate 100 L/h, cone gas flow 200 L/h, source temperature 79℃, desolvation temperature 180 ℃. Mass range was set to *m/z* 50 –1800; scan duration was 1.000 second; LM and HM resolution were set to 12.0 and a total number 4497 scans were collected.

Selected Ion monitoring – MS Tuning parameters

The capillary voltage was held at 3.00 kV, cone voltage at 14.00 V, and extraction cone voltage at 3.00 V and RF lens at 0.30 V. The desolvation settings were optimized: desolvation gas flow rate 300 L/h, cone gas flow 200 L/h, source temperature 79℃, desolvation temperature 175 ℃. LM and HM resolution were set to 12.0 and a total of 2553 scans were collected.

SIR Mass selection profile

16 channels were set up with 0.100 second dwell time and 2.000 Da span on each channel as follow: $[Ph_3PCH_2C_6H_4I]^+$ **1$_0$**, *m/z* 478; $[Ph_3PCH_2(C_6H_4)_2I]^+$ **1$_1$**, *m/z* 554; $[Ph_3PCH_2(C_6H_4)_3I]^+$ **1$_2$**, *m/z* 630; $[Ph_3PCH_2(C_6H_4)_4I]^+$ **1$_3$**, *m/z* 706; $[Ph_3PCH_2(C_6H_4)_5I]^+$ **1$_4$**, *m/z* 782; $[(Ph_3P)_2Pd(C_6H_4CH_2PPh_3)(I)]^+$ **2$_0$** *m/z* 1108; $[(Ph_3P)_2Pd((C_6H_4)_2\text{-}CH_2PPh_3)(I)]^+$ **2$_1$** *m/z* 1182; $[(Ph_3P)_2Pd((C_6H_4)_2\text{-}CH_2PPh_3)(I)]^+$ **2$_2$** *m/z* 1258; $[(Ph_3P)_2Pd((C_6H_4)_3\text{-}CH_2PPh_3)(I)]^+$ **2$_3$** *m/z* 1339; $[(Ph_3P)_2Pd((C_6H_4)_3\text{-}CH_2PPh_3)(I)]^+$ **2$_4$** *m/z* 1413;

$[Ph_3PCH_2(C_6H_4)C_6H_5]^+$ **3$_0$**, *m/z* 428; $[Ph_3PCH_2(C_6H_4)_2C_6H_5]^+$ **3$_1$**, *m/z* 506; $[Ph_3PCH_2(C_6H_4)_3C_6H_5]^+$ **3$_2$**, *m/z* 580; $[Ph_3PCH_2(C_6H_4)_4C_6H_5]^+$ **3$_3$**, *m/z* 657; $[Ph_3PCH_2(C_6H_4)_5C_6H_5]^+$ **3$_4$**, *m/z* 733.

Neutral loss scan - Collision-Induced dissociation tuning parameters

Two functions of the neutral loss scan were set up to detect precursor ions with a 262 Da neutral loss of the triphenylphosphine (PPh3) at two collision-induced dissociation voltages. Function 1 was set up to detect aryl species at low mass range m/z 300-1000 with CID set to 35.0 V. Function 2 was set up to detect palladium-containing species at high mass range m/z 900-1800 with CID at 15.0 V. Both functions were set to have 1 second scan time and same collision gas flow 0.22 mL/min.

MS Tuning parameter

The capillary voltage was held at 3.10 kV, cone voltage at 14.00 V, and extraction cone voltage at 2.00 V and RF lens at 0.30 V. The desolvation settings were optimized: desolvation gas flow rate 300 L/h, cone gas flow 150 L/h, source temperature 79℃, desolvation temperature 150 ℃. LM and HM resolution were set to 13.0 and a total of 1279 and 1278 scans were collected for Function 1 and Function 2.

Multiple reaction monitoring – MS Tuning parameters

The capillary voltage was held at 3.10 kV, cone voltage at 13.00 V, and extraction cone voltage at 3.00 V and RF lens at 0.30 V. The desolvation settings were optimized: desolvation gas flow rate 300 L/h, cone gas flow 200 L/h, source temperature 80℃, desolvation temperature 150 ℃. LM and HM resolution were set to 13.0 and a total of 2821 scans were collected.

MRM Mass selection profile

16 channels were set up with optimized dwell time and collision energy with a 2.000 Da span on each channel: $[Ph_3PCH_2C_6H_4I]^+$ **1$_0$**, *m/z* 478→217(0.05s, 35V); $[Ph_3PCH_2(C_6H_4)_2I]^+$ **1$_1$**, *m/z* 554→293 (0.05s, 35V); $[Ph_3PCH_2(C_6H_4)_3I]^+$ **1$_2$**, *m/z* 630→369; $[Ph_3PCH_2(C_6H_4)_4I]^+$ **1$_3$**, *m/z* 706→445 (0.05s, 35V); $[Ph_3PCH_2(C_6H_4)_5I]^+$ **1$_4$**, *m/z* 782→521 (0.07s, 35V) $[(Ph_3P)_2Pd(C_6H_4CH_2PPh_3)(I)]^+$ **2$_0$** *m/z* 1108→845 (0.05s, 15V); $[(Ph_3P)_2Pd((C_6H_4)_2\text{-}CH_2PPh_3)(I)]^+$ **2$_1$** *m/z* 1182→920 (0.05s, 15V); $[(Ph_3P)_2Pd((C_6H_4)_2CH_2PPh_3)(I)]^+$ **2$_2$** *m/z* 1258→996 (0.05s, 15V); $[(Ph_3P)_2Pd((C_6H_4)_3CH_2PPh_3)(I)]^+$ **2$_3$** *m/z* 1339→1077 (0.05s, 15V); $[(Ph_3P)_2Pd((C_6H_4)_3CH_2PPh_3)(I)]^+$ **2$_4$** *m/z* 1413→1152 (0.05s, 15V); $[Ph_3PCH_2(C_6H_4)_2OMe]^+$ **4$_0$**, *m/z* 459→197(0.06s, 35V); $[Ph_3PCH_2(C_6H_4)_3OMe]^+$ **4$_1$**, *m/z* 535→273 (0.07s, 35V); $[Ph_3PCH_2(C_6H_4)_4OMe]^+$ **4$_2$**, *m/z* 611→349 (0.06s, 35V); $[Ph_3PCH_2(C_6H_4)_5OMe]^+$ **4$_3$**, *m/z* 687→425 (0.06s, 35V); $[Ph_3PCH_2(C_6H_4)_6OMe]^+$ **4$_4$**, *m/z* 763→501 (0.08s, 35V).

Product ion scan – CID tuning conditions

All MS/MS spectra were collected using PSI-ESI-MS and the SPC reactions were monitored in full using the same tuning parameters as full scan from above. $1_{0\text{-}4}$, $3_{0\text{-}4}$, and $4_{0\text{-}4}$ were studied under CID at 30.0, 33.0, and 35.0 V; $2_{0\text{-}4}$ were studied under CID at 5.0, 10.0, 15.0, 25.0, and 35.0 V.

Chapter 4 Future Work

This work has highlighted the versatility of ESI-MS in studying the Suzuki-polycondensation (SPC). Future experimental design can be catered to address the fundamental understanding of the reaction: monitoring the reaction at different temperatures, different catalyst loading, stoichiometric ratio, using different substrates, boronic esters or ones that are employed in OLED synthesis (fluorenes) and different aryl halide coupling partners.[127] It would also be interesting to observe the SPC using a phosphine-free palladium catalyst, or with bulky phosphines such as Pd(*o*-toly), other than the standard $Pd(PPh_3)_4$ as the transmetalation step and the aryl-phosphine scrambling are competitive processes. Since the results of the AB pathway in this work is consistent with step-growth polymerization, performing the AA/BB pathway experiments may provide some insights on the whether it is a chain-growth or a step-growth polymerization using ESI-MS. Orthogonal methods such as UV-VIS may be able to shed light on the polymerization progress as the reaction solution showed a colour change throughout the course of the reaction. It would be interesting to see if the two methods will be in agreement and the PSI customized-Schlenk flask can easily cope with such setup.[64] Moreover, ion mobility mass spectrometry (IMS) is the may be capable to study the transmetalation step in SPC and SMC because ions are not only separated base on its *m/z* ratio but alsosize and shape as ions are required to travel through a drift-tube by the collision cross section of an particular ion. IMS may be able to differentiate the trans to cis isomerisation of the Pd-complex in the transmetalation step. We are confident that IMS will unravel an in-depth understanding of reaction mechanism in the upcoming research work.

Bibliography

(1) Dempster, A. J. A New Method of Positive Ray Analysis. *Physical Review* **1918**, *11* (4), 316–325.

(2) Barber, M.; Bordoli, R. S.; Sedgwick, R. D.; Tyler, A. N. Fast Atom Bombardment of Solids as an Ion Source in Mass Spectrometry. *Nature* **1981**, *293* (5830), 270–275.

(3) Stoll, R. G.; Harvan, D. J.; Hass, J. R. Liquid Secondary Ion Mass Spectrometry with a Focussed Primary Ion Source. *International Journal of Mass Spectrometry and Ion Processes* **1984**, *61* (1), 71–79.

(4) Bruce, M. I.; Liddell, M. J. Applications of Fast Atom Bombardment Mass Spectrometry (FAB MS) to Organometallic and Coordination Chemistry. *Applied Organometallic Chemistry* **1987**, *1* (3), 191–226.

(5) Hambitzer, G.; Heitbaum, J. Electrochemical Thermospray Mass Spectrometry. *Analytical Chemistry* **1986**, *58* (6), 1067–1070.

(6) Munson, M. S. B.; Field, F. H. Chemical Ionization Mass Spectrometry. I. General Introduction. *Journal of the American Chemical Society* **1966**, *88* (12), 2621–2630.

(7) Hoffmann, E. de.; Stroobant, V. *Mass Spectrometry : Principles and Applications*; J. Wiley, 2007.

(8) Becker, J. S. *Inorganic Mass Spectrometry : Principles and Applications*; John Wiley & Sons, 2007.

(9) Gross, J. H. *Mass Spectrometry*; Springer Berlin Heidelberg: Berlin, Heidelberg, 2011.

(10) Sparkman, O. D. Mass Spectrometry: Overview and History. In *Encyclopedia of Analytical Chemistry*; John Wiley & Sons, Ltd: Chichester, UK, 2000.

(11) Traeger, J. C. The Development of Electron Ionization. *The Encyclopedia of Mass Spectrometry* **2016**, *9*, 77–82.

(12) Amirav, A.; Danon, A. Short Communication Electron Impact Mass Spectrometry in Supersonic Molecular Beams. *International Journal of Mass Spectrometry and Ion Processes Elsevier Science Publishers B.V* **1990**, *97* (1), 107–113.

(13) Bruns, E. A.; Perraud, V.; Greaves, J.; Finlayson-Pitts, B. J. Atmospheric Solids Analysis Probe Mass Spectrometry: A New Approach for Airborne Particle Analysis. *Analytical Chemistry* **2010**, *82* (14), 5922–5927.

(14) Yamashita, M.; Fenn, J. B. Electrospray Ion Source. Another Variation on the Free-Jet Theme. *The Journal of Physical Chemistry* **1984**, *88* (20), 4451–4459.

(15) Zenobi, R. Ionization Methods in Mass Spectrometry. *Analytical Chemistry* **2015**, *87* (7), 3543–3543.

(16) Keski-Hynnilä, H.; Kurkela, M.; Elovaara, E.; Antonio, L.; Magdalou, J.; Luukkanen, L.; Taskinen, J.; Kostiainen, R. Comparison of Electrospray, Atmospheric Pressure Chemical Ionization, and Atmospheric Pressure Photoionization in the Identification of Apomorphine, Dobutamine, and Entacapone Phase II Metabolites in Biological Samples. *Analytical Chemistry* **2002**, *74* (14), 3449–3457.

(17) Stoddard, R. L.; Collins, S.; McIndoe, J. S. Mass Spectrometry of Organoaluminum Derivatives. In *PATAI'S Chemistry of Functional Groups*; John Wiley & Sons, Ltd: Chichester, UK, 2016; pp 1–15.

(18) Zhu, W.; Yuan, Y.; Zhou, P.; Zeng, L.; Wang, H.; Tang, L.; Guo, B.; Chen, B. The Expanding Role of Electrospray Ionization Mass Spectrometry for Probing Reactive Intermediates in Solution. *Molecules* **2012**, *17* (10), 11507–11537.

(19) Cody, R. B.; Laramée, J. A.; Durst, H. D. Versatile New Ion Source for the Analysis of Materials in Open Air under Ambient Conditions. *Analytical Chemistry* **2005**, *77* (8), 2297–2302.

(20) Takáts, Z.; Wiseman, J. M.; Gologan, B.; Cooks, R. G. Mass Spectrometry Sampling under Ambient Conditions with Desorption Electrospray Ionization. *Science (New York, N.Y.)* **2004**, *306* (5695), 471–473.

(21) Liu, J.; Wang, H.; Manicke, N. E.; Lin, J.-M.; Cooks, R. G.; Ouyang, Z. Development, Characterization, and Application of Paper Spray Ionization. *Analytical Chemistry* **2010**, *82* (6), 2463–2471.

(22) Jiang, J.; Zhang, H.; Li, M.; Dulay, M. T.; Ingram, A. J.; Li, N.; You, H.; Zare, R. N. Droplet Spray Ionization from a Glass Microscope Slide: Real-Time Monitoring of Ethylene Polymerization. *Analytical Chemistry* **2015**, *87* (16), 8057–8062.

(23) Dole, M.; Mack, L. L.; Hines, R. L.; Mobley, R. C.; Ferguson, L. D.; Alice, M. B. Molecular Beams of Macroions. *The Journal of Chemical Physics* **1968**, *49* (5), 2240–2249.

(24) Bruins, A. P. Mechanistic Aspects of Electrospray Ionization. *Journal of Chromatography A* **1998**, *794* (1–2), 345–357.

(25) Fenn, J. B.; Mann, M.; Meng, C. K.; Wong, S. F.; Whitehouse, C. M. Electrospray Ionization-Principles and Practice. *Mass Spectrometry Reviews* **1990**, *9* (1), 37–70.

(26) Rosell-Llompart, J.; Grifoll, J.; Loscertales, I. G. Electrosprays in the Cone-Jet Mode: From Taylor Cone Formation to Spray Development. *Journal of Aerosol Science* **2018**, *125*, 2–31.

(27) Konermann, L.; Ahadi, E.; Rodriguez, A. D.; Vahidi, S. Unraveling the Mechanism of Electrospray Ionization. *Analytical Chemistry* **2013**, *85* (1), 2–9.

(28) Plattner, D. A. Electrospray Mass Spectrometry beyond Analytical Chemistry: Studies of Organometallic Catalysis in the Gas Phase. *International Journal of Mass Spectrometry* **2001**, *207* (3), 125–144.

(29) Trefz, T. K.; Henderson, M. A.; Linnolahti, M.; Collins, S.; McIndoe, J. S. Mass Spectrometric Characterization of Methylaluminoxane-Activated Metallocene Complexes. *Chemistry - A European Journal* **2015**, *21* (7), 2980–2991.

(30) Trefz, T. K.; Henderson, M. A.; Wang, M. Y.; Collins, S.; McIndoe, J. S. Mass Spectrometric Characterization of Methylaluminoxane. *Organometallics* **2013**, *32* (11), 3149–3152.

(31) Beierlein, C. H.; Breit, B.; Paz Schmidt, R. A.; Plattner, D. A. Online Monitoring of Hydroformylation Intermediates by ESI-MS. *Organometallics* **2010**, *29* (11), 2521–2532.

(32) Vikse, K.; Khairallah, G. N.; McIndoe, J. S.; O'Hair, R. A. J. Fixed-Charge Phosphine Ligands to Explore Gas-Phase Coinage Metal-Mediated Decarboxylation Reactions. *Dalton Transactions* **2013**, *42* (18), 6440.

(33) Crawford, E.; Lohr, T.; Leitao, E. M.; Kwok, S.; Mcindoe, J. S. Distannoxane Speciation during Esterification Catalysis: Revealing Insights Provided by Electrospray Ionization Mass Spectrometry. *Dalton Transactions* **2009**, No. 42, 9110.

(34) Santos, L. S. What Do We Know about Reaction Mechanism? The Electrospray Ionization Mass Spectrometry Approach. *Journal of the Brazilian Chemical Society* **2011**, *22* (10), 1827–1840.

(35) Aliprantis, A. O.; Canary, J. W. Observation of Catalytic Intermediates in the Suzuki Reaction by Electrospray Mass Spectrometry. *Journal of the American Chemical Society* **1994**, *116* (15), 6985–6986.

(36) Vikse, K. L.; Henderson, M. A.; Oliver, A. G.; McIndoe, J. S. Direct Observation of Key Intermediates by Negative-Ion Electrospray Ionisation Mass Spectrometry in Palladium-Catalysed Cross-Coupling. *Chemical Communications* **2010**, *46* (39), 7412.

(37) Vikse, K. L.; McIndoe, J. S. Mechanistic Insights from Mass Spectrometry: Examination of the Elementary Steps of Catalytic Reactions in the Gas Phase. *Pure and Applied Chemistry* **2015**, *87* (4), 361–377.

(38) Vikse, K.; Naka, T.; McIndoe, J. S.; Besora, M.; Maseras, F. Oxidative Additions of Aryl Halides to Palladium Proceed through the Monoligated Complex. *ChemCatChem* **2013**, *5* (12), 3604–3609.

(39) Vikse, K. L.; Ahmadi, Z.; Manning, C. C.; Harrington, D. A.; McIndoe, J. S. Powerful Insight into Catalytic Mechanisms through Simultaneous Monitoring of Reactants, Products, and Intermediates. *Angewandte Chemie International Edition* **2011**, *50* (36), 8304–8306.

(40) Ahmadi, Z.; Oliver, A. G.; McIndoe, J. S. An Unexpected Pathway for Ligand Substitution in an Aryl Halide Complex of Palladium. *ChemPlusChem* **2013**, *78* (7), 632–635.

(41) Vikse, K. L.; Woods, M. P.; McIndoe, J. S. Pressurized Sample Infusion for the Continuous Analysis of Air- and Moisture-Sensitive Reactions Using Electrospray Ionization Mass Spectrometry. *Organometallics* **2010**, *29* (23), 6615–6618.

(42) Vikse, K. L.; Ahmadi, Z.; Luo, J.; van der Wal, N.; Daze, K.; Taylor, N.; McIndoe, J. S. Pressurized Sample Infusion: An Easily Calibrated, Low Volume Pumping System for ESI-MS Analysis of Reactions. *International Journal of Mass Spectrometry* **2012**, *323–324*, 8–13.

(43) Yunker, L. P. E. E.; Stoddard, R. L.; Mcindoe, J. S. Practical Approaches to the ESI-MS Analysis of Catalytic Reactions. *Journal of Mass Spectrometry* **2014**, *49* (1), 1–8.

(44) Henderson, W.; McIndoe, J. S. *Mass Spectrometry of Inorganic, Coordination and Organometallic Compounds*; John Wiley & Sons, Ltd: Chichester, UK, 2005.

(45) Sleno, L.; Volmer, D. A. Ion Activation Methods for Tandem Mass Spectrometry. *Journal of Mass Spectrometry* **2004**, *39* (10), 1091–1112.

(46) Enke, C. G. A Perspective on the Development of Tandem Mass Spectrometry. In *The Encyclopedia of Mass Spectrometry*; Elsevier, 2016; pp 68–76.

(47) Gross, J. H. Tandem Mass Spectrometry. In *Mass Spectrometry*; Springer International Publishing: Cham, 2017; pp 539–612.

(48) Amorim Madeira, P. J.; Helena, M. Applications of Tandem Mass Spectrometry: From Structural Analysis to Fundamental Studies. In *Tandem Mass Spectrometry - Applications and Principles*; InTech, 2012.

(49) Shukla, A. K.; Futrell, J. H. Collisional Activation and Dissociation of Polyatomic Ions. *Mass Spectrometry Reviews* **1993**, *12* (4), 211–255.

(50) Du, Z.; Douglas, D. J. A Novel Tandem Quadrupole Mass Analyzer. *Journal of the American Society for Mass Spectrometry* **1999**, *10* (11), 1053–1066.

(51) Douglas, D. J.; Konenkov, N. V. Mass Resolution of Linear Quadrupole Ion Traps with Round Rods. *Rapid communications in mass spectrometry : RCM* **2014**, *28* (21), 2252–2258.

(52) Savaryn, J. P.; Toby, T. K.; Kelleher, N. L. A Researcher's Guide to Mass Spectrometry-Based Proteomics. *PROTEOMICS* **2016**, *16* (18), 2435–2443.

(53) Chen, P. Electrospray Ionization Tandem Mass Spectrometry in High-Throughput Screening of Homogeneous Catalysts. *Angewandte Chemie International Edition* **2003**, *42* (25), 2832–2847.

(54) Chen, C.-C.; Lin, P.-C. Monitoring of Chemical Transformations by Mass Spectrometry. *Analytical Methods* **2015**, *7* (17), 6947–6959.

(55) Adlhart, C.; Chen, P. Fishing for Catalysts: Mechanism-Based Probes for Active Species in Solution. *Helvetica Chimica Acta* **2000**.

(56) Lee, E. D.; Mueck, W.; Henion, J. D.; Covey, T. R. Real-Time Reaction Monitoring by Continuous-Introduction Ion-Spray Tandem Mass Spectrometry. *Journal of the American Chemical Society* **1989**, *111* (13), 4600–4604.

(57) Eelman, M. D.; Blacquiere, J. M.; Moriarty, M. M.; Fogg, D. E. Shining New Light on an Old Problem: Retooling MALDI Mass Spectrometry for Organotransition-Metal Catalysis. *Angewandte Chemie International Edition* **2008**, *47* (2), 303–306.

(58) Bailey, G. A.; Fogg, D. E. Confronting Neutrality: Maximizing Success in the Analysis of Transition-Metal Catalysts by MALDI Mass Spectrometry. *ACS Catalysis* **2016**, *6* (8), 4962–4971.

(59) Penafiel, J.; Hesketh, A. V; Granot, O.; Scott McIndoe, J. Electron Ionization Mass Spectrometric Analysis of Air- and Moisture-Sensitive Organometallic Compounds. *Dalton Transactions* **2016**, *45* (39), 15552–15556.

(60) Agrawal, D.; Schröder, D. Insight into Solution Chemistry from Gas-Phase Experiments †. *Organometallics* **2011**, *30* (1), 32–35.

(61) Oxidative Addition and Reductive Elimination. In *The Organometallic Chemistry of the Transition Metals*; John Wiley & Sons, Inc.: Hoboken, NJ, USA, 2014; pp 163–184.

(62) 2011-Santos-Reaction-Mechanism-ESI-MS.Pdf.

(63) Instrumentation and Techniques of Mass Spectrometry. In *Mass Spectrometry in Cancer Research*; CRC Press, 2002; pp 23–79.

(64) Janusson, E.; Zijlstra, H. S.; Nguyen, P. P. T.; MacGillivray, L.; Martelino, J.; McIndoe, J. S. Real-Time Analysis of Pd 2 (Dba) 3 Activation by Phosphine Ligands. *Chemical Communications* **2017**, *53* (5), 854–856.

(65) Theron, R.; Wu, Y.; Yunker, L. P. E.; Hesketh, A. V; Pernik, I.; Weller, A. S.; McIndoe, J. S. Simultaneous Orthogonal Methods for the Real-Time Analysis of

Catalytic Reactions. *ACS Catalysis* **2016**, *6* (10), 6911–6917.

(66) Belli, R. G.; Burton, K. M. E.; Rufh, S. A.; McDonald, R.; Rosenberg, L. Inner- and Outer-Sphere Roles of Ruthenium Phosphido Complexes in the Hydrophosphination of Alkenes. *Organometallics* **2015**, *34* (23), 5637–5646.

(67) Belli, R. G.; Wu, Y.; Ji, H.; Joshi, A.; Yunker, L. P. E.; McIndoe, J. S.; Rosenberg, L. Competitive Ligand Exchange and Dissociation in Ru Indenyl Complexes. *Inorganic Chemistry* **2019**, *58* (1), 747–755.

(68) Zijlstra, H. S.; Linnolahti, M.; Collins, S.; McIndoe, J. S. Additive and Aging Effects on Methylalumoxane Oligomers. *Organometallics* **2017**, *36* (9), 1803–1809.

(69) Pape, J.; Vikse, K. L.; Janusson, E.; Taylor, N.; McIndoe, J. S. Solvent Effects on Surface Activity of Aggregate Ions in Electrospray Ionization. *International Journal of Mass Spectrometry* **2014**, *373*, 66–71.

(70) Suzuki, A. Recent Advances in the Cross-Coupling Reactions of Organoboron Derivatives with Organic Electrophiles, 1995–1998. *Journal of Organometallic Chemistry* **1999**, *576* (1–2), 147–168.

(71) Miyaura, N.; Ishiyama, T.; Ishikawa, M.; Suzuki, A. Palladium-Catalyzed Cross-Coupling Reactions of B-Alkyl-9-BBN or Trialkylboranes with Aryl and 1-Alkenyl Halides. *Tetrahedron Letters* **1986**, *27* (52), 6369–6372.

(72) Grubbs, R. H.; Chang, S. Recent Advances in Olefin Metathesis and Its Application in Organic Synthesis. *Tetrahedron* **1998**, *54* (18), 4413–4450.

(73) Louie, J.; Paul, F.; Hartwig, J. F. Catalysis with Platinum-Group Alkylamido Complexes. The Active Palladium Amide in Catalytic Aryl Halide Aminations As Deduced from Kinetic Data and Independent Generation. *Organometallics* **1996**, *15* (12), 2794–2805.

(74) Driver, M. S.; Hartwig, J. F. *Carbon-Nitrogen-Bond-Forming Reductive Elimination of Arylamines from Palladium(II) Phosphine Complexes*; 1997.

(75) Martin, R.; Buchwald, S. L. Palladium-Catalyzed Suzuki-Miyaura Cross-Coupling Reactions Employing Dialkylbiaryl Phosphine Ligands. *Accounts of chemical research* **2008**, *41* (11), 1461–1473.

(76) Johansson Seechurn, C. C. C.; Kitching, M. O.; Colacot, T. J.; Snieckus, V. Palladium-Catalyzed Cross-Coupling: A Historical Contextual Perspective to the 2010 Nobel Prize. *Angewandte Chemie International Edition* **2012**, *51* (21), 5062–5085.

(77) Heck, R. F.; Nolley, J. P. Palladium-Catalyzed Vinylic Hydrogen Substitution Reactions with Aryl, Benzyl, and Styryl Halides. *The Journal of Organic*

Chemistry **1972**, *37* (14), 2320–2322.

(78) Miyaura, N.; Yamada, K.; Suzuki, A. A New Stereospecific Cross-Coupling by the Palladium-Catalyzed Reaction of 1-Alkenylboranes with 1-Alkenyl or 1-Alkynyl Halides. *Tetrahedron Letters* **1979**, *20* (36), 3437–3440.

(79) Baba, S.; Negishi, E. A Novel Stereospecific Alkenyl-Alkenyl Cross-Coupling by a Palladium- or Nickel-Catalyzed Reaction of Alkenylalanes with Alkenyl Halides. *Journal of the American Chemical Society* **1976**, *98* (21), 6729–6731.

(80) Miyaura, N.; Suzuki, A. Palladium-Catalyzed Cross-Coupling Reactions of Organoboron Compounds. *Chemical Reviews* **1995**, *95* (7), 2457–2483.

(81) Nobel Review Magical Power of Transition Metals: Past, Present, and Future (Nobel Lecture)** Ei-Ichi Negishi* Carbometalation · Cross-Coupling · Negishi Coupling · Palladium Biography. **2010**.

(82) Suzuki, A. Cross-Coupling Reactions Of Organoboranes: An Easy Way To Construct C-C Bonds (Nobel Lecture). *Angewandte Chemie International Edition* **2011**, *50* (30), 6722–6737.

(83) Hassan, J.; Sévignon, M.; Gozzi, C.; Schulz, E.; Lemaire, M. Aryl−Aryl Bond Formation One Century after the Discovery of the Ullmann Reaction. *Chemical Reviews* **2002**, *102* (5), 1359–1470.

(84) Stille, J. K. Palladium-Katalysierte Kupplungsreaktionen Organischer Elektrophile Mit Organozinn-Verbindungen. *Angewandte Chemie* **1986**, *98* (6), 504–519.

(85) Mitchell, T. N. Palladium-Catalysed Reactions of Organotin Compounds. *Synthesis* **1992**, *1992* (09), 803–815.

(86) Kosugi, M.; Fugami, K. A Historical Note of the Stille Reaction. *Journal of Organometallic Chemistry* **2002**, *653* (1–2), 50–53.

(87) Torborg, C.; Beller, M. Recent Applications of Palladium-Catalyzed Coupling Reactions in the Pharmaceutical, Agrochemical, and Fine Chemical Industries. *Advanced Synthesis & Catalysis* **2009**, *351* (18), 3027–3043.

(88) Kostas, I. D. *Suzuki–Miyaura Cross-Coupling Reaction and Potential Applications*; MDPI, 2017.

(89) Walker, S. D.; Barder, T. E.; Martinelli, J. R.; Buchwald, S. L. A Rationally Designed Universal Catalyst for Suzuki–Miyaura Coupling Processes. *Angewandte Chemie International Edition* **2004**, *43* (14), 1871–1876.

(90) Murata, M.; Sambommatsu, T.; Watanabe, S.; Masuda, Y. An Efficient Catalyst System for Palladium-Catalyzed Borylation of Aryl Halides with Pinacolborane. *Synlett* **2006**, *2006* (12), 1867–1870.

(91) Ishiyama, T.; Ishida, K.; Miyaura, N. Synthesis of Pinacol Arylboronates via Cross-Coupling Reaction of Bis(Pinacolato)Diboron with Chloroarenes Catalyzed by Palladium(0)–Tricyclohexylphosphine Complexes. *Tetrahedron* **2001**, *57* (49), 9813–9816.

(92) Stambuli, J. P.; Kuwano, R.; Hartwig, J. F. Unparalleled Rates for the Activation of Aryl Chlorides and Bromides: Coupling with Amines and Boronic Acids in Minutes at Room Temperature. *Angewandte Chemie International Edition* **2002**, *41* (24), 4746–4748.

(93) Billingsley, K. L.; Barder, T. E.; Buchwald, S. L. Palladium-Catalyzed Borylation of Aryl Chlorides: Scope, Applications, and Computational Studies. *Angewandte Chemie* **2007**, *119* (28), 5455–5459.

(94) Mann, G.; Baranano, D.; Hartwig, J. F.; Rheingold, A. L.; Guzei, I. A. Carbon−Sulfur Bond-Forming Reductive Elimination Involving Sp-, Sp 2 -, and Sp 3 -Hybridized Carbon. Mechanism, Steric Effects, and Electronic Effects on Sulfide Formation. *Journal of the American Chemical Society* **1998**, *120* (36), 9205–9219.

(95) Phan, N. T. S.; Van Der Sluys, M.; Jones, C. W. On the Nature of the Active Species in Palladium Catalyzed Mizoroki–Heck and Suzuki–Miyaura Couplings – Homogeneous or Heterogeneous Catalysis, A Critical Review. *Advanced Synthesis & Catalysis* **2006**, *348* (6), 609–679.

(96) Hartwig, J. F. (John F. *Organotransition Metal Chemistry : From Bonding to Catalysis*.

(97) Frantz, D. E.; Weaver, D. G.; Carey, J. P.; Kress, M. H.; Dolling, U. H. Practical Synthesis of Aryl Triflates under Aqueous Conditions. *Organic Letters* **2002**, *4* (26), 4717–4718.

(98) Littke, A. F.; Fu, G. C. Palladium-Catalyzed Coupling Reactions of Aryl Chlorides. *Angewandte Chemie International Edition* **2002**, *41* (22), 4176–4211.

(99) Carrow, B. P.; Hartwig, J. F. Distinguishing Between Pathways for Transmetalation in Suzuki-Miyaura Reactions. *J. Am. Chem. Soc* **2011**, *133*, 2116–2119.

(100) Butters, M.; Harvey, J. N.; Jover, J.; Lennox, A. J. J.; Lloyd-Jones, G. C.; Murray, P. M. Aryl Trifluoroborates in Suzuki-Miyaura Coupling: The Roles of Endogenous Aryl Boronic Acid and Fluoride. *Angewandte Chemie International Edition* **2010**, *49* (30), 5156–5160.

(101) Kakino, R.; Narahashi, H.; Shimizu, I.; Yamamoto, A. Palladium-Catalyzed Direct Conversion of Carboxylic Acids into Ketones with Organoboronic Acids Promoted by Anhydride Activators. *Bulletin of the Chemical Society of Japan* **2002**, *75* (6), 1333–1345.

(102) Braga, A. A. C.; Morgon, N. H.; Ujaque, G.; Maseras, F. Computational Characterization of the Role of the Base in the Suzuki−Miyaura Cross-Coupling Reaction. *Journal of the American Chemical Society* **2005**, *127* (25), 9298–9307.

(103) *Cross-Coupling Reactions*; Miyaura, N., Ed.; Topics in Current Chemistry; Springer Berlin Heidelberg: Berlin, Heidelberg, 2002; Vol. 219.

(104) Smith, G. B.; Dezeny, G. C.; Hughes, D. L.; King, A. O.; Verhoeven, T. R. Mechanistic Studies of the Suzuki Cross-Coupling Reaction. *The Journal of Organic Chemistry* **1994**, *59* (26), 8151–8156.

(105) Thomas, A. A.; Denmark, S. E. Pre-Transmetalation Intermediates in the Suzuki-Miyaura Reaction Revealed: The Missing Link. *Science* **2016**, *352* (6283), 329–332.

(106) Rehahn, M.; Schlüter, A.-D.; Wegner, G.; Feast, W. J. Soluble Poly(Para-Phenylene)s. 1. Extension of the Yamamoto Synthesis to Dibromobenzenes Substituted with Flexible Side Chains. *Polymer* **1989**, *30* (6), 1054–1059.

(107) Krishna, A.; Lunchev, A. V.; Grimsdale, A. C. Suzuki Polycondensation. In *Synthetic Methods for Conjugated Polymers and Carbon Materials*; Wiley-VCH Verlag GmbH & Co. KGaA: Weinheim, Germany, 2017; pp 59–95.

(108) Sakamoto, J.; Rehahn, M.; Wegner, G.; Schlüter, A. D. Suzuki Polycondensation: Polyarylenes à La Carte. *Macromolecular Rapid Communications*. 2009.

(109) Schlüter, A.-D.; Hawker, C. J.; Sakamoto, J. *Synthesis of Polymers : New Structures and Methods*; Wiley-VCH, 2012.

(110) Li, G.; Zhao, Y.; Li, J.; Cao, J.; Zhu, J.; Sun, X. W.; Zhang, Q. Synthesis, Characterization, Physical Properties, and OLED Application of Single BN-Fused Perylene Diimide. *Journal of Organic Chemistry* **2015**.

(111) Chinnappan Baskar; Yee-Hing Lai, and; Valiyaveettil*, S. Synthesis of a Novel Optically Tunable Amphiphilic Poly(p-Phenylene): Influence of Hydrogen Bonding and Metal Complexation on Optical Properties1. **2001**.

(112) Renu Ravindranath, ‡; Chellappan Vijila, §; Parayil Kumaran Ajikumar, †; Fathima Shahitha Jahir Hussain, ‡; Kong Li Ng, ‡; Hezhou Wang, #; Chua Soo Jin, §,†; Wolfgang Knoll, § and; Suresh Valiyaveettil*, †,‡. Photophysical Properties of Hydroxylated Amphiphilic Poly(p-Phenylene)S. **2006**.

(113) Li, J.; Bo, Z. "AB2 + AB" Approach to Hyperbranched Polymers Used as Polymer Blue Light Emitting Materials. *Macromolecules*. 2004.

(114) Kraft, A.; Grimsdale, A. C.; Holmes, A. B. Electroluminescent Conjugated Polymers—Seeing Polymers in a New Light. *Angewandte Chemie International Edition* **1998**, *37* (4), 402–428.

(115) Friend, R. H.; Gymer, R. W.; Holmes, A. B.; Burroughes, J. H.; Marks, R. N.; Taliani, C.; C Bradley, D. D.; Dos Santos, D. A.; BreÂ das, J. L.; Lo È gdlund, M.; et al. *Electroluminescence in Conjugated Polymers*; 1999; Vol. 397.

(116) Rogers, M. E.; Long, T. E.; Turner, S. R. Introduction to Synthetic Methods in Step-Growth Polymers. In *Synthetic Methods in Step-Growth Polymers*; John Wiley & Sons, Inc.: Hoboken, NJ, USA, 2003; pp 1–16.

(117) Rusu, R.-D.; Schlüter, A. D. Progress in the Suzuki Polycondensation of Fluorene Monomers. *RSC Adv.* **2014**, *4* (100), 57026–57034.

(118) Schlu¨ter, A. D.; Schlu¨ter, S. The Tenth Anniversary of Suzuki Polycondensation (SPC). **2001**.

(119) Schlüter, A. D. The Tenth Anniversary of Suzuki Polycondensation (SPC). *Journal of Polymer Science Part A: Polymer Chemistry* **2001**, *39* (10), 1533–1556.

(120) Hohl, B.; Bertschi, L.; Zhang, X.; Schlüter, A. D.; Sakamoto, J. Suzuki Polycondensation toward High Molecular Weight Poly(m -Phenylene)s: Mechanistic Insights and End-Functionalization. *Macromolecules* **2012**, *45* (13), 5418–5426.

(121) Sangvikar, Y.; Fischer, K.; Schmidt, M.; Schlüter, A. D.; Sakamoto, J. Suzuki Polycondensation with a Hairpin Monomer. *Organic Letters* **2009**.

(122) Yokozawa, T.; Ohta, Y. Transformation of Step-Growth Polymerization into Living Chain-Growth Polymerization. *Chemical Reviews* **2016**, *116* (4), 1950–1968.

(123) Jakob, S. P.; Schlüter, A. D.; Sakamoto, J. Synthesis of Poly(m,p-Phenylene)s by Suzuki Polycondensation Using AA/BB Monomers. *Abstracts of Papers of the American Chemical Society* **2011**, *242*.

(124) Grätz, S.; Wolfrum, B.; Borchardt, L. Mechanochemical Suzuki Polycondensation – from Linear to Hyperbranched Polyphenylenes. *Green Chemistry* **2017**, *19* (13), 2973–2979.

(125) Frahn, J.; Karakaya, B.; Schäfer, A.; Schlüter, A.-D. Suzuki Polycondensation: On Catalyst Derived Phosphorus Incorporation and Reproducibility of Molecular Weights. *Tetrahedron* **1997**, *53* (45), 15459–15467.

(126) Ito, K.; Suzuki, T.; Sakamoto, Y.; Kubota, D.; Inoue, Y.; Sato, F.; Tokito, S. Oligo(2,6-anthrylene)s: Acene–Oligomer Approach for Organic Field-Effect Transistors. *Angewandte Chemie* **2003**, *115* (10), 1191–1194.

(127) Hohl, B.; Bertschi, L.; Zhang, X.; Schlüter, A. D.; Sakamoto, J. Suzuki Polycondensation toward High Molecular Weight Poly(m -Phenylene)s: Mechanistic Insights and End-Functionalization. *Macromolecules* **2012**, *45* (13),

5418–5426.

(128) Noonan, G.; Leach, A. G. A Mechanistic Proposal for the Protodeboronation of Neat Boronic Acids: Boronic Acid Mediated Reaction in the Solid State. *Organic & Biomolecular Chemistry* **2015**, *13* (9), 2555–2560.

(129) Lozada, J.; Liu, Z.; Perrin, D. M. Base-Promoted Protodeboronation of 2,6-Disubstituted Arylboronic Acids. *The Journal of Organic Chemistry* **2014**, *79* (11), 5365–5368.

(130) Liu, C.; Li, X.; Wu, Y. Base-Promoted Silver-Catalyzed Protodeboronation of Arylboronic Acids and Esters. *RSC Advances* **2015**, *5* (20), 15354–15358.

(131) Goodson, F. E.; Novak, B. M. Palladium-Mediated Soluble Precursor Route into Poly(Arylethynylenes) and Poly(Arylethylenes). *Macromolecules* **1997**, *30* (20), 6047–6055.

(132) Goodson, F. E.; Wallow, T. I.; Novak, B. M. Mechanistic Studies on the Aryl−Aryl Interchange Reaction of ArPdL 2 I (L = Triarylphosphine) Complexes. *Journal of the American Chemical Society* **1997**, *119* (51), 12441–12453.

(133) Wallow, T. I.; Goodson, F. E.; Novak, B. M. New Methods for the Synthesis of ArPdL 2 I (L = Tertiary Phosphine) Complexes. *Organometallics* **1996**, *15* (17), 3708–3716.

(134) Goodson, F. E.; Wallow, T. I.; Novak, B. M. Application of "Transfer-Free" Suzuki Coupling Protocols toward the Synthesis of "Unambiguously Linear" Poly(p -Phenylenes). *Macromolecules* **1998**, *31* (7), 2047–2056.

(135) Goodson, F. E.; Wallow, T. I.; Novak, B. M. Accelerated Suzuki Coupling Via a Ligandless Palladium Catalyst: 4-Methoxy-2′-Methylbiphenyl. In *Organic Syntheses*; John Wiley & Sons, Inc.: Hoboken, NJ, USA, 2003; pp 61–61.

(136) Yunker, L. P. E.; Ahmadi, Z.; Logan, J. R.; Wu, W.; Li, T.; Martindale, A.; Oliver, A. G.; McIndoe, J. S. Real-Time Mass Spectrometric Investigations into the Mechanism of the Suzuki–Miyaura Reaction. *Organometallics* **2018**, *37* (22), 4297–4308.

(137) Vikse, K. L.; Ahmadi, Z.; Scott McIndoe, J. The Application of Electrospray Ionization Mass Spectrometry to Homogeneous Catalysis. *Coordination Chemistry Reviews* **2014**, *279*, 96–114.

(138) Lubben, A. T.; Scott McIndoe, J.; Weller, A. S. Coupling an Electrospray Ionwization Mass Spectrometer with a Glovebox: A Straightforward, Powerful, and Convenient Combination for Analysis of Air-Sensitive Organometallics. *Organometallics* **2008**.

(139) Pentsak, E. O.; Eremin, D. B.; Gordeev, E. G.; Ananikov, V. P. Phantom

Reactivity in Organic and Catalytic Reactions as a Consequence of Microscale Destruction and Contamination-Trapping Effects of Magnetic Stir Bars. *ACS Catalysis* **2019**, No. 9, 3070–3081.

(140) Ahmadi, Z.; Yunker, L. P. E.; Oliver, A. G.; McIndoe, J. S. Mechanistic Features of the Copper-Free Sonogashira Reaction from ESI-MS. *Dalton Transactions* **2015**, *44* (47), 20367–20375.

(141) Qian, R.; Liao, Y.-X.; Guo, Y.-L.; Guo, H. ESI-FTICR-MS Studies on Gas Phase Fragmentation Reactions of ArPd(PPh3)2I Complexes. *Journal of the American Society for Mass Spectrometry* **2006**, *17* (11), 1582–1589.

Appendix

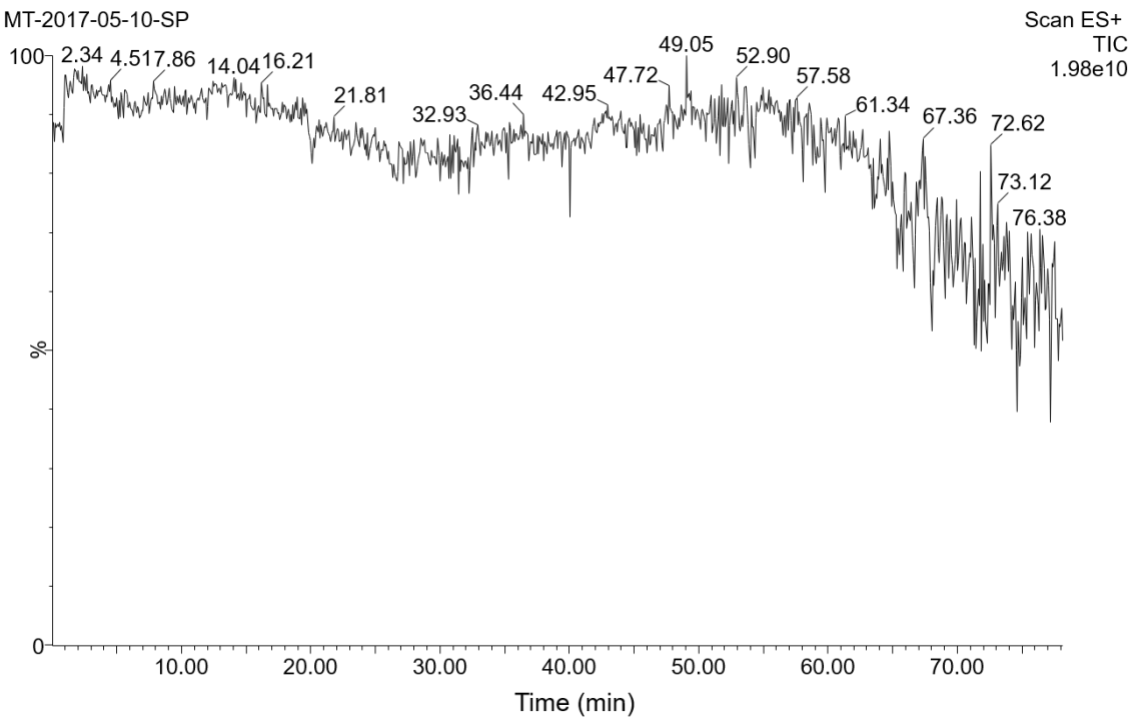

TIC of full scan SPC experiment

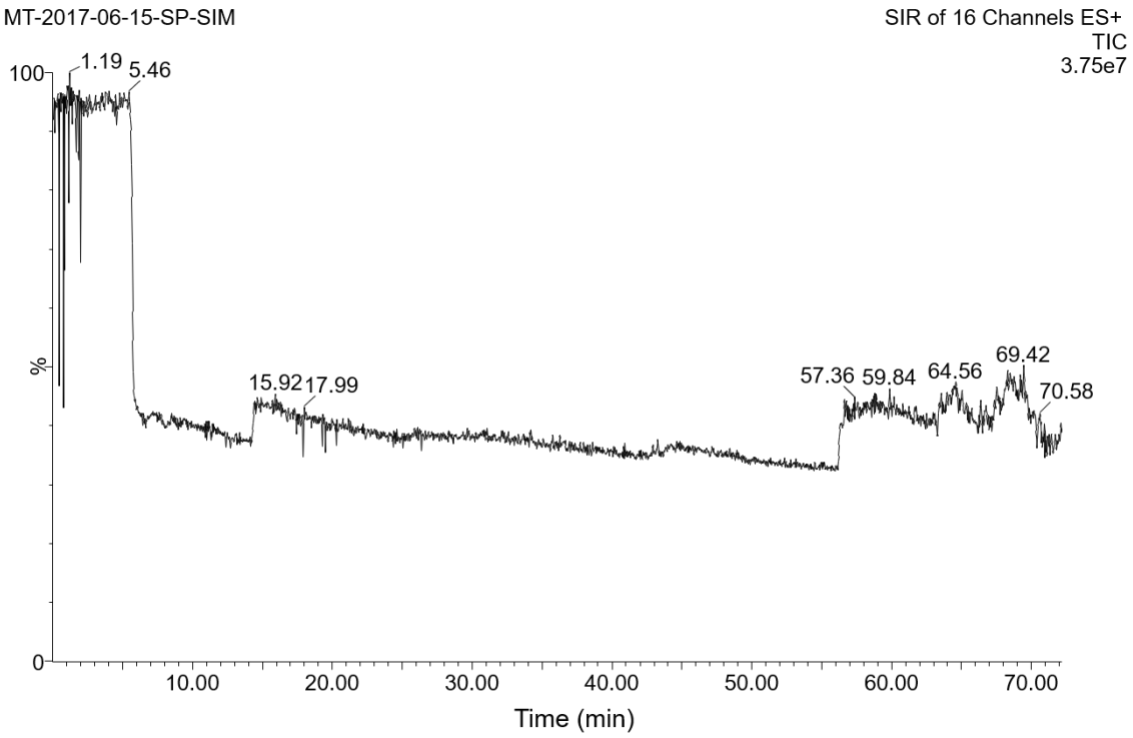

TIC of the SIR SPC experiment

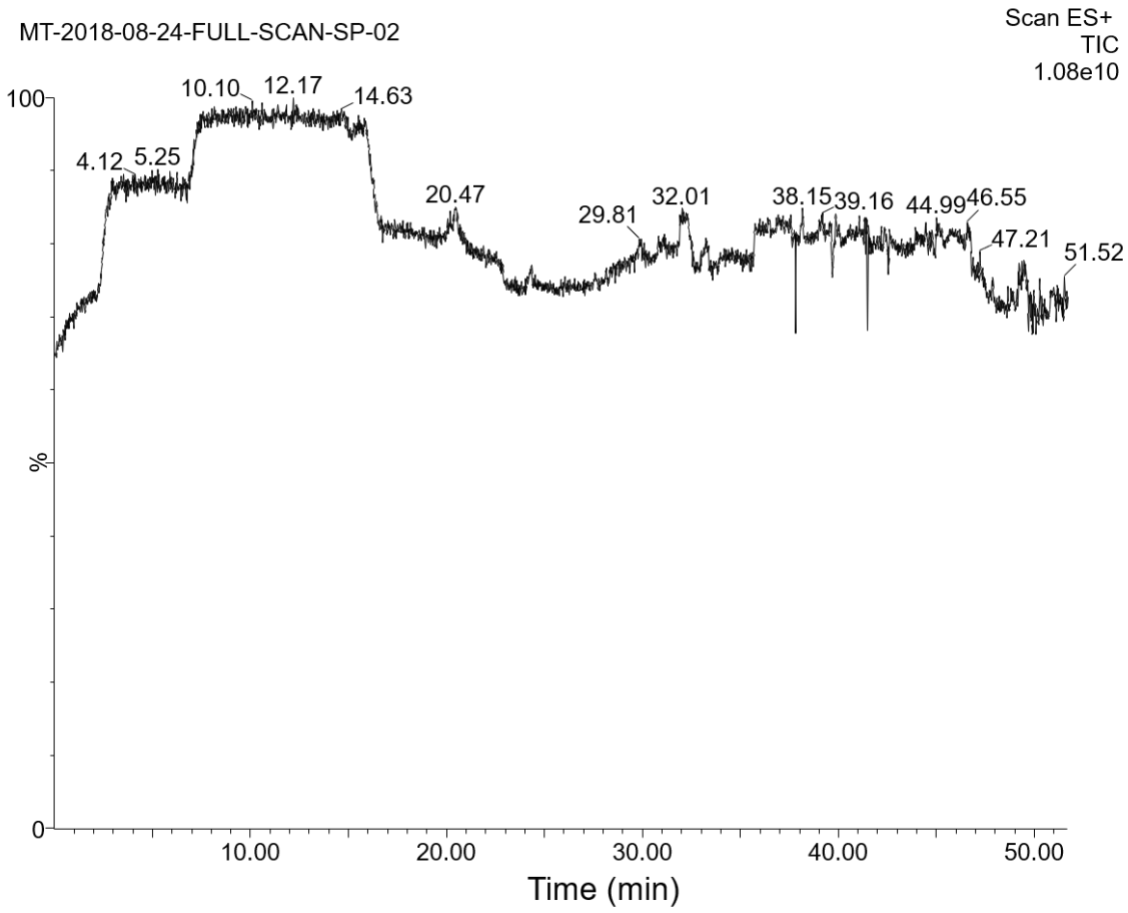

TIC of the Full scan SPC experiment using the methoxyphenylboronic acid as end-capping agent.

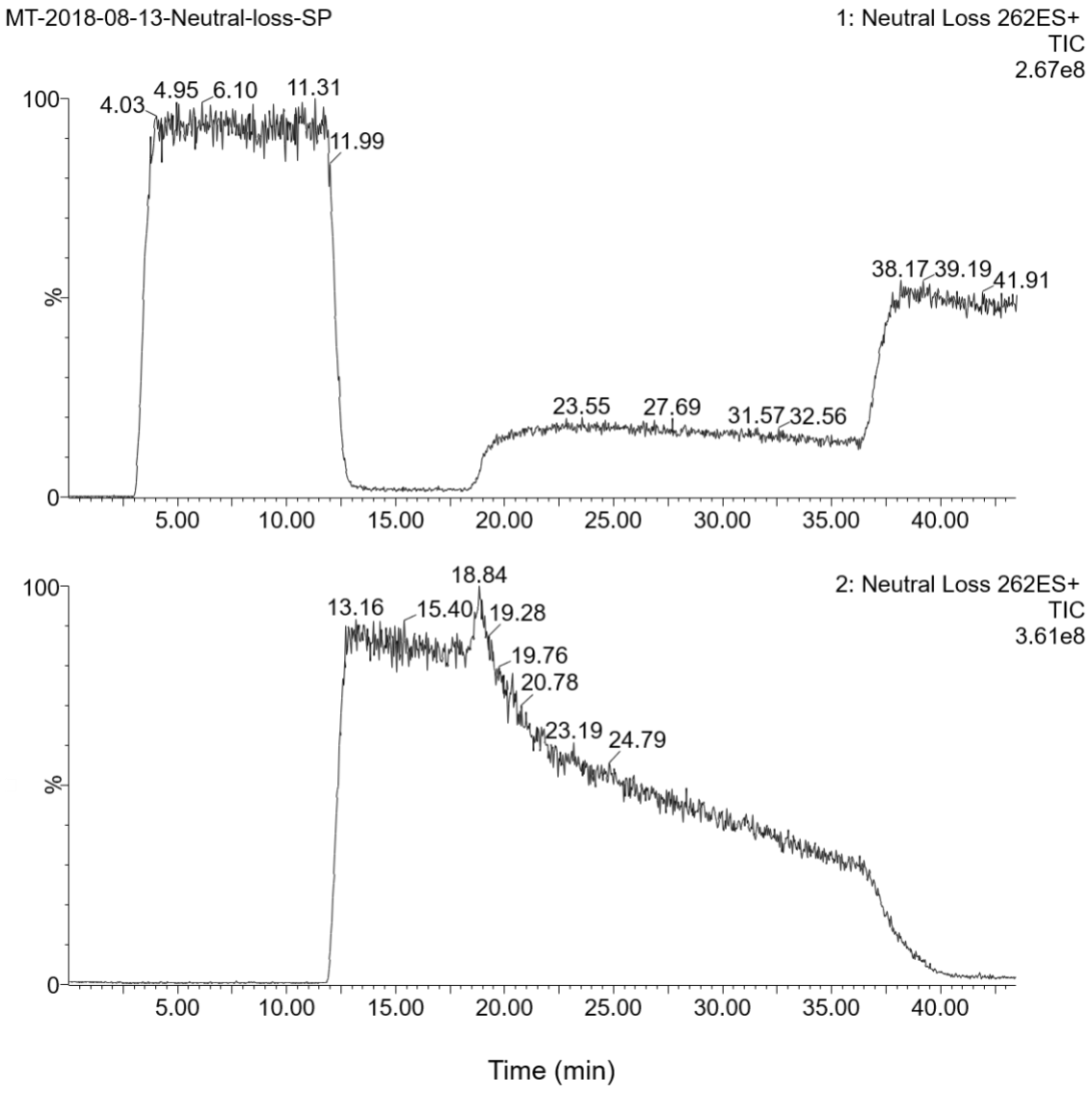

TIC of the NLS scan (two functions)

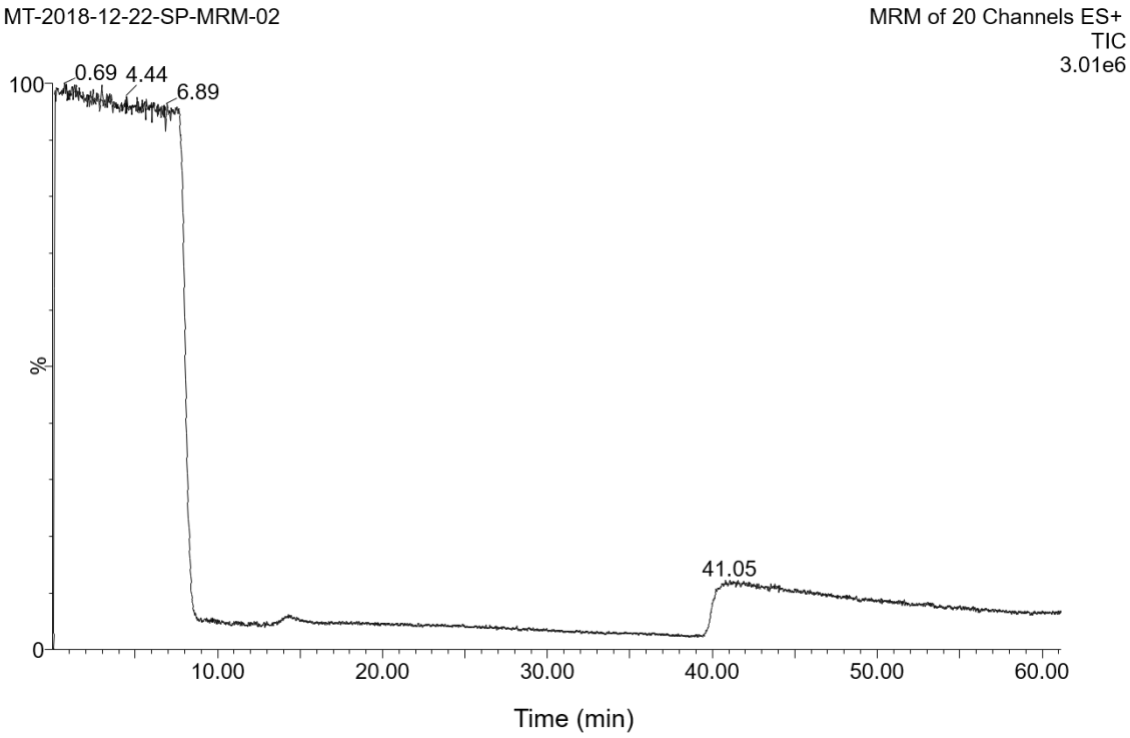

TIC of the MRM SPC experiment.